ADDIS ABABA UNIVERSITY

ADDIS ABABA INSTITUTE OF TECHNOLOGY SCHOOL OF CIVIL AND ENVIRONMENTAL ENGINEERING

PARAMETRIC ANALYSIS OF MERIDIONAL AND HOOP FORCES RESPONSE WITH RESPECT TO RISE TO RADIUS RATIO OF SPHERICAL CONCRETE SHELL

A Thesis in Structural Engineering

By Habtamu Tegegne Ewuenetu

October 2020

Addis Ababa

A Thesis

Submitted in Partial Fulfillment of the Requirements for the Degree of Master of Science in Civil Engineering (Structural Engineering)

The undersigned have examined the thesis entitled '**Parametric Analysis of Meridional and Hoop Forces Response with Respect to Rise to Radius Ratio of Spherical Concrete Shell**' Presented by **Habtamu Tegegne**, a candidate for the degree of **Master of Science** and hereby certify that it is worthy of acceptance.

Dr. SHIFFERAW TAYE		
Advisor	Signature	Date
Internal Examiner	Signature	Date
External Examiner	Signature	Date
Chair person	Signature	Date

UNDERTAKING

I certify that the paper work titled “parametric analysis of meridional and hoop forces response with respect to rise to radius ratio of spherical concrete shell” is my own work. The work has not been presented elsewhere for assessment. Where material has been used from other sources it has been properly acknowledged / referred.

_____

Habtamu Tegegne

ACKNOWLEDGMENTS

All praises to Almighty God, Merciful, and the Creator of all that exists in the universe and the Pure Virgin Saint Maryam, the Mother of God, Our Lady and Gate to Heaven. Thank You, O God, for giving me the patience, dedication and profound thought to achieve this study work. Thank you Our Lady Virgin Maryam for helping me through my university years and helping me to graduate.

It is not just to simply say 'thanks' to my principal advisor Dr. Shifferaw Taye, Associate professor of engineering mechanics & structural engineering, chief adviser (capacity building / technology transfer / policy), technical adviser / consultant (capacity building) ministry of urban development & construction, school of civil & environmental engineering, Addis Ababa Institute of Technology, Addis Ababa University, but I am really proud of being advised by him. He is caring, friendly and committed advisor. I am very much thankful to him for his inspiration, guidance, assist and extensive discussions to complete this thesis work.

I am deeply grateful to my sponsor Ethiopian Roads Authority for giving me the opportunity to join graduate program.

I would like to express my sincere gratitude to my friend, Abebe Balew, MSc in structural engineering, for his valuable supports which have contributed to the improvement of the final draft.

I would like to extend my sincere thanks to Birku Kebebew, who encourage and advised me while I had been pursuing university courses.

I am very grateful to my mother Tejtu Belachew, my sister Tsige Tegegne, and my brothers Ayitenew Tegegne and Ewnetu Tegegne for their encouragement and financial support all through my studies. I am also grateful to my other family members who have supported me along the way.

Finally I would like to thank all my friends for sharing me reference books and important information.

TABLE OF CONTENTS

LIST OF TABLES

LIST OF FIGURES

LIST OF ABBREVIATIONS

EBCS 1-1995 Ethiopian Building Code Standard for Basis of Design and Actions on Structures

EBCS 2-1995 Ethiopian Building Code Standard for Structural Use of Concrete

prEN 1991-1-4 Eurocode 1: Actions on structures – General actions – Part 1-4: Wind actions

LIST OF SYMBOLS

A	Radius of the shell
F	Rise of the shell
D	Shell span length
$\boldsymbol{t}$	Shell thickness
$\boldsymbol{h}$	Ring beam height
B	Ring beam width
$\boldsymbol{v}$	Poisson's ratio
G	Dead load
$\boldsymbol{p}$	Live load
$\mathbf{w_e}$	External wind load
C30/37	Concrete class
$\mathbf{f_{ck}}$	Characteristics cylinder compressive strength of concrete
Γ	Normal weight of concrete
E	Concrete modulus of elasticity
K	Gaussian curvature
$\frac{\mathbf{1}}{r_x}$	Principal curvature in the x direction
$\frac{\mathbf{1}}{r_y}$	Principal curvature in the y direction
$\mathbf{N_x}$	Internal hoop force in the x direction
$\mathbf{N_y}$	Internal meridional force in the y direction
$\boldsymbol{N_{xy}}$	Internal in-plane shear force in the xy direction
$\boldsymbol{N_{yx}}$	Internal in-plane shear force in the yx direction
$\mathbf{Q_x}$	Internal out of plane shear force in the x direction
$\mathbf{Q_y}$	Internal out of plane shear force in the y direction
$\mathbf{M_x}$	Internal bending force about x- axis
$\mathbf{M_y}$	Internal bending force about y- axis
$\boldsymbol{M_{xy}}$	Internal twisting couple about xy axis
$\boldsymbol{M_{yx}}$	Internal twisting couple about yx axis
$\boldsymbol{N_{\Phi}}$	Internal membrane/total meridional force
$\boldsymbol{N_{\theta}}$	Internal membrane/total hoop force

$\boldsymbol{\Phi}$	Meridional angle from center of revolution
$\boldsymbol{\alpha}$	Half central angle
$\boldsymbol{P_{\Phi}}$	External force in the Φ direction
$\boldsymbol{P_{\theta}}$	External force in the Θ direction
$\boldsymbol{P_{r}}$	External force in the r direction
$\mathbf{r}$	Radius of parallel circle
$\mathbf{r_1}$	Radius of curvature of the meridian
$\mathbf{r_2}$	Radius of curvature of the surface
$\boldsymbol{\varepsilon_{\Phi}}$	Meridian strain of the shell
$\boldsymbol{\varepsilon_{\theta}}$	Hoop strain of the shell
$\boldsymbol{\Delta r}$	Change of radius of the parallel circle
$\mathbf{v}$	Meridional displacement
$\mathbf{w}$	Displacement normal to the meridional curve
$\boldsymbol{N_{\alpha}}$	Meridional force at the base of the shell
$\boldsymbol{H_o}$	Meridional force horizontal component at the base of the shell
$\boldsymbol{V_o}$	Meridional force vertical component at the base of the shell
$\boldsymbol{H}$	Uniformly distributed radial force/ Edge shear force
$\mathbf{M_{\alpha}}$	Uniformly distributed twisting couples/ Edge moment
$\mathbf{A_R}$	Rectangular ring beam cross sectional area
$\mathbf{I_R}$	Second moment of area of ring beam
$\mathbf{c}$	Constant of integration
$\boldsymbol{\Delta H}$	Ring beam change of radius due to radial force
$\boldsymbol{T}$	Ring beam hoop force
$\boldsymbol{\Delta H^*}$	Change of ring radius due to twisting couple
$\boldsymbol{\Delta_{\alpha}}$	Ring beam torsional rotation
$\boldsymbol{D^R{}_{10}}$	Ring beam membrane radial displacement
$\boldsymbol{D^R{}_{20}}$	Ring beam membrane radial rotation
$\boldsymbol{D^D{}_{10}}$	Dome membrane displacement
$\boldsymbol{D^D{}_{20}}$	Dome membrane rotation
$\boldsymbol{\lambda}$	Damping parameter
$\boldsymbol{\psi}$	Half central angle minus meridional angle
$\boldsymbol{e^{-\lambda\psi}}$	Exponential decay term
$\boldsymbol{D^D{}_{11}}$	Dome displacement flexibility influence coefficient by edge

	shear
$D^D{}_{12}$	Dome displacement flexibility influence coefficient by edge moment
$D^D{}_{21}$	Dome rotation flexibility influence coefficient by edge shear
$D^D{}_{22}$	Dome rotation flexibility influence coefficient by edge moment
$D^R{}_{11}$	Ring displacement flexibility influence coefficient by edge shear
$D^R{}_{12}$	Ring displacement flexibility influence coefficient by edge moment
$D^R{}_{21}$	Ring rotation flexibility influence coefficient by edge shear
$D^R{}_{22}$	Ring rotation flexibility influence coefficient by edge moment
D_{11}	Dome-ring system displacement flexibility influence coefficient by edge shear
D_{12}	Dome-ring system displacement flexibility influence coefficient by edge moment
D_{21}	Dome-ring system rotation flexibility influence coefficient by edge shear
D_{22}	Dome-ring system rotation flexibility influence coefficient by edge moment
d'	Distance from dome-ring interaction center to ring beam top
y_o	Distance from dome-ring interaction center to half of ring beam height
b'	Distance from dome-ring interaction center to half of ring beam width
e	Perpendicular distance from the projection of center of dome thickness center to geometric center of ring beam
r	Internal radius of the dome
h/d	Height of wall to span of dome ratio
f/d	Rise of dome to its span ratio
γ_p	Plastering and painting unit weight
t_p	Plastering and painting thickness
q_{ref}	Reference wind pressure
$c_e(z)$	Exposure coefficient
c_{pe}	External pressure coefficient

v_{ref}	Reference wind velocity
C_{DIR}	Direction factor
C_{TEM}	Temporary (seasonal) factor
C_{ALT}	Altitude factor
ρ	Air density.
f*	Vector of elemental nodal forces
k*	Element stiffness matrix
d*	Vector of unknown element nodal degrees of freedom or generalized displacements
F*	Vector of global nodal forces
K*	Structure global or total stiffness matrix

LIST OF EQUATIONS

ABSTRACT

This paper considers a spherical concrete dome of constant span length sixty-meter and ten-centimeter thickness. Analytical and SAP2000 finite element software are employed for analysis. Ten different models for dead load, live load and wind load are done. All together thirty models are conducted and analyzed. Analysis results are done in analytically using Microsoft excel and SAP2000. Ten different rises to radius ratios are taken to determine the most efficient load carrying capacity of the shell under the action of dead, live and wind loads one after the other that generates various meridional and hoop forces. The behavior of the shell roof changes as its rise to radius ratio changes. The numerical value of rise to radius ratio that corresponds to 0.73 is taken as a reference point to study the behavior of hoop and meridional forces under gravity loads. This is the value at which edge forces are minimum. When rise to radius ratio decreases, the edge shear and edge moment increases in magnitude. As a result, the compressive hoop force is changed from compressive to tensile force drastically while the meridional force remains compressive but gets reduced in magnitude. When rise to radius ratio increases, the behavior of edge shear and edge moment increases in magnitude but show opposite sign to that of decrease in rise to radius ratio. As a result, the hoop force is changed from tensile to compressive force gradually while the meridional force remains compressive but gets negligibly increased in magnitude. Figures 5- 1, 5- 2, 5-3, 5- 4, and 5- 5 illustrate more. On this paper, the best rise to radius ratio for minimum edge disturbance effects due to gravity loads ranging from $0.72-0.74$, is recommended to resist the loads in membrane actions with negligible bending forces. However, for minimum effect of membrane meridional and hoop forces due to wind load, the best rise to radius ratio recommended ranges from $0.5 - 0.7$.

Key Words: spherical concrete shell roof, meridional force, hoop force, rise to radius ratio, SAP2000

CHAPTER 1 INTRODUCTION

A shell is defined as a body having one dimension – the thickness – small compared with the other two dimensions. The behavior of concrete shell structures is, in various aspects different from that of concrete slab structures. The most important features of shell, which make the internal force system in shells differ from those in other types of structural forms (plated structures), is their geometrical features (initial curvature). Shell structures support applied external forces efficiently by virtue of their geometrical form, i.e., spatial curvatures; as a result, shells are much stronger and stiffer than other structural forms. There are various type and complex forms of shell structures such as spherical (surface of revolution), barrel vaults, folded plates, folded plate domes and translational. Before the advancement of technology design process of shell structures was complex. Today the growth of computer modelling is accelerating the process.

The wide application of shell structures is conditioned by their efficiency of load carrying behavior, high degree of reserved strength and structural integrity, high strength to weight ratio, very high stiffness, covering of large space with no internal columns, and having extremely high aesthetic value in various architectural designs.

A doubly curved spherical shell is one of the most suitable and best structural form of shell used to cover large span structures such as churches, mosques, industrial buildings and auditoriums. It is much stiffer and stronger than a singly curved surface, such as a barrel shell. The general state of stress in a spherical shell element consists of membrane forces (meridional force, hoop force and membrane shear force) and bending forces (bending moments, twisting couples, and transverse shear forces). The bending forces normal to the shell surface, compared to membrane forces, are very small and are neglected in the membrane theory of shell. Due to this, shell roof structures carry the applied forces mostly by in plane actions, which are called membrane forces.

A doubly curved spherical concrete shell form can be shallow and hemispherical type depending on the rise of the shell. Due to this form of spherical shells i.e., as the shells makes a transition from shallow to hemispherical many effects bring the safety of the structure into question. Many researches have been reported on these effects.

Study of the literature tell that the behavior of meridional and hoop forces response of shell as the shells makes a transition from shallow to hemispherical type for loading cases of dead load, live load and wind load individually is unclear, and requires further investigation. The aim of this paper is to provide the understanding of meridional and hoop forces response as the shell translates from shallow

to hemispherical type with respect to rise to radius ratios (f/a) of spherical concrete shell roof acted upon by dead load, live load and wind load in static loading condition in order to enhance their effective design and safe use.

1.1 Research Significance

It is planned to study the variation of meridional forces NΦ and hoop forces NΘ of the spherical concrete shell as the shell translates form shallow to hemispherical type with respect to rise to radius ratio at any level of the shell by developing graphs of superimposed membrane and bending forces results for each load cases. Besides, to investigate the tendency of the shell to be extensional (tension) Moreover, it is aimed to study bending meridional and hoop forces effect on membrane fields.

1.2 Scope and Limitation

The scope of the present research paper is focused on meridional and hoop forces variation of spherical concrete shell with respect to its rise to radius ratio. The analysis of spherical shell can be carried out using analytically and finite element software. This research was done using ANSYS computer software for linear analysis subjected to axisymmetric and asymmetric static loads, and theoretically by varying shell parameters. It was done by selecting and assuming suitable shell geometry, loading condition, support condition, materials as well as other necessary parameters from manuals, codes and standards. The 60 m span and constant thickness (10 cm) rigidly supported spherical shell is analyzed for dead load, live load and wind load over the shell surface. The parameters (variables) are rise f and radius a of the shell and the constants are span d = 60 m, thickness t = 0.10 m, ring beam height h = 1.20m, width b = 0.45m, Poisson's ratio ν= 0.2, dead load g = 3.09 kN/m2, live load p = 0.25 kN/m2, and external wind load for ten models we = -0.84, -0.68, -0.48, -0.32, -0.15, 0.02, 0.11, 0.31, 0.50, and 0.69 kN/m2, support Rigidly supported. Concrete class is C30/37MPa, characteristics cylinder compressive strength of concrete fck = 30MPa, normal weight γ= 24kN/m3 and modulus of elasticity E= 32GPa.Thirty model with variable parameters of rise and radius and keeping the other dimensions, materials and support conditions constant were analyzed for each load cases. This study has the following limitations.

1. It is limited to meridional forces and hoop forces analysis using membrane and bending theory i.e., it is not complete analysis of all forces
2. It is also limited to uniform shell thickness

1.3 Objective

1.3.1 General Objective

The main objective of this research is to study the variation of meridional NΦ and hoop NΘ forces response of the shell as the shell translates form shallow to hemispherical type with respect to rise/radius ratio by plotting the graphs of superimposed membrane and bending forces results and to recommend a suitable rise to radius ratio of the shell geometries for optimum behavior of each load cases.

1.3.2 Specific Objective

It is planned to study the range of rise to radius ratio of the shell at which the bending forces are minimum. Besides, it is amid to investigate the rise to radius ratio at which the edge shear and edge moments are supposed to be zero.

1.4 Methodology

To achieve the objectives stated above, thirty model (ten models for each load cases) were analyzed in analytically using Microsoft excel and SAP2000 for dead, live, and wind load cases separately in static loading condition. The parameters (variables) are rise f, radius a. and half central angle α of the shell and the constants are span d = 60 m, thickness t = 0.10 m, ring beam height h = 1.20m, width b = 0.45m, Poisson's ratio ν= 0.2, dead load g = 3.09 kN/m^2, live load p = 0.25 kN/m^2, and external wind load for ten models w_e = -0.84, -0.68, -0.48, -0.32, -0.15, 0.02, 0.11, 0.31, 0.50, and 0.69 kN/m^2, Concrete class is C30/37MPa, characteristics cylinder compressive strength of concrete fck = 30MPa, normal weight γ= 24kN/m^3 and modulus of elasticity E= 32GPa.

CHAPTER 2 LITERATURE REVIEW

Many researches have been conducted on spherical concrete shells in order to understand the load carrying behavior of the shell by varying the rise/span ratio of the shell i.e., by changing the curvature. As a result, various conclusions were recommended by considering the analysis results with respect to the meridional angles. However, none of them have conducted the response of meridional and hoop forces with respect to rise/radius ratio of the shell. Therefore, this paper will be a very good tool to understand the meridional and hoop forces response of the shell as the shell translates form shallow to hemispherical type with respect to rise/radius ratio of the shell. For the purpose of finding supportive information for this work, review of previous work had been reviewed and explained as follows.

A paper about parametric study on behavior of concrete shell under uniform loading that was carried out by Garish G.M, Shri Mahadevan Iyer and Dr. Neeraja. D, in VIT University, Vellore concluded that there is a significant change in membrane stresses as it makes a transition from non-shallow shell to shallow shell and an appreciable change in the pattern of stress curves (rise to span ratio <0.25) can be observed in each comparison plot constructed. The study also showed that there is an exponential increase in the membrane stress in the mid-span in every stress plots comparison and slope of stress curves increases as non-shallow shells make a transition to shallow shells. The study finally recommended that tendency of a shell to extend (extensional ability) increases as rise to span decreases and a suitable rise to span ratio in the range of 0.13 to 0.16 shall be suggested for an optimum behavior of shell. [10]

Another paper on structural analysis and optimization of concrete spherical and groined shells was carried out by Ivana Mekjavic. The conclusions obtained are, varying the thickness of the shell, with the largest thickness at the supports, leads to the most effective design in terms of reduced tensile stresses, reduced deflections, and most efficient use of materials. [12]

Another study conducted on configuration of shell structures for optimum stresses by Howard Paul Harrenstien in Iowa state university concluded that it is necessary to provide proper boundary forces if constant membrane stress characteristics are desired throughout the shell. The study also showed that shells made of materials which are weak in tension will resist loads efficiently without reinforcement when they are designed by the proposed method. [11]

A study on computational structural form finding and optimization of shell structure was carried out by Andrew BORGART in Delft, The conclusions obtained are, a link is suggested between the geometry of a shell's surface via its curvature and the load path and force network, which are a result

of loading of the shell structure. In this link lies the probable solution for unveiling the relation form – force of shells, which will help architects and engineers really understand the structural behavior of shells and could help design elegant and optimum shell structures. [2]

A paper carried out on the digital workflow of parametric structural design by Marie Eliassen and Ashild Huseby in Norwegian university of science and technology summarized that a rise/span-ratio between 0.2 and 0.4 was in general the most optimal. Too low ratio lead to high moments and displacements. For high ratios the structure become less stable with large displacements and moments. [13]

A paper carried out by Garish G.M, Shri Mahadevan Iyer and Dr. Neeraja. D, in VIT University, Vellore, concluded the behavior of meridional and hoop forces by plotting the graphs of meridional and hoop stresses for various rise to span ratios with respect to meridional angles Φ for uniform loading. But in their study wind load has not been considered. This research work has a direct link with the present research work. Therefore, detailed investigation has to be conducted on the responses of meridional and hoop forces as the shell translates form shallow to hemispherical type by plotting the graphs with respect to rise/radius ratio of the shell for dead, live and wind load.

2.1 Shells

2.1.1 Definitions of Shell Structure

A shell can be defined as a curved slab whose thickness is very small compared to their other dimensions. The behavior of concrete shell structures is, in various aspects, different from that of concrete slab structures. Their behavior is difficult to analyze and they are sensitive for small change of geometry and support conditions. The most important features, which make the internal force system in shells differ from those in other types of structural forms (plated structures), is their geometrical features (initial curvature) thus curved structures resist more applied loads than flat plates with less deformation and stresses having the same span and dimensions. For this reason, the exceptional behavior of shell structures can be referred to as ‘form resistant structures. This implies a surface structure whose strength is derived from its shape, and which resist load by developing stresses in its own plane.

2.1.2 Uses of Shell Structures

Shell structures developed since ancient times. Now a day’s thin concrete shell structures such as concrete shell roofs, liquid retaining structures and water tanks, concrete silos, cooling towers, containment shells of nuclear power plants, and concrete arch dams are being increasingly used in

various industries. They also used in the construction of light weight vehicles, pressure vessels, and space structures. Recently, with the advent of various fiber-reinforced and laminated composite materials, the domain of application and range of structural efficiency of shell forms has extremely increased. The wide application of shell structures is conditioned by their efficiency of load carrying behavior, high degree of reserved strength and structural integrity, high strength to weight ratio, very high stiffness, covering of large space with no internal columns, and having extremely high aesthetic value in various architectural designs.[9]

2.1.3 Classification of Shells

Shell surfaces can be classified based on the Gaussian curvature of the surfaces, their geometrical develop ability, and their manner of generations of surface

a) *Classification According to Gaussian curvature*

The Gaussian curvature K = $\frac{1}{r_x r_y}$ is an algebraic quantity of the product of two principal curvatures. Where r_x and r_y are principal radii of curvatures, are measures of how the shell curves in the hoop and meridional directions. Depending on the quantity Gaussian curvature K = $\frac{1}{r_x r_y}$ is positive, negative, or zero at a point, they may be classified as synclastic surface, anticlastic surface (saddle surfaces), and zero Gaussian curvature surface at that point respectively.

The Gaussian curvature provides information about the load carrying behavior of shells. Synclastic surface, like domes, for such shells the edge disturbance damp out rapidly, making membrane theory valid for most of the shell surfaces. They typically show the greatest stiffness. Anticlastic surfaces (saddle surfaces) such as hyperbolic paraboloid is less stiff than synclastic structures and require more stiffness. Their edge disturbance tends to affect a greater part of the shell, making bending theory more important. Curves with Gaussian curvature K = 0 are called zero Gaussian curvature surfaces. The edge disturbance of developable surfaces are damped to a certain degree, but extend further into the shell than for synclastic surfaces. Examples are cylinders and cones.

b) Classification According to Geometrical Developability

According to geometrical developability, Shell surfaces are either developable or nondevelopable. Developable surfaces are, the ones which can be developed into a plane form without cutting/or stretching their middle surface. Surfaces with single curvature are always developable. A nondevelopable surface, on the other hand, is a surface which has to be cut and /or stretched in order to be developed into a planar form. Surfaces with double curvature are usually nondevelopable.

The classification of shell surfaces into developable and nondevelopable has some structural significance. From physical point of view, Shells with nondevelopable surface require more external energy, than do developable shells, to be stretched out, i.e., to collapse into a planar form. Hence, one may conclude that nondevelopable shells are, in general, stronger and more stable than the corresponding developable shells having the same overall dimensions.

c) Classification According to Manner of Generation of Surface

In this type of classification of surfaces, which is very useful in shell analysis and design, they classified as surfaces of revolution, translational surfaces, and ruled surfaces.

Surfaces of revolution are generated by rotating a meridional curve about an axis of revolution. It includes spherical, conical, elliptical, etc. Surface of translations are generated by the motion of the plane curve parallel to itself over another curve, the planes containing the two curves being at right angles to each other. Examples are elliptic paraboloid and hyperbolic paraboloid. Shells of ruled surface are formed by the motion of a straight line which is known as the generator or ruling. Some examples of ruled surfaces are conoid and hyperbolic paraboloid.

2.2 Assumptions of Classical Shell Theories

The following classical shell theories can be used for analysis and design of a variety of shell structures.

i) The shell is assumed to be thin, i.e., its thickness is small compared with its representative minimum radius of curvature, or lateral dimensions.
ii) Plane sections originally normal to the shell mid-surface remain plane and perpendicular to the deformed mid surface. The later assumption is equivalent to ignoring the shear deformations.
iii) The stress components normal to the shell mid-surface is very small compared with other stress components, and can be neglected.
iv) The displacements and strains are so small that their higher powers can be neglected.

2.3 Internal Force System in a Shell

Consider a shell with a general geometry. An infinitesimal element of this shell can be cut out by intersecting it with two pairs of principal plane sections which are located at arc lengths of ds_x and ds_y apart. Two intersecting planes, are from each pair the normal to the shell at the common corner point. The resulting plane curves of intersection are principal sections and are thus perpendicular to

each other, figure (2-1). The principal plane curves have principal radii of curvature which, in this figure, are designated by r_x andr_y.[9]

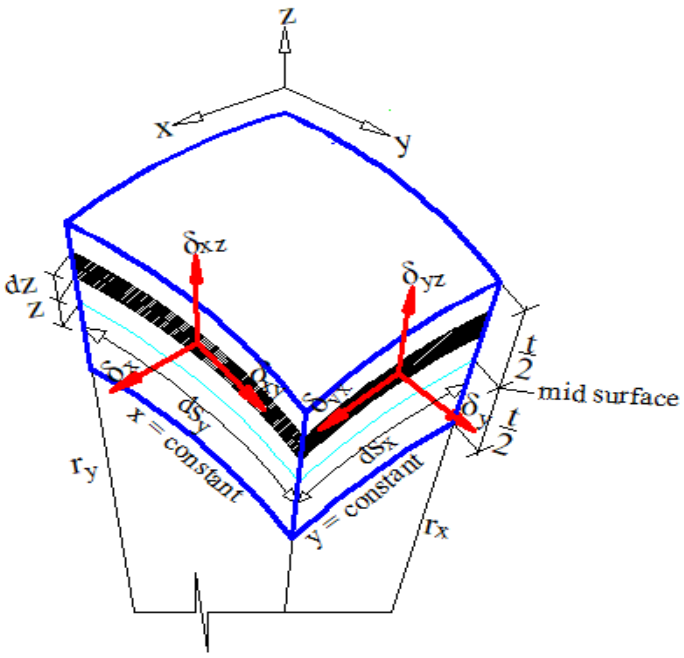

Figure 2- 1: A shell element demonstrating the principal radii of curvature and the internal stresses

In a shell structure subjected to applied external loading, temperature changes, support settlements, and deformation constraints some internal forces may develop. These forces are defined below and are shown as they act upon the element in Figure (2-2). In thin shells, the force in the z-direction (in the thickness direction) namely δ_z is very small compared to the other two normal forces δ_x and δ_y and is neglected in the classical shell theories.

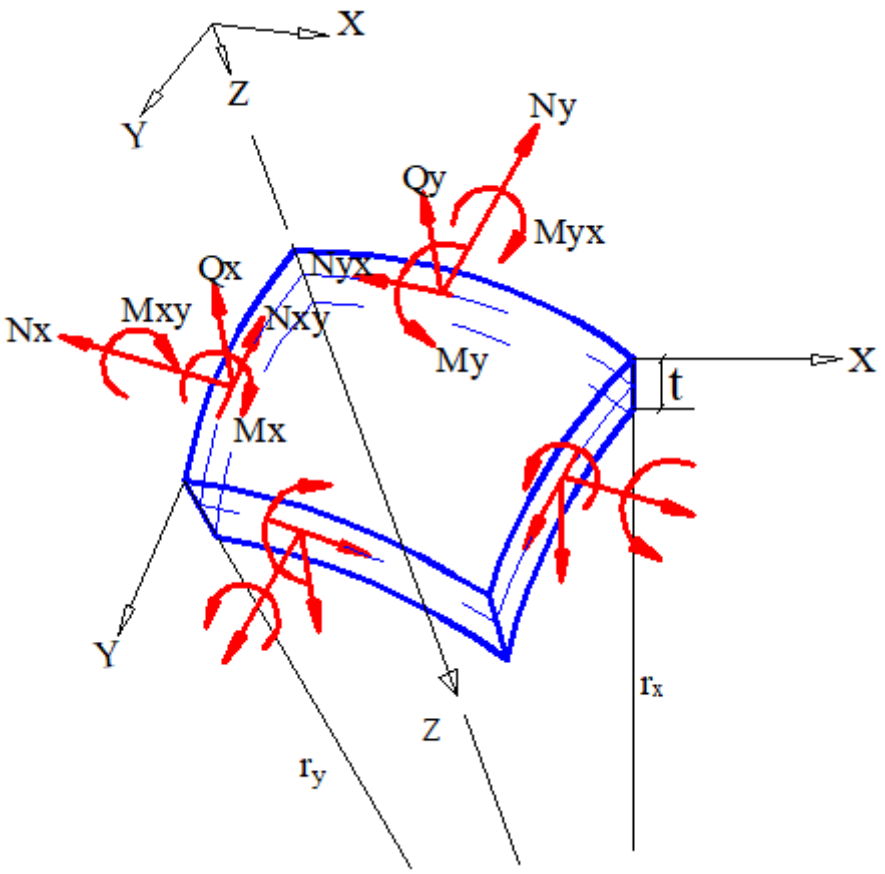

Figure 2- 2: Components of resultant internal forces in a shell element

The internal system of forces and moments acting on an infinitesimal element of the shell may be properly integrated across the shell thickness to give the so called resultant internal forces.

$$N_x = \int_{-\frac{t}{2}}^{\frac{t}{2}} \delta_x \left(1 + \frac{z}{r_y}\right) dz \quad \text{Equation 2- 1}$$

$$N_y = \int_{-\frac{t}{2}}^{\frac{t}{2}} \delta_y \left(1 + \frac{z}{r_x}\right) dz \quad \text{Equation 2- 2}$$

$$N_{xy} = \int_{-\frac{t}{2}}^{\frac{t}{2}} \delta_{xy} \left(1 + \frac{z}{r_y}\right) dz \quad \text{Equation 2- 3}$$

$$N_{yx} = \int_{-\frac{t}{2}}^{\frac{t}{2}} \delta_{yx} \left(1 + \frac{z}{r_x}\right) dz \quad \text{Equation 2- 4}$$

$$Q_x = \int_{\frac{-t}{2}}^{\frac{t}{2}} \delta_{xz}\left(1 + \frac{z}{r_y}\right)dz \quad \text{Equation 2- 5}$$

$$Q_y = \int_{\frac{-t}{2}}^{\frac{t}{2}} \delta_{yz}\left(1 + \frac{z}{r_x}\right)dz \quad \text{Equation 2- 6}$$

$$M_x = \int_{\frac{-t}{2}}^{\frac{t}{2}} z\delta_x\left(1 + \frac{z}{r_y}\right)dz \quad \text{Equation 2- 7}$$

$$M_y = \int_{\frac{-t}{2}}^{\frac{t}{2}} z\delta_y\left(1 + \frac{z}{r_x}\right)dz \quad \text{Equation 2- 8}$$

$$M_{xy} = -\int_{\frac{-t}{2}}^{\frac{t}{2}} z\delta_{xy}\left(1 + \frac{z}{r_y}\right)dz \quad \text{Equation 2- 9}$$

$$M_{yx} = \int_{\frac{-t}{2}}^{\frac{t}{2}} z\delta_{yx}\left(1 + \frac{z}{r_x}\right)dz \quad \text{Equation 2- 10}$$

where:

N_x	is internal hoop force in the x direction
N_y	is internal meridional force in the y direction
N_{xy}, N_{yx}	is internal in-plane shear forces
$\mathbf{Q_x}$, $\mathbf{Q_y}$	is internal out of plane shear forces
$\mathbf{M_x}$, $\mathbf{M_y}$	is internal bending moment forces
M_{xy}, M_{yx}	is internal twisting moment forces
$\delta_x, \delta_y, \delta_z$	is normal stresses
$\delta_{xy}, \delta_{yx}, \delta_{xz}$	is shear stresses
t	is shell thickness
r_x, r_y	is principal radii of curvature

The internal forces at each point of the shell may be placed in two groups of force fields: membrane forces (which lie inside the mid- surface of the shell); bending forces (which cause bending and twisting of the shell cross – sections). [9]

2.4 Shell Theories

The factors influencing the assumptions and domains of applications of individual shell theories have been the material type and behavior; the shell geometry; the loading conditions; the deformation ranges; the particular shell behavior desired, and the computational means. Accordingly, there are

linear and nonlinear theories, membrane and bending theories of shells. The nonlinearity can be material and / or geometrical.

Any shell theory, is, as any other theory in continuum mechanics, founded on three sets of relations (equilibrium equations, kinematic relations, and constitutive relations). To be complete, these three sets of field equations must be accompanied by the appropriate conditions of the particular shell problem.

2.4.1 The Membrane Theory

In general, the internal forces at any point of a shell, consist of ten component internal force resultants (N_x, N_y, N_{xy}, N_{yx}, M_x, M_y, M_{xy}, M_{yx}, Q_x, Q_y). These components, can be separated into two groups, entitled membrane (N_x, N_y, N_{xy}, N_{yx}) and bending (M_x, M_y, M_{xy}, M_{yx}, Q_x, Q_y) internal force field. In this terminology, M_x, M_y stands for bending moments while M_{xy}, M_{yx} represent the twisting couples. Q_x, Q_y represent the out of plane shear forces. The system is therefore statically indeterminate. As a result, deformation must be considered in order to obtain a solution. The membrane theory avoids the complexities involved with solving the statically indeterminate system by reducing the number of unknowns from ten to four (N_x, N_y, N_{xy}, $N_{yx.}$). The membrane theory accomplishes this by neglecting all normal shears, bending moments, and twisting moments in the shell. By writing the moment equation of equilibrium about the normal to the shell element (z-axis) we can conclude that $N_{xy} = N_{yx.}$. Therefore, the membrane force field will consist of the forces N_x, N_y, and $N_{xy} = N_{yx}$. This simplification of the system is based on the tendency of the shell to resist loading by means of hoop and meridional forces. [9]

a) Limitations

The validity of the results obtained by the membrane theory depend upon a number of conditions. Boundary conditions, edge constraints, concentrated load, and change in the shell geometry and/or sudden change of curvature are conditions in which the pure membrane action of shell could be disturbed. In other words, the membrane forces alone cannot satisfy the equilibrium near the region of these conditions i.e., a bending force field may develop to satisfy the specific equilibrium or deformation requirements. Therefore, the so called membrane theory would not hold throughout such shells. In these circumstances some or (all) of the bending force field components are produced near the small regions of these conditions. The range of the influence of the bending field is local and is confined to the vicinity of conditions situations. The extent of influence of bending depends on the particular shell geometry and its edge and loading conditions.

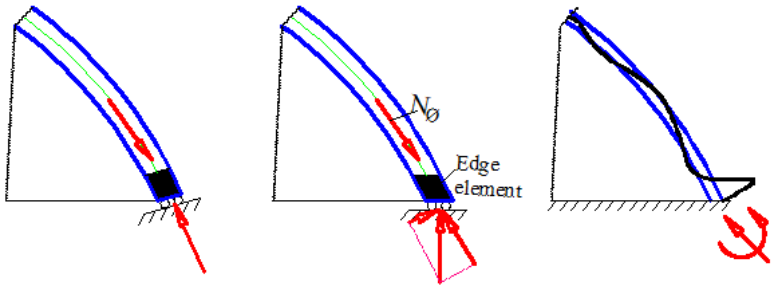

(a) membrane compatible (b)membrane incompatible (c) localized edge effects

Figure 2- 2: Membrane compatible and membrane incompatible boundary conditions in a shell

Figure (2-2) shows the shell edge with different boundary conditions. The boundary condition displayed in (a) supplies a reaction that acts only in the plane of the shell. Therefore, the support is compatible with both the membrane theory and the condition of equilibrium. The system depicted in (b) is free to translate horizontally. There is therefore a component of the reaction that acts normal to the shell surface at the edge. Yet the membrane theory neglects all forces that act out of plane, so the element is out of equilibrium. Also, the fixed boundary condition of the system in (c), is incompatible with the requirement of a pure membrane field.

The geometrical discontinuity (sudden change of curvature) and loading (concentrated load) would disturb the membrane mode of shell behavior.

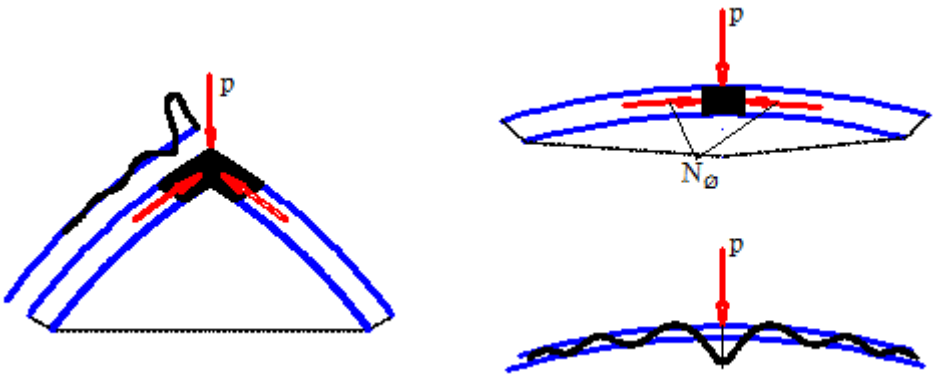

(a) geometric discontinuity (b) concentrated load

Figure 2- 3: Geometrical and loading discontinuities in shells

In the boundary conditions of (a) the membrane forces alone cannot satisfy the equilibrium near the region of the apex. The system in (b) cannot resist the load without bending because the meridional forces of the infinitesimally small at the apex have no vertical components. If, however, the size of the element taken were to be larger, a vertical reaction could be generated due to the curvature of the shell.

This implies that the loading should be distributed smoothly over the shell surface for the membrane theory to be applicable.

2.4.2 The Bending Theory

The more general and rigorous approach for solving shell problems is the so- called bending theory, also referred to as the shallow-shell theory as it is often called, and it considers the effect of the longitudinal moment and transverse shear.

The bending theory is based on two assumptions; these are:

1) The shell is so flat that the out of plane translational displacement w are much greater than the in-plane ones, u and v.
2) The shell is steep enough so that in plane stress resultants N_x, N_y, and Nxy contribute to resisting the loads that do the out of plane stress resultants Q_x and Q_y.

Both the membrane theory and the bending theory are very important and widely applicable to solving various kind of thin shell structures. The edge-load solution (bending solution), together with the membrane solution, will yield the complete solution of a shell problem.

For solving shell problems, therefore, the general procedure will be to obtain the membrane forces under a given loading, and then superimpose on these the bending theory solution for edge loads. The edge loads are determined so that the membrane and edge-load solution together satisfy the boundary conditions; i.e., the edge loads are obtained by solving equations of compatibility at the boundaries.

CHAPTER 3 SPHERICAL CONCRETE SHELL

Spherical concrete shells are shells of revolution generated by rotating a plane curve, called the meridional curve, through 360^0 about a straight line, called the axis of revolution in the plane of the curve. The axis of revolution, does not always have to intersect the meridional curve. They can be low rise and high-rise type depending on the rise and span of the shell. Spherical concrete shells mostly used for churches dome, mosques dome, silos, pressure vessels, cooling towers and water tanks.

3.1 Membrane Analysis of Spherical Concrete Shell

3.1.1 Membrane Analysis of Axisymmetric Loading

Consider an element shown in figure (3-1) taken out from the spherical concrete shell by two pairs of infinitesimally adjacent sections. The first pair of sections are meridians while the second pair contain the normal at the corner points. Since these two intersections are principal sections, they are mutually orthogonal to each other.

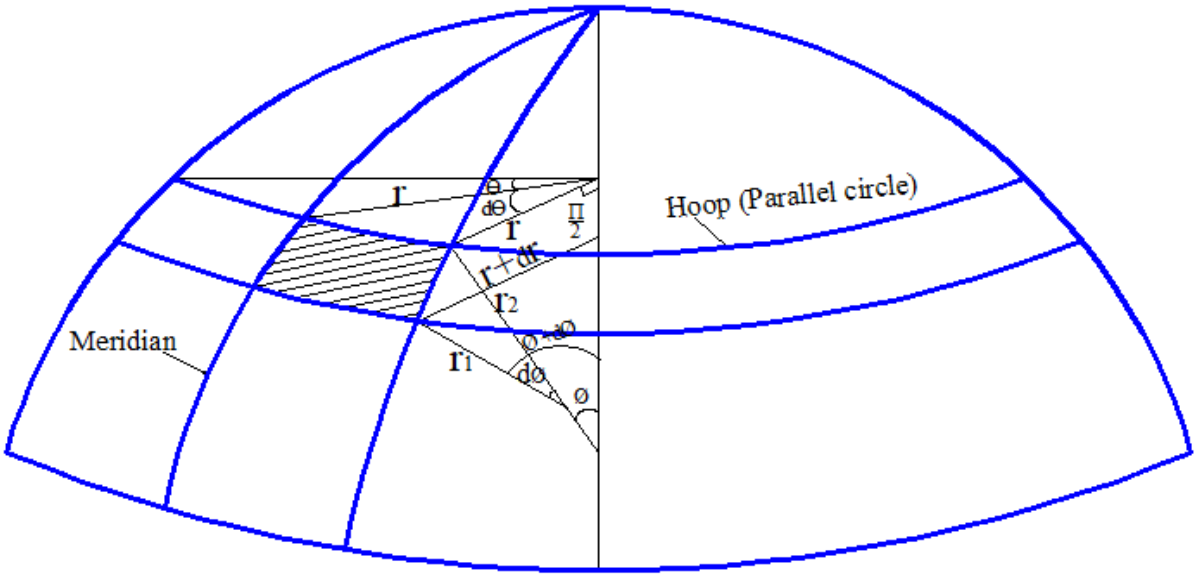

Figure 3- 1: An infinitesimal element of a spherical concrete shell surface

In the membrane analysis, we take that the bending forces M_Θ, M_Φ, $M_{\Theta\Phi}$, $M_{\Phi\Theta}$, Q_Θ, and Q_Φ are zero. Thus, there will be only three unknowns in plane stress resultants $N_{\Phi,}\ N_{\theta,}\ and\ N_{\Phi\theta} = N_{\theta\Phi}$. Three equations of equilibrium may be written in the directions of the meridian tangent, the tangent to the circles of latitude, and the normal to the element directed in ward. The external forces $P_{\Phi,}\ P_{\theta,}\ and\ P_r$ per unit area of the element act along these directions.

Geometrically complete spherical concrete shell has axisymmetric behavior. Axisymmetric behavior is independent of the variable Θ. The loading, internal forces, and deformations can vary in the Φ directions. For axisymmetric loading of spherical concrete shell, the membrane shear force $N_{\Phi\Theta}$ is zero throughout and the internal force field consist of meridional N_Φ and hoop forces N_θ only; and the direction of principal stresses coincides with the meridional and hoop directions.

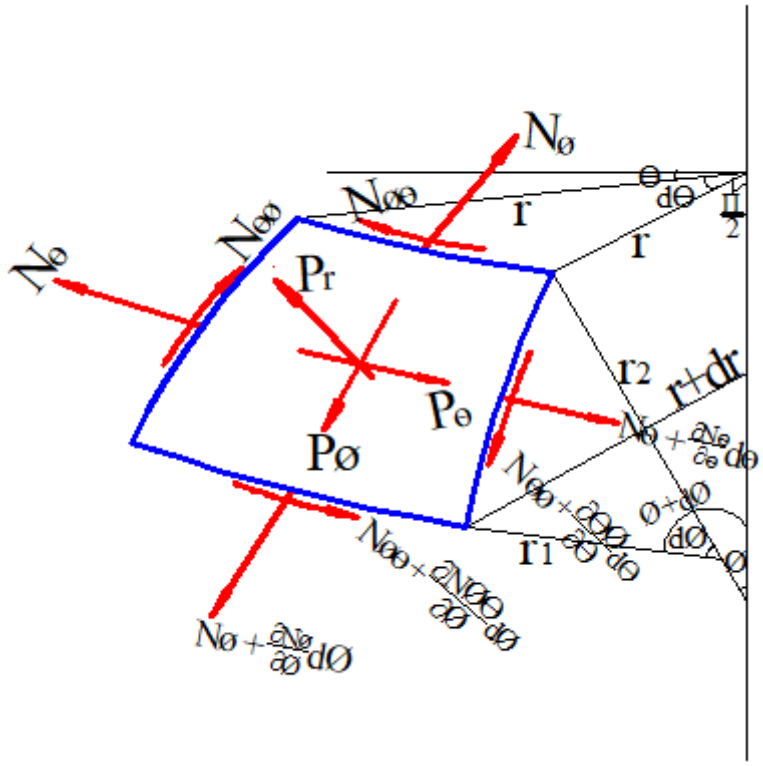

Figure 3- 2: Free body diagram of an infinitesimal element of a surface of spherical concrete shell

The above free body diagram shows the internal membrane forces and their differential variations. Because of the double curvature, the membrane forces have projections in all three directions and thus contribute to all three equilibrium equations.

The equilibrium equation in the hoop direction i.e., the summation of forces in the direction of parallel circles is:

$$\frac{\partial}{\partial \Phi}(\boldsymbol{rN_\Phi}) + \boldsymbol{r_1}\frac{\partial \boldsymbol{N_{\theta\Phi}}}{\partial \boldsymbol{\theta}} - \boldsymbol{r_1 N_\theta cos}\Phi + \boldsymbol{P}_\Phi \boldsymbol{r r_1} = \boldsymbol{0} \quad \text{..... Equation 3- 1}$$

where:

N_Φ is internal membrane meridional force in the meridional direction

N_θ is internal membrane hoop force in the circumferential direction

$N_{\theta\Phi}$ is membrane in plane shear force

r is radius of parallel circle

r_1 is radius of curvature of the meridian at any point.

P_Φ is external distributed applied load in the Φ direction

Φ is meridional angle from axis of symmetry

Equilibrium equation in the Φ direction i.e., summing forces parallel to the tangent at the meridian:

$$\frac{\partial}{\partial \Phi}(\boldsymbol{rN_{\Phi\theta}}) + \boldsymbol{r_1}\frac{\partial \boldsymbol{N_\theta}}{\partial \boldsymbol{\theta}} + \boldsymbol{r_1 N_{\theta\Phi} cos\Phi} + \boldsymbol{P_\theta r r_1} = \boldsymbol{0} \quad \text{..... Equation 3- 2}$$

where:

$N_{\Phi\theta}$ is membrane in plane shear force

r is radius of parallel circle

r_1 is radius of curvature of the meridian at any point.

P_θ is external distributed applied load in the Θ direction

Φ is meridional angle from axis of symmetry

Equilibrium equation in the r direction:

$$\frac{\boldsymbol{N_\Phi}}{\boldsymbol{r_1}} + \frac{\boldsymbol{N_\theta}}{\boldsymbol{r_2}} = \boldsymbol{P_r} \quad \text{..... Equation 3- 3}$$

where:

N_Φ is internal membrane meridional force in the meridional direction

N_θ is internal membrane hoop force in the circumferential direction

r_1 is radius of curvature of the meridian at any point.

r_2 is radius of curvature of the surface from the axis of revolution

P_r is external distributed applied load in the r direction

Φ is meridional angle from axis of symmetry

By setting all derivatives of equations (3-1), (3-2), and (3-3) equal to zero and for axisymmetric loaded spherical concrete shell $P_\theta = 0$, and integrating the combined equilibrium equation we obtain:

$$N_\Phi = \frac{1}{r_2 sin^2\Phi} - [\{\int r_1 r_2 (P_r cos\Phi - P_\Phi sin\Phi) sin\Phi d\Phi\} + c] \quad \text{.....Equation 3- 4}$$

Intersect the shell with a plane section normal to the axis of revolution at a point having an arbitrary normal angle Φ which shows the resultant of applied axisymmetric loading R as shown in figure (3-3). Figure (3-4) shows a sector of the shell lying above this plane section; it also shows the effect of the lower part on this piece, which consists of the internal meridional force uniformly distributed at the base of this sector.

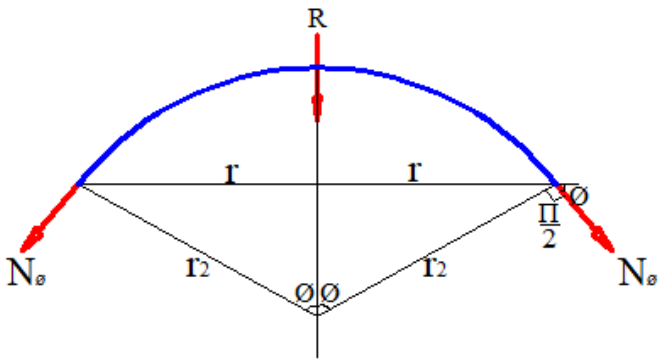

Figure 3- 3: A sector of a shell showing the resultant of axisymmetric applied loads and the reactive membrane forces

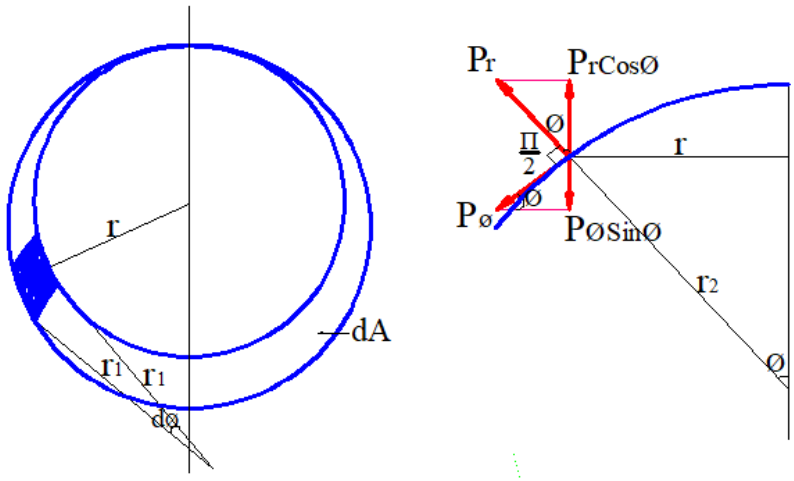

(a) (b)

Figure 3- 4: (a) ring section of the shell, (b) resultant of forces on an infinitesimal element

From figure (3-4) obseving that r = $r_2 sin\Phi$ ***and ring width is*** $r_1 d\Phi$.

An elemental area of the shell is

$dA = 2\pi r \boldsymbol{r_1 d\Phi = 2\pi r_1 r_2 sin\Phi d\Phi}$ ……..…… Equation 3- 5

We can verify that the differential of the applied forces projected in the direction of the shell axis of revolution has the value:

$dR = (\boldsymbol{P_r cos\Phi - P_\Phi sin\Phi})(\boldsymbol{2\pi r_1 r_2 sin\Phi d\Phi})$ ……..……..… Equation 3- 6

The integral of (3-4) is the resultant of applied loads R projected along the shell axis of revolution. We also note that the quantity $2\pi N_\Phi(r_2 \sin^2\Phi)$ is the sum of reactive forces projected along that axis. The constant c is the sum of applied concentrated forces, if any, along the shell axis of revolution. For shells of revolution with symmetric load conditions, c is zero. Therefore, the relation (3-4) is the equation of equilibrium for the global shell sector shown in figure (3-3).

This procedure, called the method of sections, gives the membrane force field in the form:

$$\boldsymbol{N_\Phi = -\frac{R}{2\pi r_2 sin^2\Phi}}$$ ……..…… Equation 3- 7

$$\boldsymbol{N_\theta = \frac{R}{2\pi r_1 sin^2\Phi} + P_r r_2}$$……..……..…..... Equation 3- 8

where:

N_Φ is internal membrane meridional force in the meridional direction

N_θ is internal membrane hoop force in the circumferential direction

R is resultant of applied loads projected along the shell axis of revolution

r_1 is radius of curvature of the meridian at any point.

r_2 is radius of curvature of the surface from the axis of revolution

P_r is external distributed applied load in the r direction

Φ is meridional angle from axis of symmetry

a) Membrane Forces Under Own Weight

In membrane analysis, own weight g is taken as acting along the curved length of the shell. Thus for a spherical concrete shell of radius a = $r_1 = r_2$ acted upon by its own dead load g the integral of (3-4) is the resultant R of applied loads projected along the shell axis of revolution. [9]

$R = 2\pi\int_0^{\Phi} a^2 \boldsymbol{g sin}\Phi d\Phi = 2\pi \boldsymbol{a^2 g}(1 - \cos\Phi)$ …… Equation 3- 9

where:

R is resultant of applied loads projected along the shell axis of revolution

a is radius of spherical shell

g is dead load of spherical shell

Φ is meridional angle from axis of symmetry

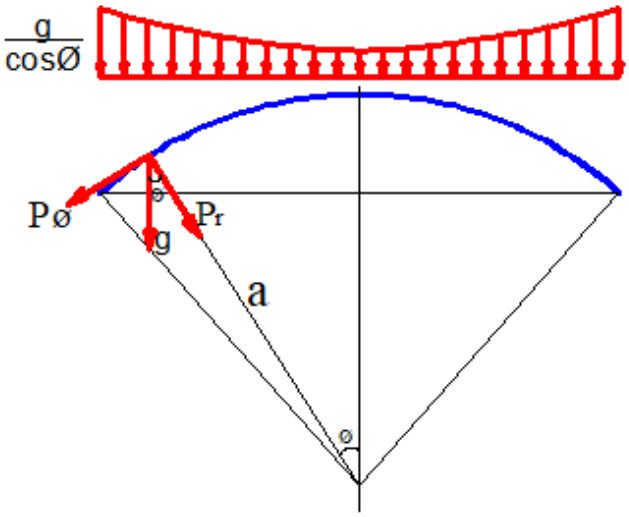

Figure 3- 5: Spherical dome under dead load

From figure (3-5) the load components can be determined as $\boldsymbol{P}_{\Phi} = g\sin\Phi$, $\boldsymbol{P}_{\boldsymbol{r}} = -g\cos\Phi$
The relations (3-7) and (3-8) give the membrane internal forces per unit length:

$$\boldsymbol{N}_{\Phi} = -\boldsymbol{ag}\left(\frac{\boldsymbol{1}}{\boldsymbol{1+cos}\Phi}\right)$$ …….....…… Equation 3- 10

$$\boldsymbol{N}_{\boldsymbol{\theta}} = \boldsymbol{ag}\left(\frac{\boldsymbol{1}}{\boldsymbol{1+cos}\Phi} - \boldsymbol{cos}\Phi\right)$$……..……..…… Equation 3- 11

where:

N_{Φ} is internal membrane meridional force in the meridional direction

N_{θ} is internal membrane hoop force in the circumferential direction

a is radius of spherical shell

g is dead load of spherical shell

Φ is meridional angle from axis of symmetry

Θ is circumferential angle

It is interesting to note that the expression (3-10) always yields negative values for N_Φ throughout the shell. Hence, the membrane meridional force N_Φ in a dome under its own weight is always compressive. Secondly at Φ = 0, both N_Φ and N_θ are equal to –ga/2. Further, the hoop force is compressive at the top, but changes sign somewhere along the meridian and becomes tensile in the lower part of the shell, i.e., the hoop forces N_θ from Φ = 0 are compression till Φ = 51^0 50'. At Φ = 51^0 50' N_θ become zero, then N_θ become tension after Φ = 51^0 50 till Φ = 90^0 .

b) Membrane Forces under Live Load

Live load P is taken as acting on the horizontal projection (plan area) only. Let the intensity of the live load be P over the horizontal projection of the spherical concrete shell surface figure (3-6). The total vertical load up to the circle of hoop corresponding to Φ = Pπa^{2}sin^{2}Φ. Making use of equation (3-7),

$$N_\Phi = -\frac{P\pi a^2 sin^2\Phi}{2\pi r_2 sin^2\Phi} = -\frac{p\,a}{2} \quad \text{..... Equation 3- 12}$$

where:

N_Φ is internal membrane meridional force in the meridional direction

a is radius of spherical shell

p is live load of spherical shell

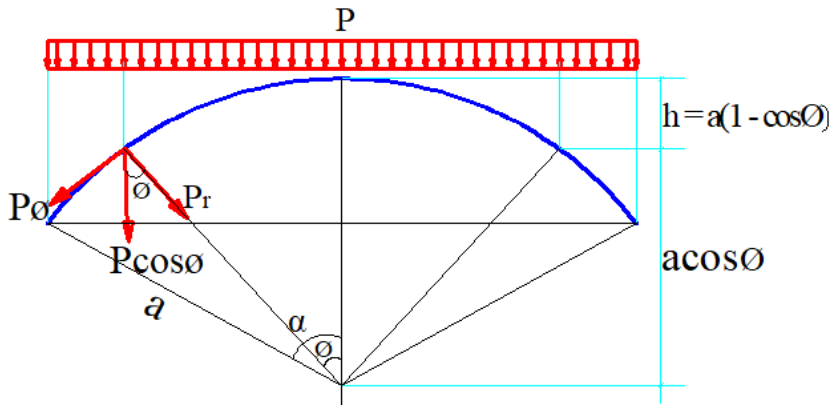

Figure 3- 6: Spherical concrete shell subjected to live load

From figure (3-6) the load components (decomposition) of the live load are $\boldsymbol{P_\Phi}$= pcosΦsinΦ, $\boldsymbol{P_r}$= - pcos^{2}Φ

From relation (3.3) and $\boldsymbol{P_r}$= - pcos^{2}Φ,

$$\boldsymbol{N_\theta = -\frac{p\,a}{2}cos2\Phi}$$ …… **Equation 3- 13**

where:

$\boldsymbol{N_\theta}$ is internal membrane hoop force in the circumferential direction

a is radius of spherical shell

$\boldsymbol{p}$ is live load of spherical shell

Φ is meridional angle from axis of symmetry

It is clear that for Φ > 45^0, N_θ will turn out to be tensile.

3.1.2 Membrane Analysis of Non-axisymmetric Loading

a) Membrane Forces under Wind Load

Spherical shells can be subjected to non-axisymmetric loading such as wind forces, and earthquake effects. Using the membrane theory, we can solve for wind loading by assuming the pressure to be made up of harmonic components. For a simple model wind forces acting on the shells of spherical concrete shell as shown in figure (3-8), the assumed wind load components (distributions) are $P_\Phi = 0$, $P_\theta = 0$, $P_r = -Psin\Phi cos\theta$. [3]

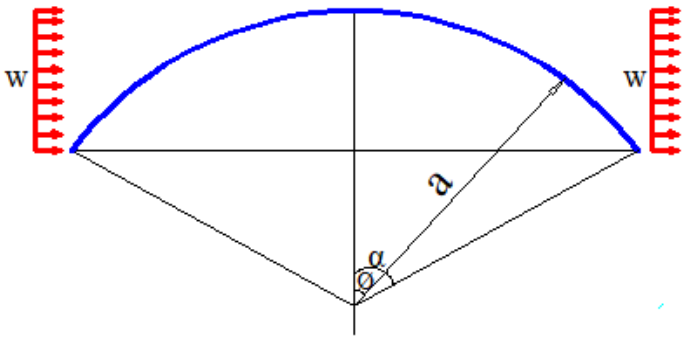

Figure 3- 7: Spherical concrete shell subjected to wind load sectional view

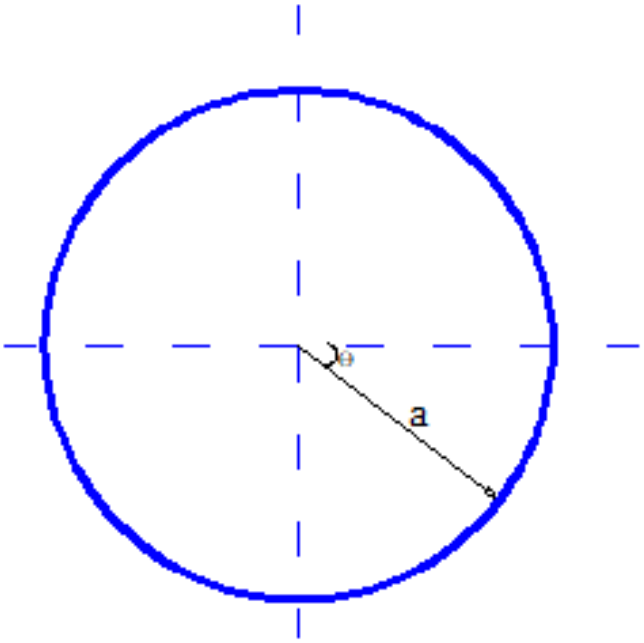

Figure 3- 8: Spherical concrete shell subjected to wind load plan view

To perform a membrane analysis of spherical shells under wind loading, we must use all three coupled simultaneous partial differential equations (3-1), (3-2), and (3-3). After some algebraic manipulations: [9]

$$N_{\Phi} = \frac{-w_e a}{3}\frac{(2+cos\Phi)(1-cos\Phi)cos\Phi}{(1+c0s\Phi)sin\Phi}cos\theta \quad \text{Equation 3- 14}$$

$$N_{\theta} = \frac{-w_e a}{3}\frac{(3+4cos\Phi+2cos^2\Phi)(1-cos\Phi)}{(1+c0s\Phi)sin\Phi}cos\theta \quad \text{Equation 3- 15}$$

where:

N_{Φ} is internal membrane meridional force in the meridional direction

N_{θ} is internal membrane hoop force in the circumferential direction

w_e is the external applied wind load on the spherical shell

a is radius of spherical shell

p is live load of spherical shell per unit area

Φ is the meridional angle

Θ is the wind blowing hoop angle

Because of the loading (wind load) is not symmetric there is a nonzero membrane shear force, $N_{\Phi\theta}$. But this research is limited to only meridional and hoop forces responses.

3.2 Displacements of Axisymmetric Shells

A spherical shell generally has meridional, hoop, and normal displacement vector components. The hoop component of the displacement vector is zero for symmetrical loading. For axisymmetric spherical shell there are only the displacement components along the meridional and normal to the shell.

Consider an infinitesimal element, AB taken from the meridional section of the shell. This element is deformed into A'B', as shown in the figure (3-9). The positive meridional displacement, v, is taken in the direction of increasing Φ, the positive normal displacement, w, is taken inwards.

The change of length of element AB is composed of two parts: one part arises from the meridional differential displacement, (dv/dΦ)dΦ; the other from the normal displacement, (w)dΦ.

The meridional strain is obtained by dividing the above change of length to the undeformed length of the element ($r_1 d\Phi$). So, the expression for the meridional strain is

$$\boldsymbol{\varepsilon_{\Phi}} = \frac{\mathbf{1}}{\boldsymbol{r_1}}\frac{\boldsymbol{dv}}{\boldsymbol{d\Phi}} - \frac{\boldsymbol{w}}{\boldsymbol{r_1}} \quad \text{..... Equation 3- 16}$$

where:

$\boldsymbol{\varepsilon_{\Phi}}$ is meridional strain

v is meridional displacement

w is displacement normal to the meridional curve

Φ is meridional angle from axis of symmetry

r_1 is radius of curvature of the meridian at any point.

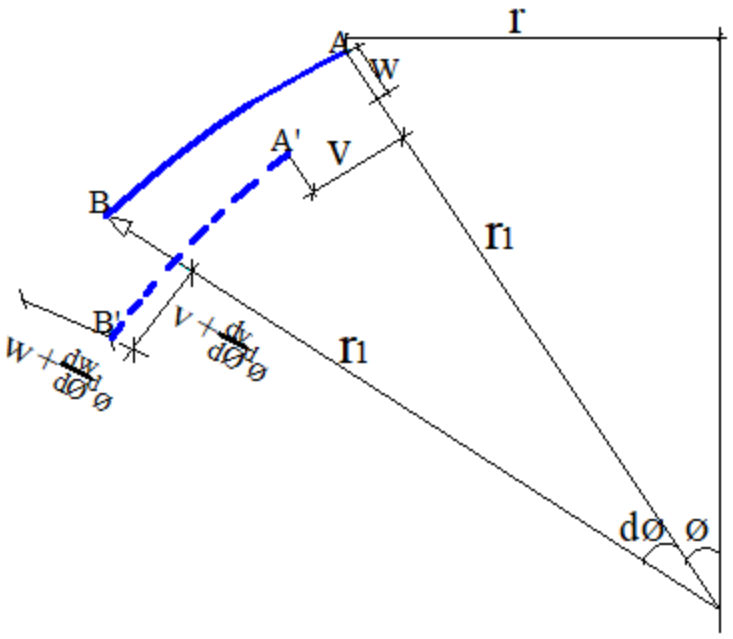

Figure 3- 9: A meridional element of the shell and its symmetrically deformed configuration

To determine the hoop strain, we consider a hoop element of the shell. Figure (3-10) shows the change of radius, Δr, of the parallel circle passing through this element. Referring to this figure, the expression for the change of radius is

$\Delta r = v\cos\Phi - w\sin\Phi$ …….…… Equation 3- 17

where:

Δr is change of radius of parallel circle

v is meridional displacement

Φ is meridional angle from axis of symmetry

w is displacement normal to the meridional curve

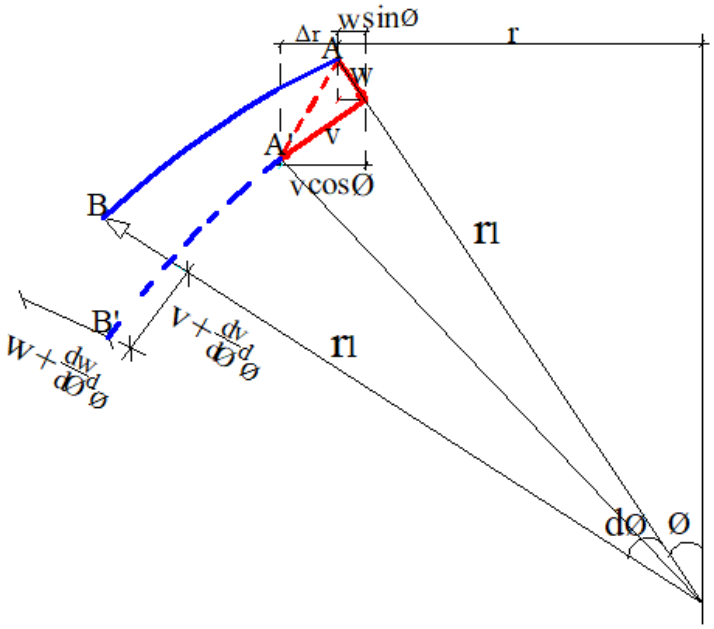

Figure 3- 10: Shell displacement components leading to the change of radius of a typical parallel circle:

Since the circumferential length change is proportional to the change in the radius, so the hoop strain is

$\boldsymbol{\varepsilon_\theta = \frac{1}{r}}$ **(vcosΦ – wsinΦ)…….....…… Equation 3- 18**

Since r = $r_2 sin\Phi$

$$\boldsymbol{\varepsilon_\theta = \frac{v}{r_2}\cot\Phi - \frac{w}{r_2}}$$ **……..……...… Equation 3- 19**

where:

ε_θ is hoop strain

v is meridional displacement

Φ is meridional angle from axis of symmetry

r_2 is radius of curvature of the surface from the axis of revolution

Expressions (3-16) and (3-18) constitute the strain-displacement relations of a rotational shell undergoing axisymmetric deformations. If we eliminate the normal displacement function, w, between these relations, we obtain the following differential equation for the meridional displacement components v.

$$\boldsymbol{\frac{dv}{d\Phi} - v\cot\Phi = r_1\varepsilon_\Phi - r_2\varepsilon_\theta}$$ …….…..…..…… Equation 3- 20

Having obtained the kinematic relations and equilibrium equations we now write down the third group of governing relations, i.e., the constitutive relations. If the shell is linearly elastic and isotropic, the two-dimensional elastic constitutive relations, for a local state of plane stress are:

$$\boldsymbol{\varepsilon}_{\Phi} = \frac{\mathbf{1}}{\boldsymbol{Et}} (\boldsymbol{N}_{\Phi} - \boldsymbol{\upsilon N_{\theta}}) \quad \text{..... Equation 3- 21}$$

$$\boldsymbol{\varepsilon_{\theta}} = \frac{\mathbf{1}}{\boldsymbol{Et}} (\boldsymbol{N_{\theta}} - \boldsymbol{\upsilon N}_{\Phi}) \quad \text{..... Equation 3- 22}$$

Substituting these relations into (3-20) we obtain the membrane rotation of meridional curve at the edge of the shell, $\Delta\alpha$

$$\frac{\boldsymbol{dv}}{\boldsymbol{d}\Phi} - \boldsymbol{v}\boldsymbol{cot}\Phi = \frac{\mathbf{1}}{\boldsymbol{Et}} [\boldsymbol{N}_{\Phi}(\boldsymbol{r_1} + \boldsymbol{\upsilon r_2}) - \boldsymbol{N_{\theta}}(\boldsymbol{r_2} + \boldsymbol{\upsilon r_1})] \text{..... Equation 3- 23}$$

The horizontal displacement, i.e., the change in radius of the parallel circle is

$$\delta = \boldsymbol{r_2}\ \sin\alpha\boldsymbol{\varepsilon_{\theta}} = \frac{\boldsymbol{r_2 sin}\Phi}{\boldsymbol{Et}} (\boldsymbol{N_{\theta}} - \boldsymbol{\upsilon N}_{\Phi}) \quad \text{..... Equation 3- 24}$$

The general solution to the above equation (3-20), obtained by direct integration, is

$$\boldsymbol{v} = \sin\Phi \left[\int \frac{\frac{\mathbf{1}}{\boldsymbol{Et}}[N_{\Phi}(r_1 + \upsilon r_2) - N_{\theta}(r_2 + \upsilon r_1)]}{\boldsymbol{sin}\Phi} \boldsymbol{d}\Phi + \boldsymbol{c}\right] \text{..... Equation 3- 25}$$

where:

υ is meridional displacement

Φ is meridional angle from axis of symmetry

N_{Φ} is internal membrane meridional force in the meridional direction

N_{θ} is internal membrane hoop force in the circumferential direction

r_1 is radius of curvature of the meridian at any point.

r_2 is radius of curvature of the surface from the axis of revolution

υ is Poisson's ratio

c is constant of integration

Here the constant c is determined from the boundary conditions. When the displacement v is calculated, w is found from their relations. [9]

3.3 Membrane Deformation of Spherical Concrete Shell

Consider a spherical shell subjected to its own weight, g. To determine deformations field in this shell by substituting membrane forces obtained in relation (3.10) and (3.11), and noting that $r_1 = r_2 =$ a into (3-24).

$$\boldsymbol{v} = \frac{\mathbf{a^2}\boldsymbol{g}(\mathbf{1}+\boldsymbol{v})}{\boldsymbol{Et}}\boldsymbol{sin}\Phi\left[\mathbf{ln}(\mathbf{1}+\boldsymbol{cos}\Phi) - \frac{\mathbf{1}}{\mathbf{1}+\boldsymbol{cos}\Phi}\right] + \boldsymbol{csin}\Phi \text{.....Equation 3- 26}$$

where:

v is meridional displacement

a is radius of spherical shell

g is dead load of spherical shell

υ is Poisson's ratio

E is concrete modulus of elasticity

t is shell thickness

Φ is meridional angle from axis of symmetry

c is constant of integration

At the lower edge of the shell i.e., at $\Phi = \alpha$, we have v = 0, so that

$$\text{c} = \frac{\mathbf{a^2}\boldsymbol{g}(\mathbf{1}+\boldsymbol{v})}{\boldsymbol{Et}}\left[\frac{\mathbf{1}}{\mathbf{1}+\boldsymbol{cos\alpha}} - \mathbf{ln}(\mathbf{1}+\boldsymbol{cos\alpha})\right] \text{..... Equation 3- 27}$$

where:

c is constant of integration

a is radius of spherical shell

g is dead load of spherical shell

υ is Poisson's ratio

E is concrete modulus of elasticity

t is shell thickness

α is half central angle

With v(Φ) determined, we can find w(Φ) from the relation (3-19)

$$w = \frac{-a^2 g}{Et}\left(\frac{1}{1+\cos\Phi} - \cos\Phi\right) + \frac{a^2 g(1+\upsilon)}{Et}\cos\Phi\left[\ln(1+\cos\Phi) - \frac{1}{1+\cos\Phi}\right] + c\cos\Phi$$ ... Equation 3- 28

where:

w is displacement normal to the meridional curve

a is radius of spherical shell

g is dead load of spherical shell

υ is Poisson's ratio

E is concrete modulus of elasticity

t is shell thickness

Φ is meridional angle from axis of symmetry

c is constant of integration

3.3.1 Membrane Analysis of Dome-Ring Interaction

Figure (3-11a) shows the membrane field of dome-ring interaction of spherical shell. The membrane deformations caused by these sorts of interaction and the adopted sign convention are shown in figures (3-11b) and (3-11c), respectively.

The meridional force N_α has horizontal, H_o and vertical, V_o components at the base of the shell.

$$H_o = N_\alpha \cos\alpha \quad and \quad V_o = N_\alpha \sin\alpha$$ .....Equation 3- 29

where:

H_o is meridional force horizontal component at the base of the shell

N_α is meridional force at the base of the shell

α is half central angle

V_o is meridional force vertical component at the base of the shell

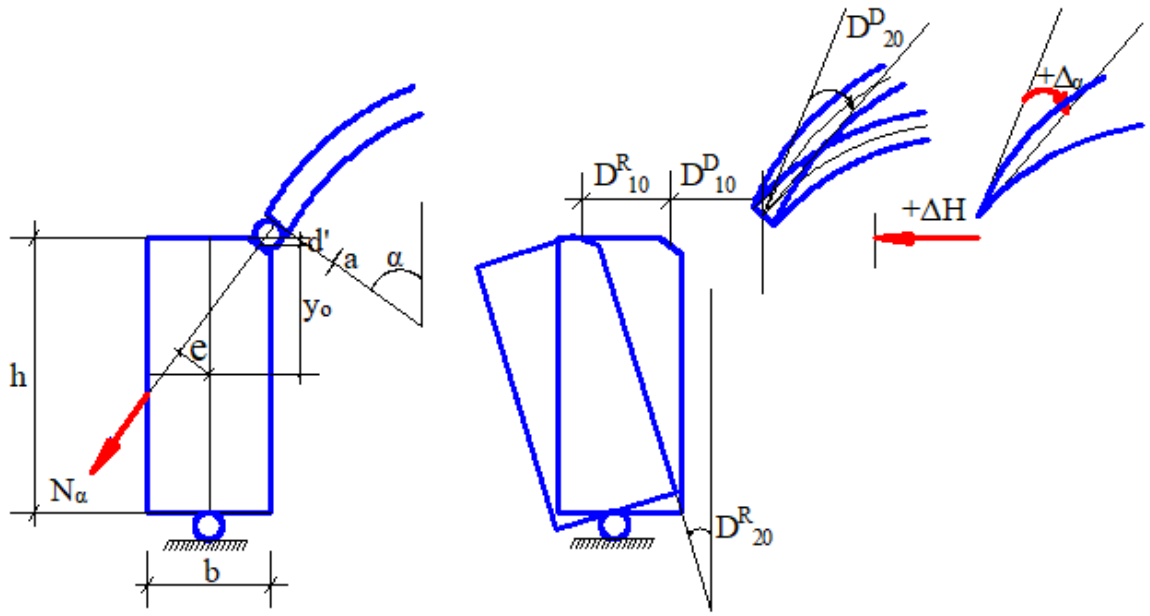

(a) (b) (c)

Figure 3- 11: Membrane dome-ring interaction, (a) membrane meridional force, (b) membrane ring deformation (c) Membrane dome deformations.

The vertical component is absorbed by the vertical support while the horizontal component is taken by the ring and it will be acted as radial force on the ring. Again the meridional force N_α acts on the ring section with an eccentricity, e. thus an eccentric meridional force induced torsional couple M_α on the ring.In general the ring is subjected to a uniformly distributed radial force, H and a uniformly distributed twisting couple M_α due to eccentric meridional force at the base of the shell. Figure (3-12) shows the free-body diagram of this ring segment.

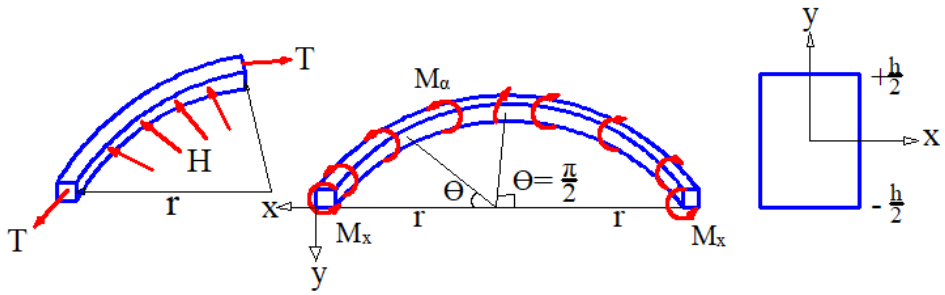

(a) (b) (c)

Figure 3- 12: Free body diagram of ring segment under radial force and twisting couple

Figure (3-12a) the change of radius of this ring due to a radial force is:

$$\mathbf{\Delta H} = -\frac{Hr}{EA_R}.\boldsymbol{r} = -\frac{r^2}{EA_R}\boldsymbol{H} \quad \text{Equation 3- 30}$$

where:

ΔH is ring beam change of radius due to radial force

r is spherical shell internal radius

H is uniformly distributed radial force/ edge shear force

E is concrete modulus of elasticity

A_R is rectangular ring beam cross sectional area

And the corresponding change of ring radius due to twisting couple is:

$$\mathbf{\Delta H^*} = -\frac{r^2 y}{EI_R}\boldsymbol{M_\alpha} \quad \text{Equation 3- 31}$$

where:

ΔH^* is change of ring radius due to twisting couple

r is spherical shell internal radius

y is height of ring section above the neutral axis

M_α is uniformly distributed twisting couples/edge moment

E is concrete modulus of elasticity

I_R is second moment of area of ring beam

Due to difference in the radius change, each section of the ring would undergo the following torsional rotation:

$$\boldsymbol{\Delta_\alpha = \frac{|\Delta H|^*}{y} = \frac{r^2}{EI_R} M_\alpha}$$ .....Equation 3- 32

where:

Δ_α is ring beam torsional rotation

r is spherical shell internal radius

M_α is uniformly distributed twisting couples/edge moment

E is concrete modulus of elasticity

I_R is second moment of area of ring beam

Therefore, the total radial displacement of the ring due to horizontal component of meridional force at the base of the shell, $H_O = N_\alpha cos\alpha$ and torsional couple, $M_{O\alpha} = N_\alpha e$ of a spherical shell subjected to its own weight, g with the rectangular ring cross sectional area $A_R =$ b x h, radius$r_1 = r_2 =$ a, and $N_\alpha = -\frac{ag}{1+cos\alpha}$ are:

i) Ring

By combining (3-30) and (3-31):

$$\boldsymbol{D^R{}_{10} = \frac{r^2}{EA_R} N_\alpha cos\alpha + \frac{r^2 y_o}{EI_R} N_\alpha e = (cos\alpha + \frac{12 y_o e}{h^2}) \frac{r^2}{Ebh} (\frac{ag}{1+cos\alpha})}$$ ..... Equation 3-

where:

$D^R{}_{10}$ is ring beam membrane radial displacement

α is half central angle

y_o is distance from dome-ring interaction center to half of ring beam height

e is perpendicular distance from the projection of dome thickness center to geometric center of ring beam

r is spherical shell internal radius

E is concrete modulus of elasticity

b is ring beam width

h is ring beam height

a is radius of spherical shell

g is dead load of spherical shell

And from (3-32):

$$\boldsymbol{D^R_{20}} = \frac{r^2}{EI_R}\boldsymbol{N_\alpha e} = -\frac{12r^2e}{Ebh^3}\left(\frac{ag}{1+cos\alpha}\right) \quad \text{Equation 3- 33}$$

where:

D^R_{20} is ring beam membrane radial rotation

r is spherical shell internal radius

e is perpendicular distance from the projection of dome thickness center to geometric center of ring beam

α is half central angle

E is concrete modulus of elasticity

b is ring beam width

h is ring beam height

a is radius of spherical shell

g is dead load of spherical shell

i.) Dome

The expression for the membrane horizontal displacement of the edge parallel circle, ΔH and the membrane rotation of meridional curve at the edge of the shell, Δα, from equations (3-23) and (3-24) are:

$$\boldsymbol{\Delta^D H = D^D_{10} = \frac{r_2 sin\Phi}{Et}(N_\theta - \upsilon N_\Phi)}$$ …… Equation 3- 34

$$\boldsymbol{\Delta^D_{\alpha=} D^D_{20} = \frac{1}{Et}[N_\Phi(r_1 + \upsilon r_2) - N_\theta(r_2 + \upsilon r_1)]}$$ …… Equation 3- 35

Similarly, for a spherical shell subjected to its own weight, g with radius$r_1 = r_2 =$ a and $N_\Phi = -\frac{ag}{1+cos\alpha}$, equation (3-35) and (3-36) become:

$$\boldsymbol{D^D_{10} = \frac{a^2 g}{Et}(\frac{1+\upsilon}{1+cos\Phi} - cos\Phi)sin\Phi}$$ …… Equation 3- 36

where:

D^D_{10} is dome membrane displacement

a is radius of spherical shell

g is dead load of spherical shell

υ is Poisson's ratio

E is concrete modulus of elasticity

t is shell thickness

Φ is meridional angle from axis of symmetry

$$\boldsymbol{D^D_{20} = \frac{ag}{Et}(2 + \upsilon)sin\Phi}$$ …… Equation 3- 37

where:

D^D_{20} is dome membrane rotation

a is radius of spherical shell

g is dead load of spherical shell

υ is Poisson's ratio

E is concrete modulus of elasticity

t is shell thickness

Φ is meridional angle from axis of symmetry

3.4 Bending Analysis of Axisymmetric Spherical Concrete Shell

Spherical concrete shells are provided with edge rings. Edge rings in a shell structure create some bending field in the vicinity of the ring due to the difference in stiffness between the shell and the ring. The edge ring effects in an axisymmetric spherical concrete shell consists of uniformly distributed bending moment, shear force and vertical reaction, figure (3-13)

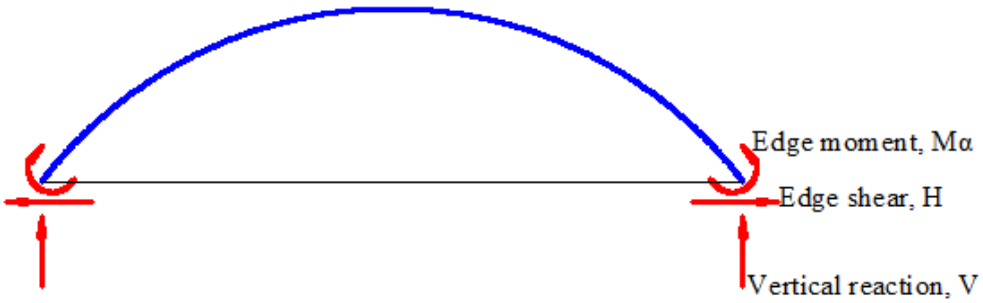

Figure 3- 13: Edge forces in an axisymmetric spherical shell

Each of these edge forces (edge shear and edge moment) produces bending field of forces and displacements in a spherical shell. The stresses due to these bending fields must be superposed on the membrane field stresses to obtain the total field of internal forces in the shell. Calculations based on more exact theories and experimental results show that the edge effects decrease as we move away from the edge.

3.4.1 Influence Coefficients for Axisymmetric Spherical Concrete Shell

a) The Dome Influence Coefficients

To determine the internal forces and displacements due to edge effects the redundant edge forces (M_α and H) should be computed from the compatibility relations of influence coefficients of bending analysis and membrane deformations.

Consider figure (3-14) in which the shell is acted upon by a uniformly distributed edge moment and edge shear separately.

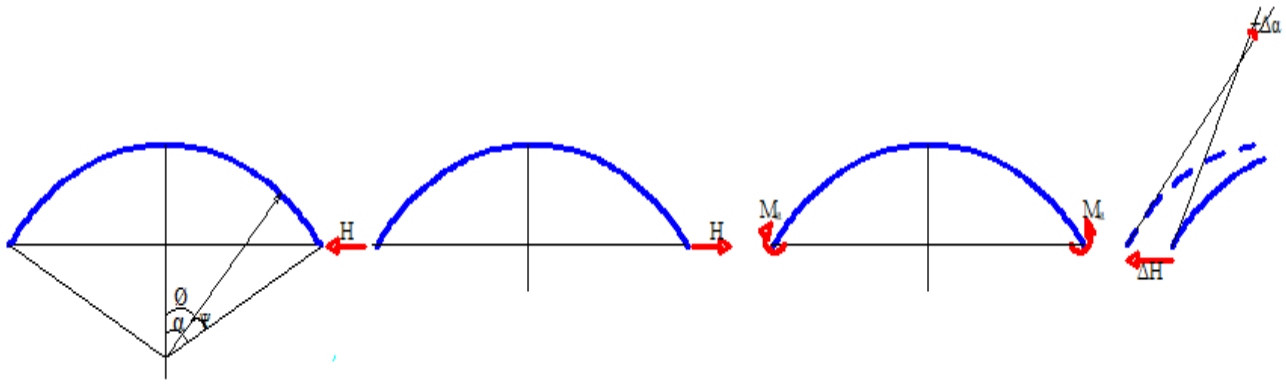

(a) shear force (b) bending moment (c) sign conventions

Figure 3- 14: Axisymmetric shell under separate application of edge forces

The expressions for internal edge forces and edge displacements due to a distributed edge moment, M_α and edge shear force, H have been derived and tabulated in table (3-1). The dome influence coefficients for bending analysis can be calculated from table (3-1). Specifically, for$M_\alpha = 1$ we shall get the bending moment flexibility influence coefficients of the dome. Again, for H = 1, these expressions give the flexibility influence coefficient of the dome due to shear force. [9]

Table 3- 1: Flexibility influence coefficient for axisymmetric shells

	H	M_α
N_Φ	$-\sqrt{2}\cot(\alpha-\psi)\,sin\alpha e^{-\lambda\psi}\sin\left(\lambda\psi-\frac{\pi}{4}\right)H$	$\frac{-2\lambda}{a}\cot(\alpha-\psi)e^{-\lambda\psi}\sin(\lambda\psi)M_\alpha$
N_θ	$-2\lambda sin\alpha e^{-\lambda\psi}\sin\left(\lambda\psi-\frac{\pi}{2}\right)H$	$\frac{-2\sqrt{2}}{a}\lambda^2 e^{-\lambda\psi}\sin(\lambda\psi-\frac{\pi}{4})M_\alpha$
M_Φ	$\frac{a}{\lambda}sin\alpha e^{-\lambda\psi}\sin(\lambda\psi)\,H$	$\sqrt{2}\,e^{-\lambda\psi}\sin(\lambda\psi+\frac{\pi}{4})M_\alpha$
ΔH	$\frac{2a\lambda sin^2\alpha}{Et}H$	$\frac{2\lambda^2 sin\alpha}{Et}M_\alpha$
Δα	$\frac{2\lambda^2 sin\alpha}{Et}H$	$\frac{4\lambda^3}{Eat}M_\alpha$

The exponential decay term $e^{-\lambda\psi}$ in the equations of table (3-1) can be physically explained as the damping in the system. The rate at which the edge effects are damped out in the system is dependent upon the damping parameter λ. The magnitude of λ is determined by the geometry and material properties of the shell as:

$$\lambda = \sqrt[4]{3\,(1-\upsilon^2)(\frac{a}{t})^2} \quad \text{..... Equation 3- 38}$$

where:

λ is damping parameter

υ is Poisson's ratio

a is radius of spherical shell

t is shell thickness

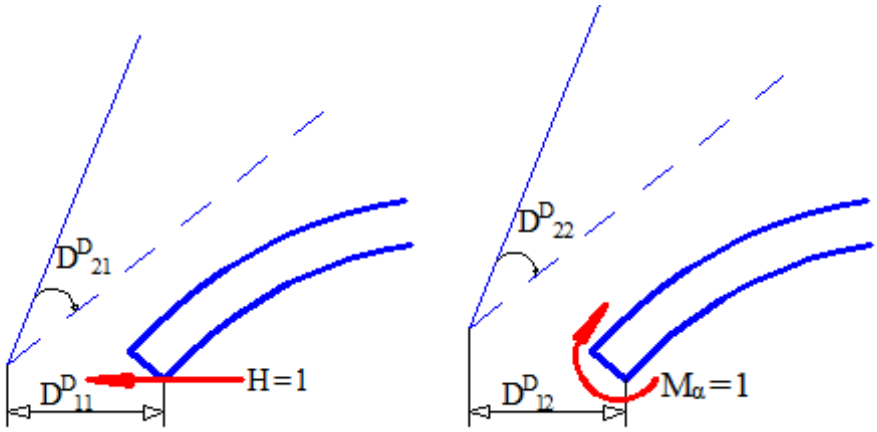

Figure 3- 15: Positive sign convention for the influence coefficients of the dome

Therefore, the flexibility influence coefficients of the dome from table (3-1) are:

$$D^D_{11} = \frac{2a\lambda sin^2\alpha}{Et} \quad \text{..... Equation 3- 39}$$

$$D^D_{12} = \frac{2\lambda^2 sin\alpha}{Et} \quad \text{..... Equation 3- 40}$$

$$D^D_{21}\frac{2\lambda^2 sin\alpha}{Et} = D^D_{12} \quad \text{..... Equation 3- 41}$$

$$D^D_{22} = \frac{4\lambda^3}{Eat} \quad \text{..... Equation 3- 42}$$

where:

D^D_{11} is dome displacement flexibility influence coefficient by edge shear

D^D_{12} is dome displacement flexibility influence coefficient by edge moment

$D^D{}_{21}$ is dome rotation flexibility influence coefficient by edge shear

$D^D{}_{22}$ is dome rotation flexibility influence coefficient by edge moment

λ is damping parameter

υ is Poisson's ratio

α is half central angle

a is radius of spherical shell

E is concrete modulus of elasticity

t is shell thickness

b) The Ring Influence Coefficients

Consider the ring subjected to edge forces H and as shown in figure (3-15). The ring deformations due to the force H, applied at y_o are:

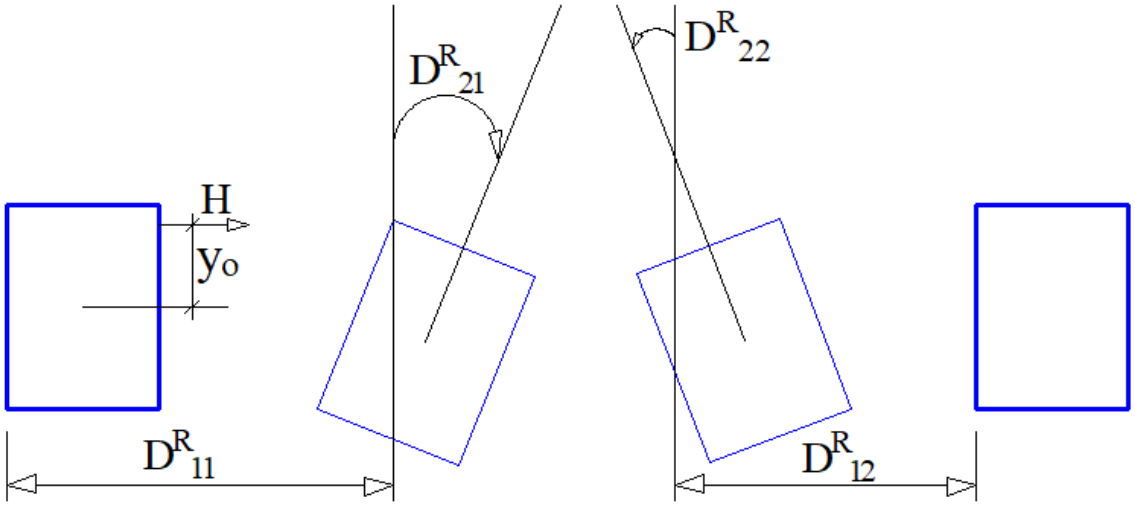

Figure 3- 16: Applied edge force to ring and positive sign conventions for the ring influence coefficients

From equation (3-30) and (3-31),

$\boldsymbol{\Delta H_1 = \frac{r^2}{EA_R} H}$ and $\boldsymbol{\Delta H_2 = \frac{r^2 Y_o^2}{EI_R} H}$ ……..... Equation 3- 43 , (e = $\boldsymbol{y_o}$)

From (3-32),

$$\boldsymbol{\Delta_{\alpha}} = -\frac{r^2 y_o}{EI_R}\boldsymbol{H} \quad \text{..... Equation 3- 44}$$

By combining ΔH_1 and ΔH_2 and putting H =1 from the above relations, the influence coefficients due to shear force become:

$$\boldsymbol{D^R_{11}} = \frac{r^2}{Ebh} + \frac{12r^2 Y_o^2}{Ebh^3} \quad \text{..... Equation 3- 45}$$

$$\boldsymbol{D^R_{21}} = -\frac{12r^2 y_o}{Ebh^3} \quad \text{..... Equation 3- 46}$$

The ring deformations due to a torsional couple M_α are:

From relation (3.31) and (3-32) for $M_\alpha = 1$ we have

$$\boldsymbol{D^R_{12}} = -\frac{12r^2 y_o}{Ebh^3} = \boldsymbol{D^R_{21}} \quad \text{..... Equation 3- 47}$$

$$\boldsymbol{D^R_{22}} = \frac{12r^2}{Ebh^3} \quad \text{..... Equation 3- 48}$$

where:

$D^R{}_{11}$ is ring displacement flexibility influence coefficient by edge shear

$D^R{}_{12}$ is ring displacement flexibility influence coefficient by edge moment

$D^R{}_{21}$ is ring rotation flexibility influence coefficient by edge shear

$D^R{}_{22}$ is ring rotation flexibility influence coefficient by edge moment

E is concrete modulus of elasticity

b is ring beam width

h is ring beam height

y_o is distance from dome-ring interaction center to half of ring beam height

r is spherical shell internal radius

To determine the influence coefficients for the dome-ring system, the influence coefficients of the dome and the ring should be combined. Therefore, the system influence coefficients are:

$$\boldsymbol{D_{11} = D^{D}_{11} + D^{R}_{11}}$$ …….…….. Equation 3- 49

$$\boldsymbol{D_{12} = D^{D}_{12} + D^{R}_{12} = D_{21}}$$ ……..….. Equation 3- 50

$$\boldsymbol{D_{22} = D^{D}_{22} + D^{R}_{22}}$$ ……..…...… Equation 3- 51

where:

D_{11} is dome-ring system displacement flexibility influence coefficient by edge shear

D_{12} is dome-ring system displacement flexibility influence coefficient by edge moment

D_{21} is dome-ring system rotation flexibility influence coefficient by edge shear

D_{22} is dome-ring system rotation flexibility influence coefficient by edge moment

The numerical values of the parameters in the dome-ring system are shown in figure (3-17)

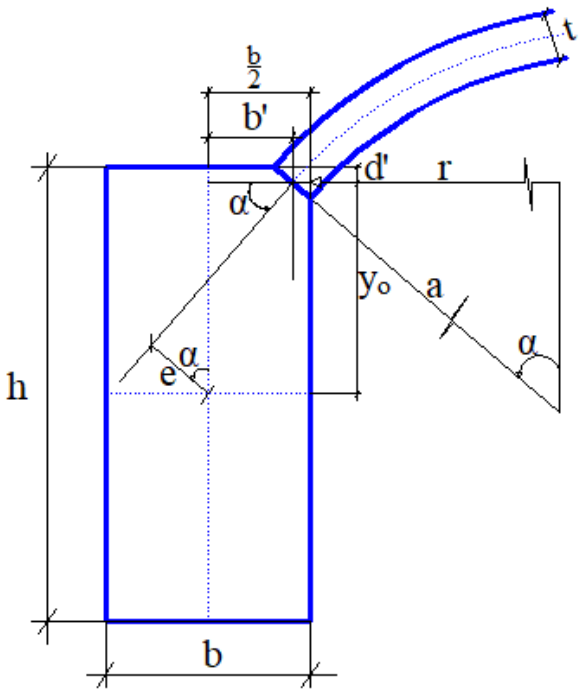

Figure 3- 17: Spherical concrete dome with a ring

From the geometry of figure (3-17) we have

$$\boldsymbol{d' = \frac{t}{2}cos\alpha}$$ ..... Equation 3- 52

$$\boldsymbol{y_o = \frac{h}{2} - d'}$$ ..... Equation 3- 53

$$\boldsymbol{b' = \frac{b}{2} - \frac{t}{2}sin\alpha}$$ ..... Equation 3- 54

$$\boldsymbol{e = \left(\frac{h}{2} - d' - b'tan\alpha\right)cos\alpha}$$ ..... Equation 3- 55

$$\boldsymbol{r = asin\alpha - \frac{t}{2}sin\alpha}$$ ..... Equation 3- 56

where:

d' is distance from dome-ring interaction center to ring beam top

y_o is distance from dome-ring interaction center to half of ring beam height

b' is distance from dome-ring interaction center to half of ring beam width

e is perpendicular distance from the projection of dome thickness center to geometric center of ring beam

r is spherical shell internal radius

λ is damping parameter

υ is Poisson's ratio

α is half central angle

a is radius of spherical shell

t is shell thickness

3.5 Force Method of Dome Ring Analysis

The deformation results obtained in membrane and bending theory should be combined to satisfy the compatibility requirements at the shell boundaries. The compatibility requirements, expressed in terms of known membrane displacements and unknown edge forces, yield a set of simultaneous algebraic

equations from which the redundant edge forces can be determined. The compatibility relations which express the continuity of radial displacement and rotation at the dome ring junction are:

$$\boldsymbol{D^D}_{\mathbf{10}} + \boldsymbol{D^D}_{\mathbf{11}}\boldsymbol{H} + \boldsymbol{D^D}_{\mathbf{12}}\boldsymbol{M_\alpha} = -(\boldsymbol{D^R}_{\mathbf{10}} + \boldsymbol{D^R}_{\mathbf{11}}\boldsymbol{H} + \boldsymbol{D^R}_{\mathbf{12}}\boldsymbol{M_\alpha})$$ ……. Equation 3- 57

$$\boldsymbol{D^D}_{\mathbf{20}} + \boldsymbol{D^D}_{\mathbf{21}}\boldsymbol{H} + \boldsymbol{D^D}_{\mathbf{22}}\boldsymbol{M_\alpha} = -(\boldsymbol{D^R}_{\mathbf{20}} + \boldsymbol{D^R}_{\mathbf{21}}\boldsymbol{H} + \boldsymbol{D^R}_{\mathbf{22}}\boldsymbol{M_\alpha})$$ …..... Equation 3- 58

Using the parameters defined in relations (3.50), (3.51, and (3.52) the compatibility relations, requiring zero horizontal displacement and zero meridional rotation at the edge, are as follows:

$\Sigma\Delta H = \boldsymbol{D_{11}H} + \boldsymbol{D_{12}M_\alpha} + \boldsymbol{D_{10}} = \mathbf{0}$ ……..... Equation 3- 59

$\Sigma\Delta H = \boldsymbol{D_{21}H} + \boldsymbol{D_{22}M_\alpha} + \boldsymbol{D_{20}} = \mathbf{0}$ ……..….. Equation 3- 60

where:

$D_{10} = D^D{}_{10} + D^R{}_{10}$

$D_{20} = D^D{}_{20} + D^R{}_{20}$

By solving linear simultaneous equations of (3-61) and (3-62), the redundant edge forces are:

$$\boldsymbol{H} = -\frac{\boldsymbol{D_{22}D_{10} - D_{12}D_{20}}}{\boldsymbol{D_{22}D_{11} - D_{12}^2}}$$ ……...…… Equation 3- 61

$$\boldsymbol{M_\alpha} = -\frac{\boldsymbol{D_{11}D_{20} - D_{12}D_{10}}}{\boldsymbol{D_{22}D_{11} - D_{12}^2}}$$ ……..….. Equation 3- 62

where:

H is uniformly distributed radial force/ edge shear force

M_α is uniformly distributed twisting couples/edge moment

D_{10} is dome-ring system membrane displacement

D_{20} is dome-ring system membrane rotation

D_{11} is dome-ring system displacement flexibility influence coefficient by edge shear

D_{12} is dome-ring system displacement flexibility influence coefficient by edge moment

D_{21} is dome-ring system rotation flexibility influence coefficient by edge shear

D_{22} is dome-ring system rotation flexibility influence coefficient by edge moment

CHAPTER 4 MATERIALS AND METHODS

4.1 Materials

In this study Ethiopian Building Code Standard (EBCS 2 – 1995) is adopted for strength classes for concrete. The concrete having properties of characteristics 28-day compressive cylinder strength f_{ck} of C30/37Mpa, normal weight γ value of 24kN/m3, modulus of elasticity E value of 32Gpa, and poison's ratio ν value of 0.20 has been used for each load case.

4.2. Geometrical Dimension Selection

The geometry of the spherical shell for this study were selected for 60 m span with ring beam b x h (0.45 x 1.20m) by varying rise to radius ratio as the shells makes a transition from shallow to hemispherical type. Thirty models (ten models for each load case) each spans 60m with change of rise to radius ratio from 0.10 to 1.00 were selected for dead, live, and wind load cases separately. The geometrical dimension of half central angle α of each model can be determined by applying the following mathematical formula.

$$\text{Sin}\alpha = \frac{d/2}{a} \quad \text{..... Equation 4- 1}$$

where:

$d/2$ is half span of spherical concrete dome

a is radius of spherical dome

As a general guide line, thin shells are defined as shells with a radius to thickness ratio between 20 and 1000. [1].

From table (4.1), the radius to thickness ratio $\frac{a}{t}$ is in the range of (688.5 to 300). The selected radii are in the given range.

The geometrical details of each model were tabulated as shown in table (4-1)

Table 4- 1: Spherical shell dimensions of each model

Model		Geometric dimensions						
	Edge beam (b x h) (m)	Thickness (m)	Span (m)	Rise (m)	Radius (m)	Rise/Radius ratio	Rise/Span ratio	Half central angle (degree)
1	0.45 X 1.20	0.10	60.00	6.88	68.85	0.10	0.115	25.83
2	0.45 X 1.20	0.10	60.00	10.00	50.00	0.20	0.17	36.87
3	0.45 X 1.20	0.10	60.00	12.60	42.01	0.30	0.21	45.56
4	0.45 X 1.20	0.10	60.00	15.00	37.50	0.40	0.25	53.13
5	0.45 X 1.20	0.10	60.00	17.32	34.64	0.50	0.29	60.00
6	0.45 X 1.20	0.10	60.00	19.64	32.73	0.60	0.33	66.42
7	0.45 X 1.20	0.10	60.00	22.01	31.45	0.70	0.37	72.53
8	0.45 X 1.20	0.10	60.00	24.49	30.62	0.80	0.41	78.45
9	0.45 X 1.20	0.10	60.00	27.14	30.15	0.90	0.45	84.27
10	0.45 X 1.20	0.10	60.00	30.00	30.00	1.00	0.50	90.00

For this study the minimum rise to radius ratio for buckling requirement (for model 1) is 0.10, at which the critical buckling load is 3.38 kN/m2 which is greater than the maximum applied dead load, 3.09 kN/m2 and the maximum rise to radius ratio (for model 10) is 1.0. Thus, by considering the minimum and maximum rise to radius ratios, for other models the intervals have been considered to be 0.10 and their corresponding other variable parameters have been determined by applying mathematical formulas as shown in table 4-1.

4.3. Load Determination

For this study the concrete shell structure is subjected to dead, live and wind load separately and Ethiopian Building Code Standard (EBCS 1 – 1995) is adopted to determine each load.

4.3.1 Dead load

Dead load g is determined by adding self-weight of the shell and plastering and painting finishing. According to Ethiopian Building Code Standard (EBCS 1-1995) of table 2.1 concrete has a specific weight of $24kN/m^3$ and cement plastering mortar $23kN/m^3$. These weights multiplied by their thicknesses, gives a surface load.

g = $(\boldsymbol{\gamma} \times \boldsymbol{t}) + \boldsymbol{\gamma_p} \times \boldsymbol{t_p}$ ……..… Equation 4- 2

where:

g is dead load of spherical shell

γ is normal weight of concrete

t is shell thickness

γ_p is normal weight of plastering and painting

t_p is thickness of plastering and painting

g = $24kN/m^3$*0.10 m + $23kN/m^3$*0.03 m

g = $3.09kN/m^2$

4.3.2 Live load

In this study the live load p considered is roof maintenance load which shall be assumed to act vertically over the area protected by the roof. From Ethiopian Building Code Standard (EBCS 1-1995) of table 2.14 loads for roofs of category H (roofs not accessible except for normal maintenance, repair, painting and minor repairs) is $0.25kN/m^2$.

p = $0.25kN/m^2$

4.3.3 Wind load

To determine the wind load the structure is considered to be built in Debre Maryam (an island in Lake Tana located 11º37’ north 37º23’ east, 1786 meter above sea level), Ethiopia and the blowing direction is considered to be zero to determine the maximum internal forces. Wind action calculations depend on the location of the structure as well as the shape and size of the structure. The action on the structure caused by the wind pressure is assumed to act normal to the surface. The total wind pressure acting on individual zones of the structure is proportional to the difference in between external and internal wind pressure acting on the surface of the structure. However, for this study, only external pressure w_e and thus only the external pressure coefficient is determined for the roof surface.

$\boldsymbol{w_e} = \boldsymbol{q_{ref}} \boldsymbol{c_e}(\boldsymbol{z}) \boldsymbol{c_{pe}}$……. Equation 4- 3

where:

w_e is external wind pressure for each part of the structure

q_{ref} is reference wind pressure

$c_e(z)$ is exposure coefficient

c_{pe} is external pressure coefficient

1) Reference Wind Velocity

The reference wind velocity v_{ref} is the 10 minute mean wind velocity at 10m above ground having an annual probability of exceedance of 0.02 (commonly referred to as having a mean return period of 50 years).

$\boldsymbol{v_{ref}} = \boldsymbol{C_{DIR}C_{TEM}C_{ALT}v_{ref,o}}$ ……..…. Equation 4- 4

where:

$v_{ref,o}$ is basic value of the reference wind velocity to be taken as 22m/sec.

C_{DIR} is direction factor to be taken as 1.0.

C_{TEM} is temporary (seasonal) factor to be taken as 1.0.

C_{ALT} is altitude factor to be taken as 1.0.

The reference wind velocity v_{ref} is to be taken as 22m/sec

$v_{ref} = 22 m/s\,ec$

2) Reference Wind Pressure

The reference mean wind velocity pressure $\boldsymbol{q_{ref}}$ shall be determined from

$$\boldsymbol{q_{ref} = \frac{1}{2}\rho v^2_{ref}} \quad \text{..... Equation 4- 5}$$

where:

$\boldsymbol{q_{ref}}$ is reference wind pressure

ρ is air density.

$\boldsymbol{v_{ref}}$ is reference wind velocity

The air density is affected by altitude and depends on the temperature and pressure to be expected in the region during wind storms. A temperature of 20^0C has been selected as appropriate for Ethiopia and the values of air density in Debre Maryam (an island in Lake Tana located 11º37' north 37º23' east, 1786 meter above sea level), Ethiopia by interpolation from table 3.1 in EBCS 1-1995 is $0.97\ \text{kg/m}^3$

$$q_{\text{ref}} = \frac{1}{2} * 0.97\ \text{kg/m}^3 * (22\text{m/s ec})^2$$

$$q_{\text{ref}} = 0.23\ \text{kN/m}^2$$

3) Exposure Coefficient

The exposure coefficient $c_e(z)$ takes into account the effects of terrain roughness, topography and height above ground. Although this is not clearly stated for spherical shell in Ethiopian Building code standard (EBCS 1-1995), it is calculated according to Eurocode 1: actions on structures- general actions - part 1-4: wind actions -prEN 1991-1-4-2004. Since the structure is planned in an open area (Debre Maryam) without obstacles terrain category I is chosen with the recommended orography factor c_o value is 1 and turbulent factor value k_1 is 1.

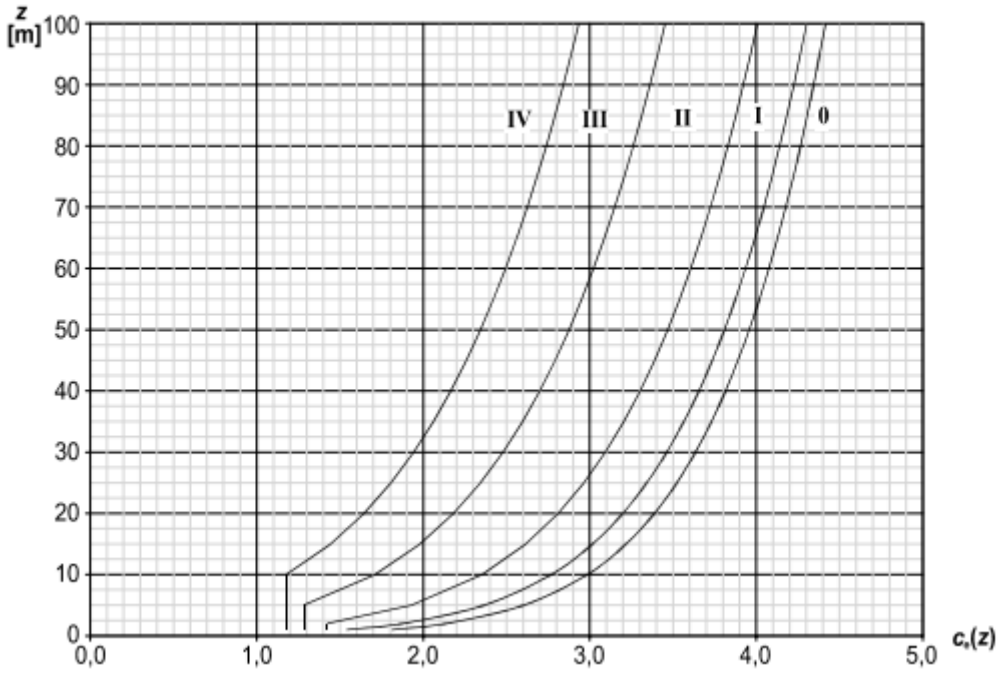

Figure 4- 1: Illustration of the exposure factors (Eurocode 1- prEN 1991-1-4-2004)

Table 4- 2: Exposure Coefficient of each model

Model	Reference height, z (m)	Exposure Coefficient, $c_e(z)$
1	21.88	3.25
2	25.00	3.34
3	27.6	3.40
4	30.00	3.45
5	32.32	3.50
6	34.64	3.56
7	37.01	3.60
8	39.49	3.64
9	42.14	3.68
10	45.00	3.73

The rise of the dome f for each model (ten models) is in the range of 6.88m to 30.00m as shown in table 4-1 and the assumed height of the wall of the structure h is 15m. Hence the value for the Exposure Coefficient for each model is tabulated as shown in table 4-2.

4) External Pressure Coefficient

The external Pressure Coefficient for each loaded zone area greater than $10m^2$ $c_{pe,10}$ is presented graphically in EBCS 1-1995.

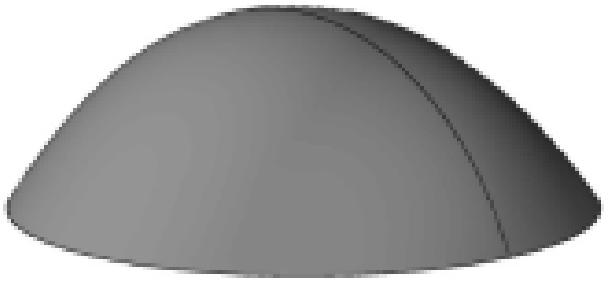

Figure 4- 2: Structure with spherical roof shape used in the wind action calculations

In accordance with figure 4-3 and 4-4 the following values are obtained: The rise of the dome f (the total height of spherical roof) in this study is in the range of 6.88m to 30.00m, the assumed height of the wall of the structure h is 15m and the span of the dome d is 60.00m. Hence giving the following relations:

h/d = 0.25

f/d = 0.11 to 0.50

where:

h/d is height of wall to span of dome ratio

f/d is rise of dome to its span ratio

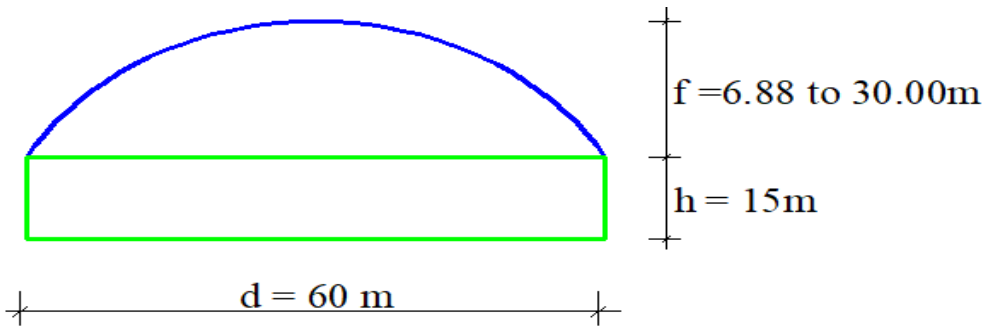

Figure 4- 3: Section drawing of the spherical roof shape with dimensions

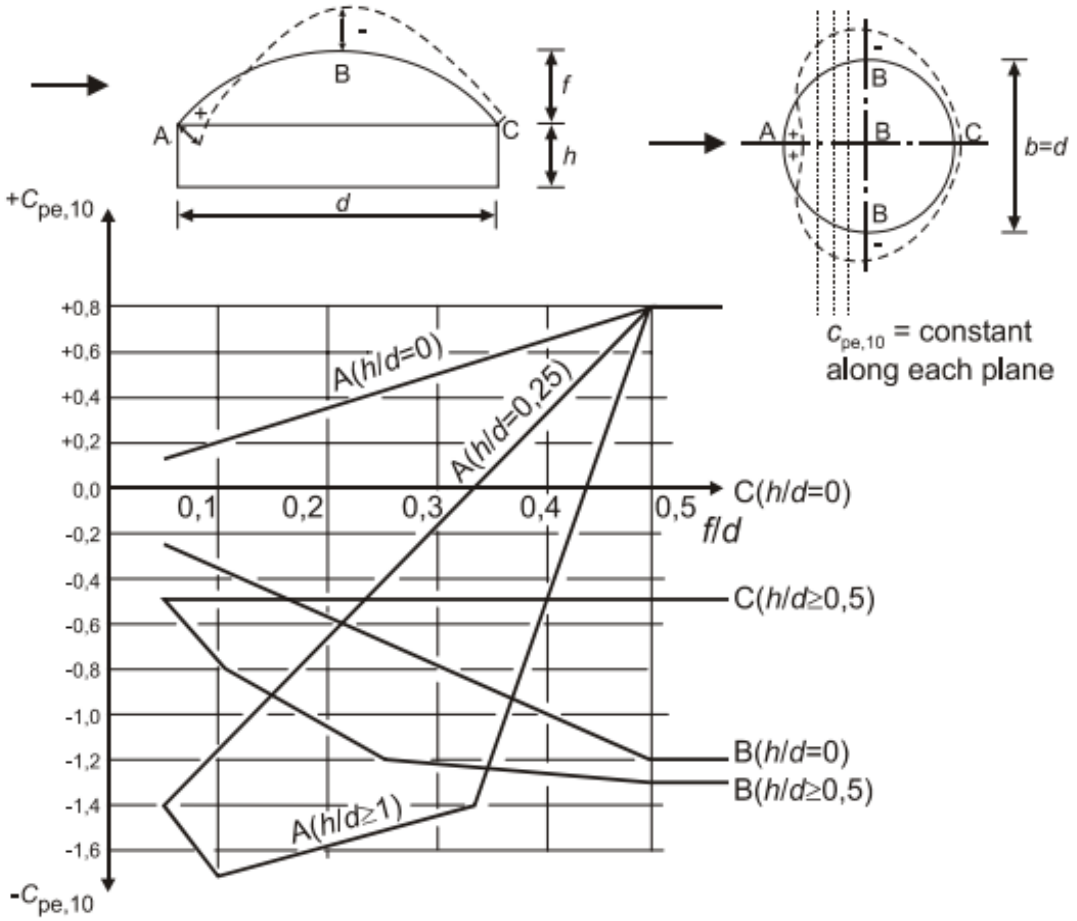

Figure 4- 4: External pressure coefficient for domes with circular base (Eurocode 1- prEN 1991-1-4-2004)

The values of external pressure coefficient for each model are extracted and interpolated from the graph presented in figure 4-4 and tabulated in table 4-2 below together with reference wind pressure and exposure coefficients which are obtained above. Hence the external wind pressure for each part of the zone obtained with equation 4-2.

For ten models the distribution of the wind pressure with the different wind zones have been obtained as shown in table 4-3, However, the values which has been taken (considered) for each model finite element analysis are zone A values. Positive sign is into the surface and negative sign is away from the surface (suction).

Table 4- 3: External pressure coefficients of spherical roof shape and wind pressures corresponding to the wind zones

Model	h/d	f/d	Zone	$c_{pe,10}$	q_{ref} (kN/m^2)	$c_e(z)$	w_e (kN/m^2)
1	0.25	0.11	A	-1.12	0.23	3.25	-0.84
			B	-0.58			-0.43
			C	-0.25			-0.19
2		0.17	A	-0.89		3.34	-0.68
			B	-0.65			-0.50
			C	-0.25			-0.19
3		0.21	A	-0.62		3.40	-0.48
			B	-0.79			-0.62
			C	-0.25			-0.20
4		0.25	A	-0.40		3.45	-0.32
			B	-0.95			-0.75
			C	-0.25			-0.20
5		0.29	A	-0.19		3.50	-0.15
			B	-1.03			-0.83
			C	-0.25			-0.20
6		0.33	A	0.02		3.56	0.02
			B	-1.10			-0.90
			C	-0.25			-0.20
7		0.37	A	0.13		3.60	0.11
			B	-1.15			-0.95
			C	-0.25			-0.21
8		0.41	A	0.37		3.64	0.31
			B	-1.19			-1.00
			C	-0.25			-0.21
9		0.45	A	0.59		3.68	0.50
			B	-1.26			-1.07
			C	-0.25			-0.21
10		0.50	A	0.80		3.73	0.69
			B	-1.25			-1.07
			C	-0.25			-0.21

4.4. Finite Element Analysis Method

The finite element method is a numerical method that generates approximate solution to engineering problems and mathematical physics which are usually expressed in terms of differential equations. It is used for stress analysis, heat transfer, fluid flow, electromagnetic potential etc.

Use of several materials within the same structure, complicated or discontinuous geometries, and complicated loading makes the closed form (analytical) solution of structural problems very difficult. Hence, we need to rely on numerical methods, such as the finite element method, for acceptable

solutions. The structure is partitioned into an equivalent system of smaller units (finite elements) interconnected at points common to two or more elements (nodes) and/or boundary lines and/or surfaces is called discretization. In the finite element method, equations are formulated for each finite elements and then combined to obtain the solution of the entire model.

The general steps of the finite element method for the structural stress-analysis problem are described in Logan's text as follows.

Step 1 Discretize and Select the Element type

Step 1 involves dividing the body into an equivalent system of finite elements with associated nodes and choosing the most appropriate element type to model most closely the actual physical behavior. The element must be small enough to give usable results and large enough to reduce computational effort. Thus, some engineering judgement must be used. Small elements are generally desirable where the results are changing rapidly, such as where changes in geometry occur; large elements can be used where results are relatively constant.

The choice of the elements depends on the physical makeup of the body under actual loading conditions and on how close to the actual behavior the analyst wants the result to be. Judgment must be used in choosing one-, two-, or three-dimensional idealizations.

Step 2 Select a Displacement Function

The displacement function is defined within the element using the nodal values of the element. Frequently used functions are linear, quadratic, and cubic polynomials because they are simple to work with in finite element formulation. Trigonometric series can also be used. The displacement functions of a two-dimensional element is a function of the coordinates in its plane. The functions are expressed in terms of the nodal unknowns. The same general displacement function can be used repeatedly for each element.

Step 3 Define the Strain/Displacement and Stress/Strain Relationship

Strain/displacement and stress/strain relationships are necessary for deriving the equations for finite elements. For example, in the case of one-dimensional deformation, say, in the x direction, stain ε_x is related to the displacement u by $\varepsilon_x = du/dx$ for small strains. Stresses must be related to stains through the stress/strain relation called Hooke's law. Being able to define the materials behavior accurately is most important in obtaining acceptable results. Hooke's low, $\sigma_x = E\varepsilon_x$, is used in stress analysis, where $\sigma_x =$ stress in the x direction and E = modulus of elasticity.

Step 4 Derive the Element Stiffness Matrix and Equations

The stiffness and element equations relating nodal forces to nodal displacements are obtained and written in compact matrix form are:

$\{f^*\} = [k^*]\{d^*\}$ ……...…… Equation 4- 6

where:

f^* is vector of elemental nodal forces

k^* is element stiffness matrix

d^* is vector of unknown element nodal degrees of freedom or generalized displacements, n. These may include actual displacements, slopes, or even curvatures.

Step 5 Assemble the Element Equations to Obtain the Global or Total Equations and Introduce Boundary Conditions

The individual element equations generated in step 4 can now be added together using a method of superposition (called the direct stiffness method), whose basis is nodal force equilibrium, to obtain the global equations for the whole structure. There must be consistency in the deformation of the structure, that is, element sharing a node will have the same displacements at that node.

The final assembled or global equation written in matrix form is

$\{F^*\} = [K^*]\{d^*\}$ ……..…….... Equation 4- 7

where:

F^* is vector of global nodal forces

K^* is structure global or total stiffness matrix

d^* is vector of known and unknown structure nodal degree of freedom or generalized displacements.

The global stiffness matrix [K*] is a singular matrix. Thus, certain boundary conditions must be invoked (from constraints or supports) so that the structure remains in place. The applied loads have been accounted for in the global force matrix {F*}.

Step 6 Solve for the Unknown Degrees of Freedom (or Generalized Displacements)

The equation {F*} = [K*]{d*}is a set of simultaneous algebraic equations that can be written in expanded matrix form as

$$\begin{Bmatrix} F_1^* \\ F_2^* \\ \vdots \\ F_n^* \end{Bmatrix} = \begin{bmatrix} K_{11}^* & K_{12}^* & \dots & K_{1n}^* \\ K_{21}^* & K_{22}^* & \dots & K_{2n}^* \\ \vdots & & & \vdots \\ K_{n1}^* & K_{n2}^* & \dots & K_{nn}^* \end{bmatrix} \begin{Bmatrix} d_1^* \\ d_2^* \\ \vdots \\ d_n^* \end{Bmatrix} \quad \text{..... Equation 4- 8}$$

Where n is the total number of unknown nodal degrees of freedom.

These equations can be solved for the d*'s by using an elimination method such as Gauss's method. The d*'s are called the primary unknowns, because they are the first quantities to be determined in using the finite element method.

Step 7 Solve for the Elements strains and Stresses

Important secondary quantities of strains and stress (or moment and shear force) can be obtained because they can be directly expressed in terms of the displacements determined in step 6. The equations given in step 3 can be used.

Step 8 Interpret the Results

The final goal is to interpret and analyze the results for use in the design/ analysis process. The determinations of locations in the structure where large deformations and stresses occur is important in making design/analysis decisions. [4]

SAP 2000 (Structural Analysis Program) version is used for modeling and analysis of spherical concrete shell roof with dead, live and wind load individually. FEM includes geometrical modeling, assigning material properties and support conditions, analyzing and obtaining outputs

CHAPTER 5 RESULT AND DISCUSSION

5.1. Theoretical Results

5.1.1. Edge shear and edge moment due to gravity loads

The values of edge shear and edge moments of all models are computed and tabulated in table 5.3 as shown below.

Table 5- 1: Edge shear and edge moments of each models

Models	Rise to Radius	Edge shear and Edge moment of each models			
		Due to dead load		Due to live load	
		H (kN/m)	Mα (kN.m/m)	H (kN/m)	Mα (kN.m/m)
1	0.10	39.58	-19.92	3.20	-1.64
2	0.20	22.63	-13.40	1.83	-1.08
3	0.30	15.26	-9.80	1.23	-0.79
4	0.40	10.64	-7.14	0.86	-0.58
5	0.50	7.13	-4.83	0.58	-0.39
6	0.60	4.11	-2.64	0.33	-0.21
7	0.70	1.22	-0.38	0.10	-0.03
8	0.80	-1.79	2.08	-0.15	0.17
9	0.90	-5.15	4.89	-0.42	0.40
10	1.00	-9.09	8.22	-0.74	0.66

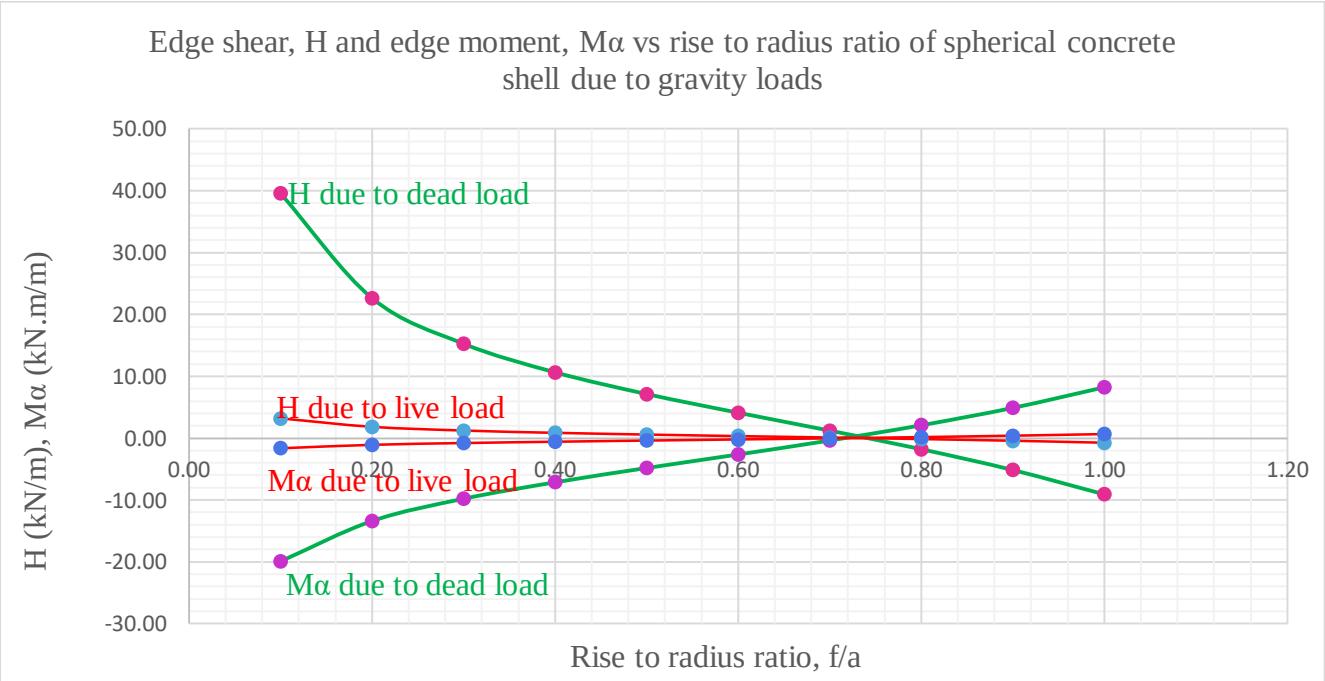

Figure 5- 1: Edge shears and edge moments vs rise to radius ratio

The two graphs crossed each other at rise to radius ratio of 0.73. The numerical value of rise to radius ratio that corresponds to 0.73 is taken as a reference point to study the behavior of hoop and meridional forces under gravity loads. This is the value at which edge forces are minimum. When rise to radius ratio decreases, the edge shear and edge moment increases in magnitude. When rise to radius ratio increases, the behavior of edge shear and edge moment increases in magnitude but show opposite sign to that of decrease in rise to radius ratio. The edge moment cross the x axis at rise to radius ratio of 0.716 (reverse curvature point with zero magnitude). Thus, its line of action is out ward to the dome up to 0.716 and towards the dome after 0.716. While, the edge shear line of action is outward to the dome up to 0.74 and towards after 0.73. It is zero at 0.74.

5.1.2. Bending forces due to dead load

Table 5- 2: Bending meridional and hoop forces of each models

Φ (°)	bending meridional and hoop forces due to gravity load for each model, NΦ and NΘ (kN/m)																			
	model 1		model 2		model 3		model 4		model 5		model 6		model 7		model 8		model 9		model 10	
	$N_Ø$	$N_Θ$	$N_Ø$	$N_Θ$	$N_Ø$	$N_Θ$	$N_Ø$	$N_Θ$	$N_Ø$	$N_Θ$	$N_Ø$	$N_Θ$	$N_Ø$	$N_Θ$	$N_Ø$	$N_Θ$	$N_Ø$	$N_Θ$	$N_Ø$	$N_Θ$
0.00	0.00	0.00	0.00	0.00	0.00	0.00	0.00	0.00	0.00	0.00	0.00	0.00	0.00	0.00	0.00	0.00	0.00	0.00	0.00	0.00
0.02	-0.01	-0.04	0.00	0.00	0.00	0.00	0.00	0.00	0.00	0.00	0.00	0.00	0.00	0.00	0.00	0.00	0.00	0.00	0.00	0.00
0.06	-1.45	-21.54	0.00	0.02	0.00	0.00	0.00	0.00	0.00	0.00	0.00	0.00	0.00	0.00	0.00	0.00	0.00	0.00	0.00	0.00
0.10	35.62	502.63	0.07	-0.07	0.00	-0.02	0.00	0.00	0.00	0.00	0.00	0.00	0.00	0.00	0.00	0.00	0.00	0.00	0.00	0.00
0.13			-0.71	-14.37	0.01	0.29	0.00	-0.01	0.00	0.00	0.00	0.00	0.00	0.00	0.00	0.00	0.00	0.00	0.00	0.00
0.20			18.11	336.38	-0.18	-7.24	0.01	0.24	0.00	-0.01	0.00	0.00	0.00	0.00	0.00	0.00	0.00	0.00	0.00	0.00
0.23					-0.76	-2.87	0.03	0.15	0.00	0.01	0.00	0.00	0.00	0.00	0.00	0.00	0.00	0.00	0.00	0.00
0.30					10.68	249.12	-0.30	-8.21	0.01	0.23	0.00	0.00	0.00	0.00	0.00	0.00	0.00	0.00	0.00	0.00
0.36							0.57	68.94	-0.04	-3.02	0.00	0.14	0.00	0.00	0.00	0.00	0.00	0.00	0.00	0.00
0.40							6.38	187.28	-0.24	-5.11	0.01	-0.02	0.00	0.01	0.00	0.00	0.00	0.00	0.00	0.00
0.50									3.57	135.42	-0.14	-2.43	0.00	0.01	0.00	-0.04	0.00	0.01	0.00	0.00
0.60											1.64	87.87	-0.05	-2.00	0.00	0.58	0.00	-0.14	0.00	0.01
0.66													0.01	11.64	0.03	0.86	0.00	0.17	0.00	-0.10
0.70													0.36	40.59	0.01	-4.09	0.01	1.66	0.00	-0.27
0.80															-0.36	-9.61	0.04	-8.06	0.01	3.14
0.83																	-0.05	-29.15	0.03	5.68
0.90																	-0.51	-65.93	0.03	-13.88
1.00																			0.00	-131.48

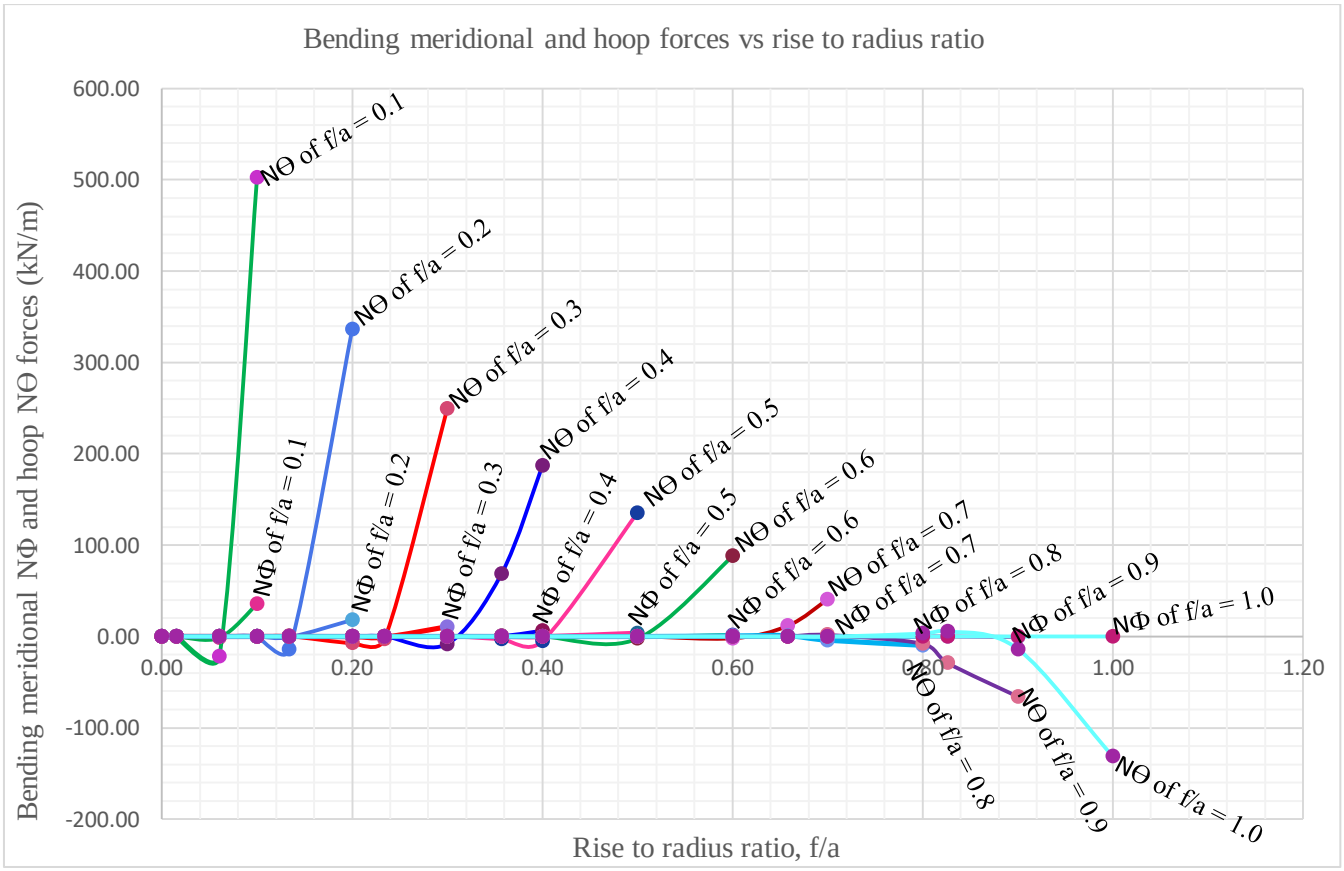

Figure 5- 2: Bending meridional and hoop forces of all model due to dead load vs meridional angle

When the shell become shallower and shallower with respect to 0.73, the bending hoop forces are maximum tensile type at edge and gradually decreased and changed to tensile type. Finally they damp out in the range of rise to radius ratio 0.030 – 0.086. While, the tensile bending meridional forces are small and theirs value are increased for more flat types of models 3, 2, and 1.

When the shell rise increased, the compressive type bending hoop forces are maximum at the edge and gradually decreased and changed to tensile type and damp out in the range of 0.030 – 0.044. But the bending meridionals are insignificant. These results are also valid qualitatively due to live load.

5.1.3. Superimposed forces due to Dead load

Table 5- 3: Superimposed meridional and hoop forces of all models

Rise/radius	Superimposed meridional and hoop forces due to gravity load for each model, NΦ and NΘ (kN/m)																			
	Model 1		Model 2		Model 3		Model 4		Model 5		Model 6		Model 7		Model 8		Model 9		Model 10	
	$N_Ø$	$N_Θ$	$N_Ø$	$N_Θ$	$N_Ø$	$N_Θ$	$N_Ø$	$N_Θ$	$N_Ø$	$N_Θ$	$N_Ø$	$N_Θ$	$N_Ø$	$N_Θ$	$N_Ø$	$N_Θ$	$N_Ø$	$N_Θ$	$N_Ø$	$N_Θ$
0.00	-106.37	-106.37	-77.25	-77.25	-64.91	-64.91	-57.98	-57.98	-53.52	-53.52	-50.57	-50.57	-48.59	-48.59	- 47.31	-47.31	-46.58	-46.58	-46.35	-46.35
0.02	-107.20	-102.37	-77.84	-74.31	-65.40	-62.44	-58.43	-55.78	-53.93	-51.48	-50.95	-48.64	-48.96	-46.74	-47.67	-45.51	-46.94	-44.81	-46.70	-44.59
0.06	-111.13	-111.77	-79.66	-65.51	-66.92	-55.06	-59.79	-49.19	-55.18	-45.40	-52.14	-42.90	-50.10	-41.22	-48.78	-40.13	-48.03	-39.52	-47.79	-39.32
0.10	-76.34	423.11	-81.24	-57.82	-68.32	-48.54	-61.03	-43.35	-56.33	-40.01	-53.23	-37.80	-51.15	-36.33	-49.80	-35.37	-49.03	-34.82	-48.79	-34.65
0.13			-83.50	-65.37	-69.56	-42`.56	-62.15	-38.30	-57.36	-35.34	-54.20	-33.39	-52.08	-32.08	-50.70	-31.24	-49.93	-30.76	-49.68	-30.60
0.20			-67.73	298.61	-72.30	-38.97	-64.42	-28.11	-59.47	-26.17	-56.19	-24.72	-53.99	-23.76	-52.56	-23.13	-51.76	-22.77	-51.50	-22.66
0.23					-74.26	-28.81	-65.64	-23.02	-60.61	-21.37	-57.27	-20.21	-55.03	-19.42	-53.57	-18.90	-52.75	-18.61	-52.49	-18.52
0.30					-65.67	234.58	-68.51	-21.19	-62.94	-11.75	-59.49	-11.32	-57.16	-10.88	-55.65	-10.60	-54.80	-10.43	-54.52	-10.38
0.36							-70.02	64.99	-65.20	-6.67	-61.56	-3.31	-59.16	-3.31	-57.59	-3.22	-56.71	-3.17	-56.43	-3.16
0.40							-66.10	190.17	-67.14	-2.44	-63.20	2.51	-60.74	2.44	-59.13	2.37	-58.23	2.33	-57.94	2.32
0.50									-67.79	153.26	-67.56	14.42	-64.78	16.21	-63.08	15.73	-62.11	15.53	-61.80	15.45
0.60											-70.60	119.65	-69.46	28.54	-67.58	30.31	-66.55	29.13	-66.21	29.14
0.66													-72.40	50.82	-70.48	39.00	-69.42	37.73	-69.08	37.26
0.70													-74.38	86.16	-72.76	40.28	-71.64	45.34	-71.30	43.19
0.80															-79.19	50.28	-77.59	50.91	-77.23	61.81
0.83																	-79.43	34.05	-78.95	68.56
0.90																	-85.22	9.48	-84.25	61.15
1.00																			-92.70	-38.78

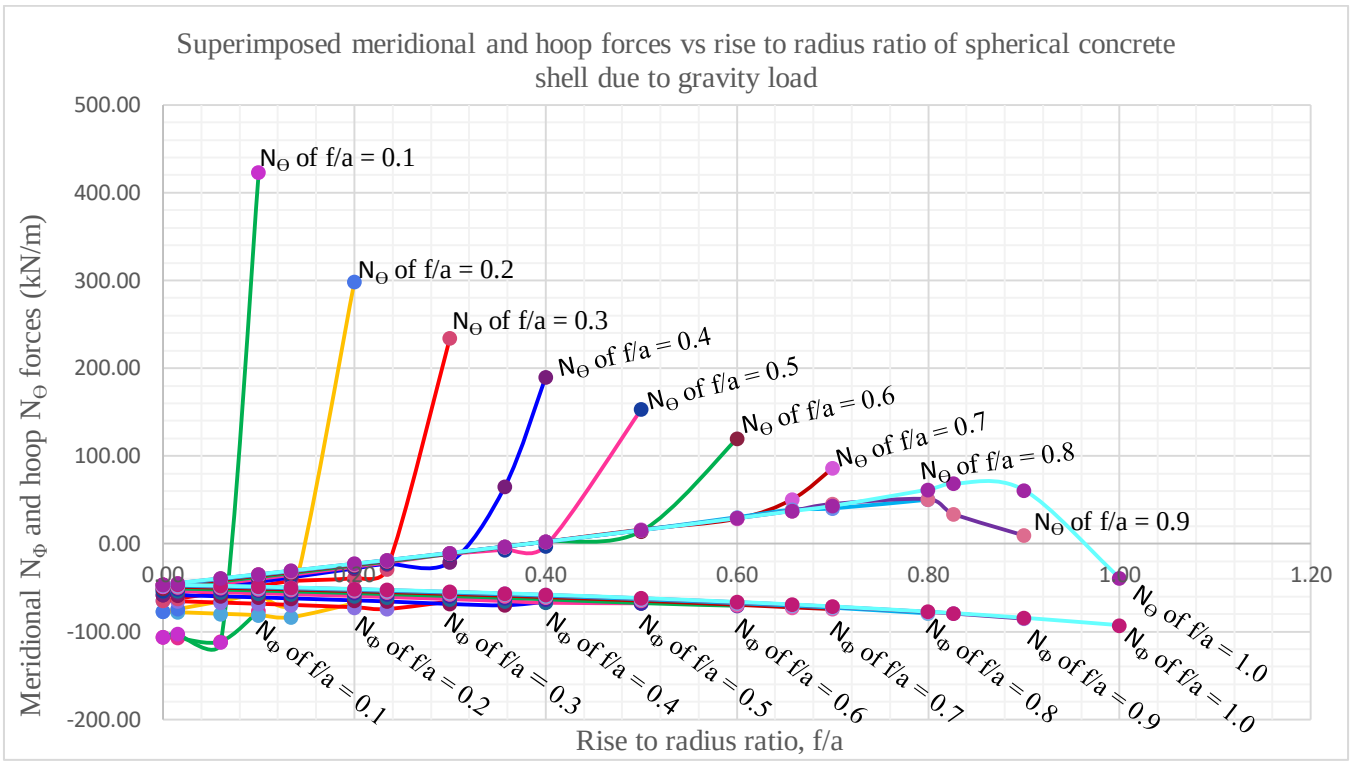

Figure 5- 3: Superimposed meridional and hoop forces vs rise to radius ratio due to dead load

The rise to radius ratio that corresponds to 0.73 is taken as a reference point to study the behavior of superimposed hoop and meridional forces due to dead as shown on figure 5-3. This is the value at which bending forces are minimum. When rise to radius ratio decreases, i.e., as the shell becomes shallower and shallower, the edge shear and the edge moment increases in magnitude. As a result, the linear membrane compressive hoop forces are changed to tensile type exponentially. While, the compressive meridionals are decreased in magnitude for more flat types (models 3, 2, and 1) and for others they have been affected slightly. When rise to radius ratio increases, the behavior of edge shear and edge moment increases in magnitude but show opposite sign to that of decrease in rise to radius ratio. Thus, the linear membrane tensile hoop forces are decreased, for hemispherical type, it is changed to compressive type. While the meridionals have not been affected.

5.1.4 Superimposed forces due to Live load

Table 5-4: Superimposed meridional and hoop forces of all models due to dead load

Rise/radius	Superimposed meridional and hoop forces due to live load for each model (kN/m)																			
	Model 1		Model 2		Model 3		Model 4		Model 5		Model 6		Model 7		Model 8		Model 9		Model 10	
	N_ϕ	N_θ	N_ϕ	N_θ	N_ϕ	N_θ	N_ϕ	N_θ	N_ϕ	N_θ	N_ϕ	N_θ	N_ϕ	N_θ	N_ϕ	N_θ	N_ϕ	N_θ	N_ϕ	N_θ
0.00	-8.61	-8.61	-6.25	-6.25	-5.25	-5.25	-4.69	-4.69	-4.33	-4.33	-4.09	-4.09	-3.93	-3.93	-3.83	-3.83	-3.77	-3.77	-3.75	-3.75
0.02	-8.61	-8.09	-6.25	-5.87	-5.25	-4.93	-4.69	-4.41	-4.33	-4.07	-4.09	-3.84	-3.93	-3.69	-3.83	-3.60	-3.77	-3.54	-3.75	-3.52
0.06	-8.72	-8.34	-6.25	-4.79	-5.25	-4.02	-4.69	-3.59	-4.33	-3.32	-4.09	-3.13	-3.93	-3.01	-3.83	-2.93	-3.77	-2.89	-3.75	-2.87
0.10	-5.72	35.33	-6.24	-3.88	-5.25	-3.26	-4.69	-2.91	-4.33	-2.69	-4.09	-2.54	-3.93	-2.44	-3.83	-2.37	-3.77	-2.34	-3.75	-2.33
0.13			-6.31	-4.29	-5.25	-2.60	-4.69	-2.35	-4.33	-2.16	-4.09	-2.05	-3.93	-1.97	-3.83	-1.91	-3.77	-1.88	-3.75	-1.87
0.20			-4.79	25.47	-5.27	-2.06	-4.69	-1.29	-4.33	-1.21	-4.09	-1.15	-3.93	-1.10	-3.83	-1.07	-3.77	-1.06	-3.75	-1.05
0.23					-5.31	-1.14	-4.69	-0.80	-4.33	-0.75	-4.09	-0.71	-3.93	-0.68	-3.83	-0.66	-3.77	-0.65	-3.75	-0.65
0.30					-4.39	20.26	-4.72	-0.57	-4.33	0.10	-4.09	0.08	-3.93	0.08	-3.83	0.07	-3.77	0.07	-3.75	0.07
0.36							-4.65	6.39	-4.33	0.51	-4.09	0.72	-3.93	0.68	-3.83	0.66	-3.77	0.65	-3.75	0.65
0.40							-4.17	16.47	-4.35	0.80	-4.09	1.14	-3.93	1.10	-3.83	1.07	-3.77	1.06	-3.75	1.05
0.50									-4.04	13.12	-4.10	1.85	-3.93	1.97	-3.83	1.91	-3.77	1.88	-3.75	1.88
0.60											-3.96	9.89	-3.94	2.51	-3.83	2.65	-3.77	2.55	-3.75	2.55
0.66													-3.93	3.95	-3.83	3.00	-3.77	2.90	-3.75	2.86
0.70													-3.90	6.51	-3.83	2.81	-3.77	3.22	-3.75	3.05
0.80															-3.86	2.74	-3.77	2.81	-3.75	3.70
0.83																	-3.77	1.18	-3.75	3.98
0.90																	-3.81	-1.64	-3.75	2.55
1.00																			-3.75	-6.89

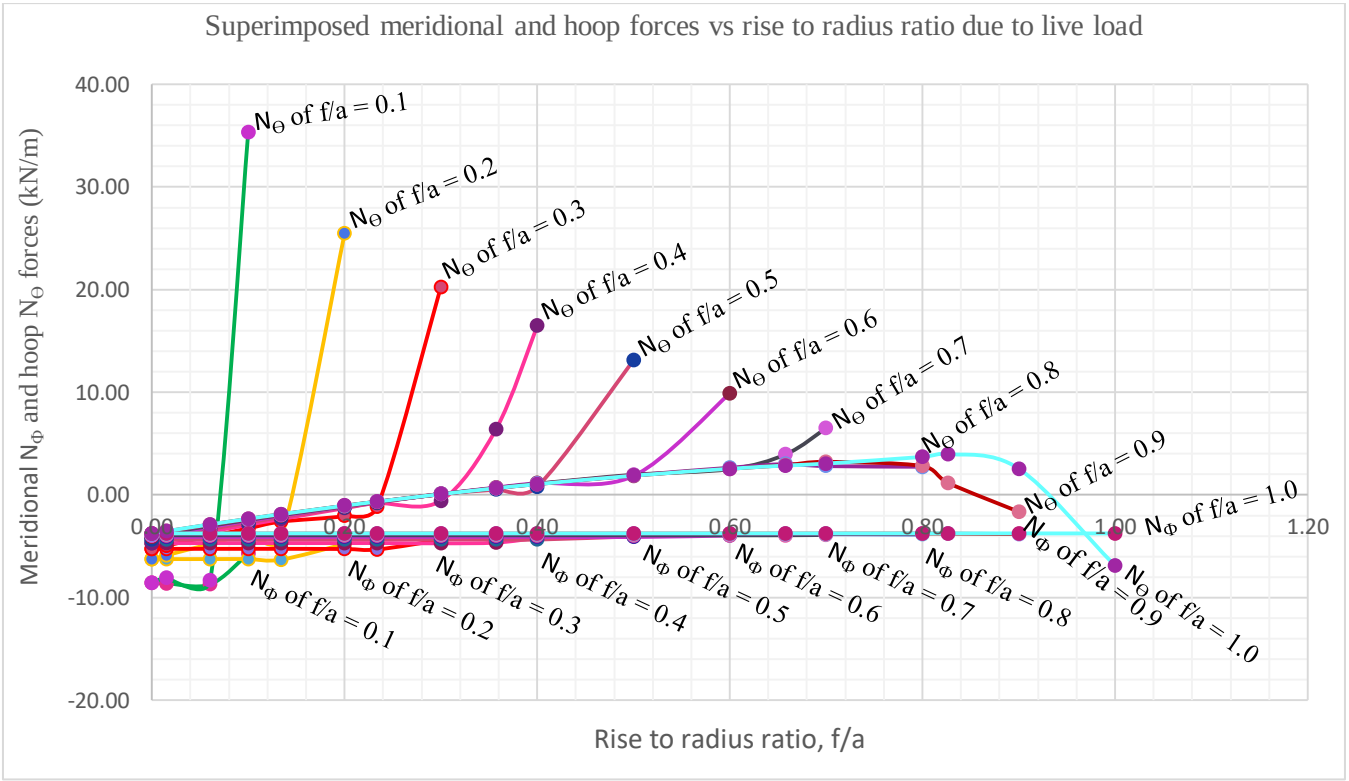

Figure 5- 4: Superimposed meridional and hoop forces vs rise to radius ratio due to live load

Figure 5-4 explains the fact that the numerical value of rise to radius ratio that corresponds to 0.73 is taken as a reference point to study the behavior of superimposed hoop and meridional forces under live load. This is the value at which edge forces are minimum so that all internal forces and axisymmetric deformations due to edge effects are minimum. When rise to radius ratio decreases that is to say, as the shell becomes shallower and shallower, the edge shear and the edge moment increases in magnitude. As a result, the superimposition of bending and membrane fields lead the hoop force an abrupt change from compressive to tensile force being nearly vertical line graphically while the meridional force remains compressive but gets reduced in magnitude. When rise to radius ratio increases, the behavior of edge shear and edge moment also increases in magnitude but show opposite sign to that of decrease in rise to radius ratio. For the rise to radius ratio 0.8, bending effects are small while for the rise to radius ratio 0.9, the tensile hoop total force decreases and after an angle Φ around 81.9^0 it is changed to compressive type. For hemispherical dome, the hoop force is changed from tensile to compressive type with high slope change after an angle Φ approximately 86.00^0. However; for all models except 1 and 2, the effect of bending field in the compressive membrane meridional forces are insignificant. Figure 5.2 explains more about this discussion.

5.1.5. Membrane meridional and hoop forces due to wind load

In this study, the theoretical method of bending forces of ring beam have not been considered. However; summary of membrane meridional and hoop forces for each model are tabulated below. For rise to radius ratio value less than 0.5 the wind load acted on the dome is suction type as a result the internal membrane meridional and hoop forces are tensile type while for greater or equal to 0.50, the wind pressure acted towards the dome and the membrane forces are compressive type. Figure 5-3 illustrates more about these values and their significance. For minimum effect of membrane meridional and hoop forces due to wind load, the best rise to radius ratio recommended ranges from $0.5-0.7$

Table 5- 5: Membrane meridional and hoop forces of all models due to wind load

Rise/radius	Membrane meridional and hoop forces for each model, NΦ and NΘ (kN/m)																			
	Model 1		Model 2		Model 3		Model 4		Model 5		Model 6		Model 7		Model 8		Model 9		Model 10	
	NØ	NΘ	NØ	NΘ	NØ	NΘ	NØ	NΘ	NØ	NΘ	NØ	NΘ	NØ	NΘ	NØ	NΘ	NØ	NΘ	NØ	NΘ
0.00	0	0	0	0	0	0	0	0	0	0!	0	0	0	0	0	0	0	0	0	0
0.02	2.50	7.54	1.47	4.44	0.87	2.63	0.52	1.57	0.22	0.68	-0.03	-0.09	-0.15	-0.45	-0.41	-1.24	-0.65	-1.97	-0.89	-2.70
0.06	4.84	14.94	2.85	8.78	1.69	5.21	1.00	3.10	0.43	1.34	-0.05	-0.17	-0.29	-0.89	-0.79	-2.45	-1.26	-3.89	-1.73	-5.35
0.10	6.07	19.13	3.57	11.24	2.12	6.67	1.26	3.97	0.55	1.72	-0.07	-0.22	-0.36	-1.14	-1.00	-3.14	-1.58	-4.99	-2.17	-6.85
0.13			4.04	12.96	2.40	7.69	1.43	4.57	0.62	1.98	-0.08	-0.25	-0.41	-1.32	-1.13	-3.62	-1.79	-5.75	-2.46	-7.89
0.20			4.70	15.70	2.79	9.31	1.66	5.54	0.72	2.40	-0.09	-0.30	-0.48	-1.60	-1.31	-4.38	-2.08	-6.96	-2.86	-9.56
0.23					2.94	10.03	1.75	5.97	0.76	2.58	-0.10	-0.33	-0.50	-1.72	-1.38	-4.72	-2.19	-7.50	-3.01	-10.29
0.30					3.14	11.26	1.87	6.70	0.81	2.90	-0.10	-0.37	-0.54	-1.93	-1.48	-5.30	-2.35	-8.42	-3.22	-11.56
0.36							1.93	7.26	0.84	3.15	-0.11	-0.40	-0.56	-2.09	-1.53	-5.75	-2.42	-9.13	-3.33	-12.53
0.40							1.95	7.65	0.84	3.31	-0.11	-0.42	-0.56	-2.21	-1.54	-6.05	-2.45	-9.61	-3.36	-13.20
0.50									0.83	3.67	-0.10	-0.46	-0.55	-2.44	-1.52	-6.70	-2.42	-10.64	-3.32	-14.61
0.60											-0.10	-0.50	-0.52	-2.65	-1.42	-7.28	-2.26	-11.56	-3.10	-15.87
0.66													-0.48	-2.77	-1.32	-7.60	-2.10	-12.07	-2.88	-16.57
0.70													-0.45	-2.85	-1.23	-7.82	-1.96	-12.42	-2.69	-17.06
0.80															-0.95	-8.35	-1.51	-13.26	-2.07	-18.21
0.83																	-1.36	-13.49	-1.86	-18.52
0.90																	-0.87	-14.13	-1.19	-19.41
1.00																			0.00	-20.70

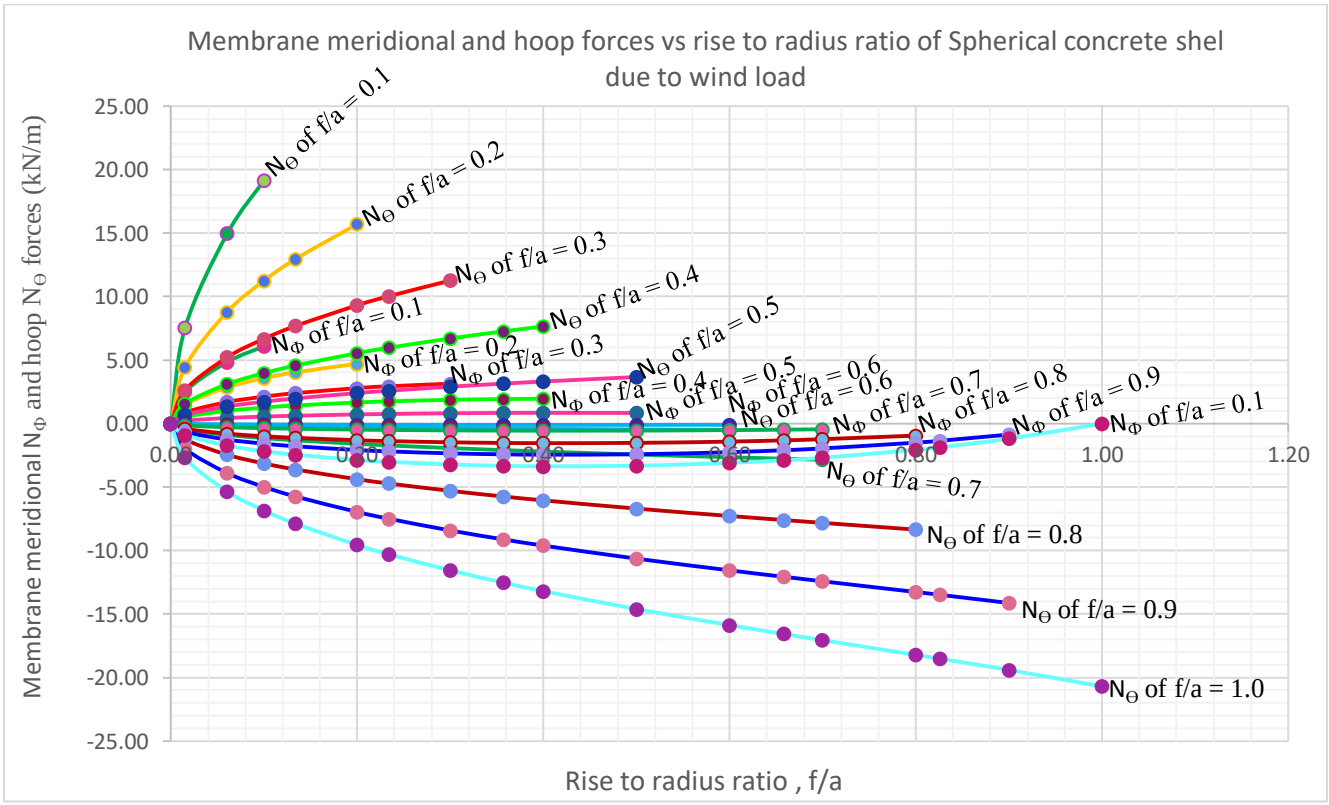

Figure 5- 5: Membrane meridional and hoop forces vs rise to radius ratio due to wind load

5.2. Software Results

5.2.1. Resultant forces due to dead load

Table 5- 6: Resultant meridional and hoop forces of all models

Rise to radius	Resultant meridional NΦ and hoop NΘ forces due to dead load for each model, (kN/m)																			
	model 1		model 2		model 3		model 4		model 5		model 6		model 7		model 8		model 9		model 10	
	NØ	NΘ	NØ	NΘ	NØ	NΘ	NØ	NΘ	NØ	NΘ	NØ	NΘ	NØ	NΘ	NØ	NΘ	NØ	NΘ	NØ	NΘ
0.00	-106.93	-106.89	-77.88	-77.83	-65.60	-65.53	-58.70	-58.62	-54.35	-54.25	-51.48	-51.36	-49.60	-49.45	-48.42	-48.24	-47.83	-47.61	-47.75	-47.48
0.02	-107.04	-102.59	-77.73	-74.59	-65.31	-62.73	-58.31	-56.04	-53.88	-51.79	-50.92	-48.96	-48.96	-47.01	-47.69	-45.71	-46.98	-45.09	-46.78	-44.85
0.06	-109.42	-92.20	-79.42	-66.34	-66.69	-55.91	-59.50	-50.09	-54.94	-46.35	-51.92	-43.82	-49.87	-42.19	-48.53	-41.21	-47.81	-40.51	-47.53	-40.49
0.10	-108.84	-21.67	-81.01	-58.73	-68.01	-49.66	-60.72	-44.45	-56.04	-41.19	-52.91	-39.18	-50.84	-37.64	-49.49	-36.63	-48.72	-36.14	-48.46	-36.06
0.13			-82.42	-52.77	-69.20	-44.27	-61.76	-39.61	-57.02	-36.72	-53.84	-34.89	-51.76	-33.48	-50.32	-32.89	-49.53	-32.52	-49.29	-32.32
0.20			-84.35	-16.84	-71.70	-33.18	-63.89	-30.23	-59.02	-27.78	-55.70	-26.58	-53.97	-23.77	-52.09	-25.08	-51.28	-24.83	-50.99	-24.77
0.23					-73.06	-27.44	-65.13	-25.12	-60.10	-23.28	-56.75	-22.30	-54.51	-21.51	-53.08	-20.89	-52.15	-21.04	-51.86	-21.10
0.30					-75.87	-15.17	-67.21	-14.70	-62.40	-13.48	-58.89	-13.79	-56.55	-13.29	-54.99	-13.24	-54.45	-11.93	-54.71	-10.40
0.36							-70.16	-5.19	-64.53	-6.03	-60.84	-6.03	-58.48	-5.77	-56.90	-5.71	-56.04	-5.58	-55.61	-6.04
0.40							-72.72	-14.56	-66.17	1.54	-62.50	-0.13	-59.95	-0.33	-58.38	-0.25	-57.34	-0.73	-57.00	-1.01
0.50									-72.37	-14.50	-66.50	16.11	-63.90	13.24	-62.04	12.41	-61.14	12.30	-60.65	11.44
0.60											-73.94	-14.82	-68.23	30.79	-66.35	25.83	-65.31	25.51	-64.95	25.27
0.66													-70.70	35.23	-69.12	35.28	-67.98	33.10	-67.68	33.30
0.70													-77.16	-15.47	-71.24	45.01	-70.13	38.96	-69.75	39.12
0.80															-82.04	-16.45	-75.65	59.34	-75.38	53.73
0.83																	-77.08	65.34	-77.03	57.79
0.90																	-88.80	-17.79	-81.70	75.24
1.00																			-97.82	-15.98

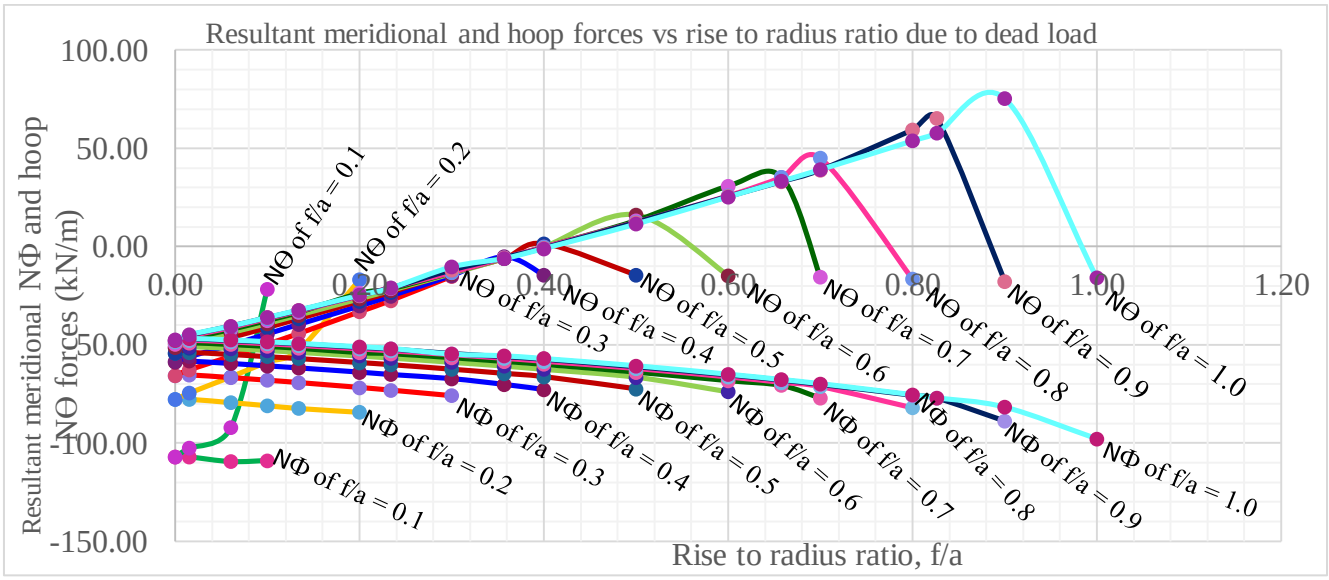

Figure 5- 6: Resultant meridional and hoop forces vs rise to radius ratio due to dead

5.2.2. Resultant forces due to live load

Table 5- 7: Resultant meridional and hoop forces of all models

Rise to radius	Resultant meridional NΦ and hoop NΘ forces due to live load for each model, (kN/m)																			
	model 1		model 2		model 3		model 4		model 5		model 6		model 7		model 8		model 9		model 10	
	NØ	NΘ	NØ	NΘ	NØ	NΘ	NØ	NΘ	NØ	NΘ	NØ	NΘ	NØ	NΘ	NØ	NΘ	NØ	NΘ	NØ	NΘ
0.00	-8.65	-8.65	-6.30	-6.30	-5.31	-5.30	-4.75	-4.74	-4.40	-4.39	-4.17	-4.15	-4.01	-4.00	-3.92	-3.90	-3.87	-3.85	-3.86	-3.84
0.02	-8.60	-8.13	-6.25	-5.91	-5.25	-4.98	-4.69	-4.45	-4.33	-4.11	-4.10	-3.89	-3.94	-3.74	-3.84	-3.64	-3.78	-3.59	-3.76	-3.57
0.06	-8.60	-6.77	-6.25	-4.89	-5.25	-4.12	-4.68	-3.69	-4.33	-3.43	-4.10	-3.24	-3.93	-3.13	-3.83	-3.08	-3.77	-3.00	-3.75	-3.02
0.10	-8.40	-1.68	-6.25	-4.00	-5.25	-3.40	-4.69	-3.04	-4.33	-2.82	-4.10	-2.67	-3.93	-2.58	-3.83	-2.52	-3.77	-2.52	-3.75	-2.49
0.13			-6.24	-3.26	-5.25	-2.76	-4.68	-2.49	-4.33	-2.32	-4.10	-2.20	-3.93	-2.13	-3.83	-2.10	-3.77	-2.08	-3.75	-2.09
0.20			-6.20	-1.24	-5.25	-1.62	-4.68	-1.49	-4.33	-1.39	-4.10	-1.32	-3.93	-1.29	-3.82	-1.26	-3.77	-1.25	-3.75	-1.25
0.23					-5.24	-1.00	-4.68	-0.99	-4.33	-0.93	-4.10	-0.90	-3.93	-0.87	-3.82	-0.85	-3.77	-0.87	-3.75	-0.86
0.30					-5.29	-1.06	-4.68	-0.04	-4.33	-0.10	-4.10	-0.11	-3.93	-0.11	-3.82	-0.15	-3.79	-0.15	-3.75	-0.15
0.36							-4.67	0.75	-4.33	0.57	-4.10	0.52	-3.93	0.50	-3.82	0.47	-3.77	0.43	-3.75	0.40
0.40							-4.79	-0.96	-4.33	1.15	-4.10	0.96	-3.93	0.90	-3.82	0.88	-3.77	0.84	-3.75	0.83
0.50									-4.48	-0.90	-4.10	2.06	-3.93	1.78	-3.82	1.71	-3.77	1.68	-3.75	1.65
0.60											-4.28	-0.86	-3.92	2.74	-3.83	2.42	-3.77	2.40	-3.75	2.37
0.66													-3.89	2.83	-3.83	2.84	-3.77	2.72	-3.75	2.72
0.70													-4.15	-0.83	-3.82	3.26	-3.77	2.93	-3.75	2.93
0.80															-4.07	-0.81	-3.76	3.63	-3.75	3.33
0.83																	-3.74	3.78	-3.75	3.43
0.90																	-4.04	-0.81	-3.74	3.87
1.00																			-4.04	-0.81

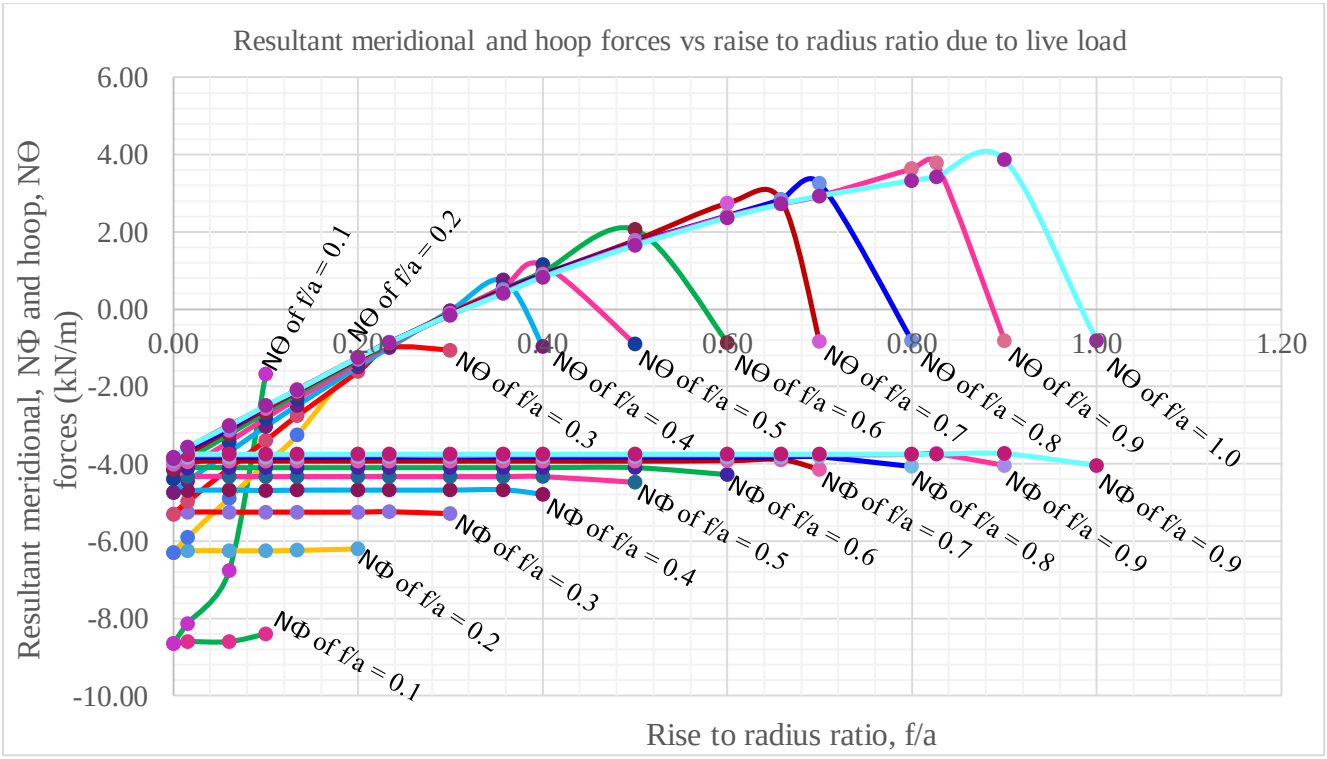

Figure 5- 7: Resultant meridional and hoop forces vs rise to radius ratio due to live load

5.2.3. Resultant forces due to wind load

Table 5- 8: Resultant meridional and hoop forces of all models

Rise to radius, f/a	Membrane meridional and hoop forces due to wind load for each models (kN/m)																			
	Model 1		Model 2		Model 3		Model 4		Model 5		Model 6		Model 7		Model 8		Model 9		Model 10	
	$N_Ø$	$N_Θ$	$N_Ø$	$N_Θ$	$N_Ø$	$N_Θ$	$N_Ø$	$N_Θ$	$N_Ø$	$N_Θ$	$N_Ø$	$N_Θ$	$N_Ø$	$N_Θ$	$N_Ø$	$N_Θ$	$N_Ø$	$N_Θ$	$N_Ø$	$N_Θ$
0.00	0.27	0.27	0.17	0.17	0.12	0.12	0.07	0.07	0.03	0.03	0.00	0.00	-0.02	-0.02	-0.06	-0.06	-0.09	-0.10	-1.23	-1.36
0.02	3.64	5.77	4.28	1.12	3.63	-0.51	2.61	-0.75	1.34	-0.58	-0.20	0.10	-1.13	0.64	-3.30	1.95	-5.58	3.52	-8.09	5.26
0.06	-1.63	22.91	1.33	9.80	1.79	4.70	1.55	2.26	0.86	0.77	-0.13	-0.08	-0.81	-0.25	-2.43	-0.42	-4.14	-0.36	-6.19	-0.02
0.10	-4.13	7.00	-0.42	14.52	0.84	7.62	0.97	4.01	0.62	1.52	-0.10	-0.17	-0.64	-0.76	-1.95	-1.83	-3.40	-2.68	-5.18	-3.05
0.13			-1.43	18.50	0.15	9.61	0.59	5.22	0.42	2.02	-0.08	-0.23	-0.53	-1.11	-1.66	-2.77	-2.97	-4.10	-4.57	-4.93
0.20			-3.50	7.29	-0.74	12.43	-0.07	7.09	0.15	2.86	-0.05	-0.33	-0.34	-1.66	-1.16	-4.23	-2.20	-6.38	-3.50	-8.11
0.23					-1.21	14.72	-0.38	7.87	0.02	3.22	-0.03	-0.38	-0.26	-1.90	-0.93	-4.92	-1.68	-7.90	-2.74	-10.48
0.30					-2.59	5.98	-0.99	9.59	-0.23	3.84	0.00	-0.46	-0.11	-2.30	-0.52	-5.97	-1.04	-9.57	-1.91	-12.76
0.36							-1.43	10.95	-0.44	4.33	0.03	-0.52	0.03	-2.61	-0.17	-6.84	-0.48	-10.95	-1.20	-14.54
0.40							-1.87	4.48	-0.60	4.90	0.05	-0.56	0.12	-2.83	0.08	-7.44	-0.10	-11.84	-0.69	-15.75
0.50									-0.97	2.30	0.09	-0.69	0.36	-3.28	0.70	-8.70	0.86	-13.71	0.54	-18.29
0.60											0.14	-0.34	0.60	-3.95	1.36	-9.80	1.91	-15.56	1.92	-20.75
0.66													0.73	-3.94	1.79	-10.68	2.57	-16.43	2.78	-22.08
0.70													0.87	-2.05	2.09	-11.67	2.74	-16.65	2.99	-22.24
0.80															2.84	-6.35	4.01	-19.70	4.65	-24.50
0.83																	4.35	-20.55	5.17	-25.23
0.90																	5.35	-11.39	6.63	-28.87
1.00																			8.73	-17.47

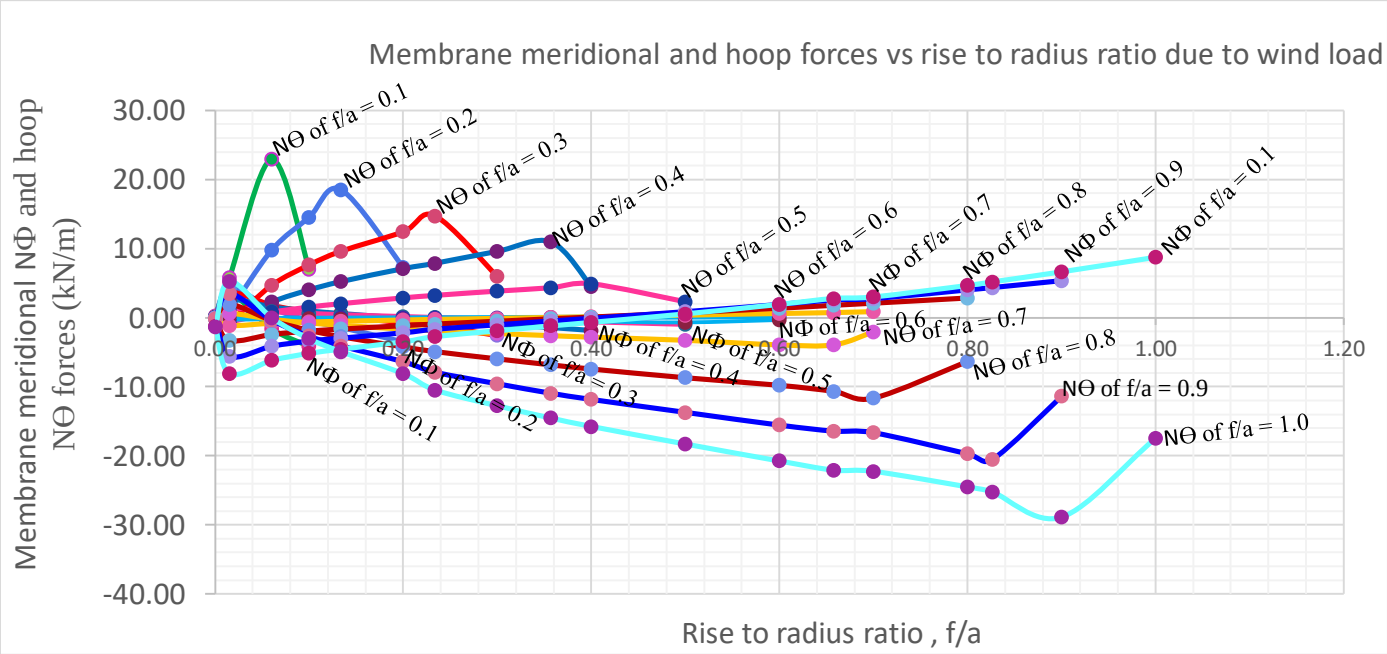

Figure 5- 8: Resultant meridional and hoop forces vs rise to radius ratio due to wind load

The software method analysis for each load cases have been performed for edge fixed boundary conditions. After analyzing all the models of spherical concrete domes with different rises gives similar values as theoretical values except around the edge due to variation of stiffness of default fixed support of dome and theoretically used ring beam. Further the followings have been observed.

1. In the case of fixed support, while moving from the apex to the edge the value of resultant hoop force is smaller than the theoretical values and changes its sign from tensile to compressive type after model 4. Thus the default fixed support is more stiffened than the theoretically used ring beam stiffness.
2. The rate of change of hoop forces from apex to edge are significant for more flatter type models.

CHAPTER 6 CONCLUSIONS AND RECCOMENDATIONS

6.1. Conclusions

According to the results and discussions on chapter five, the following major conclusions of ring beam effects on membrane forces are made for gravity loads by taking rise to radius ratio equal to 0.73 as a reference point, the value at which the edge shear and edge moments are minimum.

1. When rise to radius ratio decreased the linear type compressive membrane hoop forces are changed to exponential type superimposed hoop forces. While, the meridionals are slightly affected.
2. When rise to radius ratio increased the linear type tensile membrane hoop forces are decreased in magnitude and for hemispherical type they have been changed to compressive type around the edge. Whereas the meridionals have not been affected.
3. For rise to radius ratio up to 0.716 and 0.74 the edge moment and edge shear acted on the ring beam are outward to the dome respectively.
4. For rise to radius ratio after to 0.716 and 0.74 the edge moment and edge shear acted on the ring beam are towards the dome respectively.
5. The range of x-axis crossing points of rise to radius ratio (zero edge forces points) are the minimum bending forces ranges.
6. For rise to radius ratio value less than 0.5 the wind load acted on the dome is suction type as a result the internal membrane meridional and hoop forces are tensile type while for greater or equal to 0.50, the wind pressure acted towards the dome, thus the internal membrane meridional and hoop forces are compressive type.
7. For wind load the minimum membrane forces are in the range of 0.60 to 0.70.

6.2. Recommendations

Detailed and careful study of rise to radius ratio of a given spherical concrete dome of specified span length is the fundamental and most dominant issue to design it with insignificant edge effects so as to resist the external applied load in membrane behavior with insignificant bending fields.

In this particular paper, the range 0.72 – 0.74 of rise to radius ratio of the shell for gravity loads is best recommended. Within this range, the bending internal forces are minimum. Thus the range of x-axis crossing points of rise to radius ratio (zero edge forces points) are recommended to resist the external forces which acted on the dome in membrane actions with minimum bending forces due to ring beam.

Further works are needed to study the behavior and effect of bending forces on membrane forces by varying shell thickness from edge to apex.

REFERENCES

1) Andreas Hauso (2014), Analysis Methods for Thin Concrete Shells of Revolution, MSc thesis, Norwegian University of Science and Technology.
2) Andrew Borgart & Lonneke Tiggeler (2009), Computational Structural Form Finding and Optimization of Shell Structures, Delft, Netherlands.
3) D.P. Billington, (1982), Thin shell Concrete structure, Second Edition, McGraw-Hill, New York – Toronto.
4) Daryl L.Logan, A First Course in the Finite Element Method, Fourth Edition, United States.
5) David B. Farnsworth Jr. (1999), Behavior of Shell Structures,MSc thesis, Massachusetts Institute of Technology.
6) Ethiopian Building Code Standard EBCS-1, (1995), Basis of Design and Actions on Structures, Addis Ababa, Ethiopia.
7) Ethiopian Building Code Standard EBCS-2, (1995), Structural Use of Concrete, Addis Ababa, Ethiopia.
8) Eurocode 1, (prEN 1991-1-4), Actions on Structures – General Actions – Part 1-4: Wind Actions, Brussels.
9) Farshad, M., (1992), Design and Analysis of Shell Structure, EMPA, Switzerland.
10) Girish G M, Shri Mahadevan Iyer & Dr. Neeraja D (2015), Parametric Study on Behavior of Concrete Shell Under Uniform Loading', International Journal of Engineering & Technology, Vol.4 Issue 03, India.
11) Howard Paul Harrenstien, (1959), Configuration of Shell Structures for optimum stresses, PhD thesis, Iowa State University.
12) Ivana Mekjavic & Piculin, (2015), Structural Analysis and Optimization of Concrete Spherical and GroinedShells,Researchgate.Availablefrom:https://www.researchgate.net/publication/2651437360.
13) M. Eliassen and A. Huseby, (2018), The Digital workflow of Parametric Structural Design, MSc thesis, Norwegian University of Science and Technology.

APPENDIX A: Theoretical analysis results due to dead and live load

Table 0-1: Bending and membrane meridional and hoop forces of model 1 due to dead load

	ψ = α-Ø		Bending field (kN/m)		Membrane field (kN/m)		Total field (kN/m)	
$Ø^0$	Deg.	Rad.	NΘ	NØ	NΘ	NØ	NΘ	NØ
0.00	25.83	0.45	0.00	0.00	-106.37	-106.37	-106.37	-106.37
10.00	15.83	0.28	-0.04	-0.01	-102.33	-107.19	-102.37	-107.20
20.00	5.83	0.10	-21.54	-1.45	-90.24	-109.68	-111.77	-111.13
25.83	0.00	0.00	502.63	35.62	-79.52	-111.97	423.11	-76.34

According to this table, bending fields are negligible up to10 degrees but near the edge of the shell at an angle of 25.83 degrees, these forces reach their maximum value. This fact is the general behavior of shallow shell whose rise is 6.88m. The membrane fields are compressive throughout the shell. As the angle increases, the meridional force decreases while the hoop force increases. The total hoop force is compressive up to an angle nearly 22 degrees but becomes tensile force just away from 22 degrees with an abrupt increase in value. The total meridional force is tensile over the surface and decrease in value with increase of meridional angle.

Table 0-2: Bending and membrane meridional and hoop forces of model 2 due to dead load

	ψ = α-Ø		Bending field (kN/m)		Membrane field (kN/m)		Total field (kN/m)	
$Ø^0$	Deg.	Rad.	NΘ	NØ	NΘ	NØ	NΘ	NØ
0.00	36.87	0.64	0.00	0.00	-77.25	-77.25	-77.25	-77.25
10.00	26.87	0.47	0.00	0.00	-74.31	-77.84	-74.31	-77.84
20.00	16.87	0.29	0.02	0.00	-65.53	-79.65	-65.51	-79.66
25.83	11.04	0.19	-0.07	0.07	-57.75	-81.31	-57.82	-81.24
30.00	6.87	0.12	-14.37	-0.71	-51.00	-82.80	-65.37	-83.50
36.87	0.00	0.00	336.38	18.11	-37.77	-85.83	298.61	-67.73

According to this table, bending fields are negligible up to25.83 degrees but near the edge of the shell at an angle of 36.87 degrees, these forces reach their maximum value. The membrane fields are compressive throughout the shell. As the angle increases, the meridional force decreases while the hoop force increases. The total hoop force is compressive up to an angle nearly 31.5 degrees but becomes tensile force just away from 32 degrees with an abrupt increase in value. The total meridional force is tensile over the surface and show an abrupt decrease in value just about angle of 36.87. Similar

discussion can be made in the same way as these two tables with some modification of values of results.

Table 0-3: Bending and membrane meridional and hoop forces of model 3 due to dead load

	ψ = α-Ø		Bending field (kN/m)		Membrane field (kN/m)		Total field (kN/m)	
Ø^0	Deg.	Rad.	NΘ	NØ	NΘ	NØ	NΘ	NØ
0.00	45.56	0.80	0.00	0.00	-64.91	-64.91	-64.91	-64.91
10.00	35.56	0.62	0.00	0.00	-62.44	-65.40	-62.44	-65.40
20.00	25.56	0.45	0.00	0.00	-55.06	-66.92	-55.06	-66.92
25.83	19.73	0.34	-0.02	0.00	-48.52	-68.32	-48.54	-68.32
30.00	15.56	0.27	0.29	0.01	-42.85	-69.57	-42.56	-69.56
36.87	8.69	0.15	-7.24	-0.18	-31.73	-72.12	-38.97	-72.30
40.00	5.56	0.10	-2.87	-0.76	-25.94	-73.50	-28.81	-74.26
45.56	0.00	0.00	249.12	10.68	-14.54	-76.35	234.58	-65.67

Table 0-4: Bending and membrane meridional and hoop forces of model 4 due to dead load

	ψ = α-Ø		Bending field (kN/m)		Membrane field (kN/m)		Total field (kN/m)	
Ø^0	Deg.	Rad.	NΘ	NØ	NΘ	NØ	NΘ	NØ
0.00	53.13	0.93	0.00	0.00	-57.98	-57.98	-57.98	-57.98
10.00	43.13	0.75	0.00	0.00	-55.78	-58.43	-55.78	-58.43
20.00	33.13	0.58	0.00	0.00	-49.19	-59.79	-49.19	-59.79
25.83	27.30	0.48	0.00	0.00	-43.35	-61.03	-43.35	-61.03
30.00	23.13	0.40	-0.01	0.00	-38.28	-62.15	-38.30	-62.15
36.87	16.26	0.28	0.24	0.01	-28.35	-64.43	-28.11	-64.42
40.00	13.13	0.23	0.15	0.03	-23.17	-65.67	-23.02	-65.64
45.56	7.57	0.13	-8.21	-0.30	-12.99	-68.21	-21.19	-68.51
50.00	3.13	0.05	68.94	0.57	-3.95	-70.59	64.99	-70.02
53.13	0.00	0.00	187.28	6.38	2.90	-72.48	190.17	-66.10

Table 0-5: Bending and membrane meridional and hoop forces of model 5 due to dead load

	ψ = α-Ø		Bending field (kN/m)		Membrane field (kN/m)		Total field (kN/m)	
Ø^0	Deg.	Rad.	NΘ	NØ	NΘ	NØ	NΘ	NØ
0.00	60.00	1.05	0.00	0.00	-53.52	-53.52	-53.52	-53.52
10.00	50.00	0.87	0.00	0.00	-51.48	-53.93	-51.48	-53.93
20.00	40.00	0.70	0.00	0.00	-45.40	-55.18	-45.40	-55.18
25.83	34.17	0.60	0.00	0.00	-40.01	-56.33	-40.01	-56.33
30.00	30.00	0.52	0.00	0.00	-35.34	-57.36	-35.34	-57.36
36.87	23.13	0.40	-0.01	0.00	-26.16	-59.47	-26.17	-59.47
40.00	20.00	0.35	0.01	0.00	-21.39	-60.61	-21.37	-60.61
45.56	14.44	0.25	0.23	0.01	-11.99	-62.96	-11.75	-62.94
50.00	10.00	0.17	-3.02	-0.04	-3.65	-65.16	-6.67	-65.20
53.13	6.87	0.12	-5.11	-0.24	2.68	-66.90	-2.44	-67.14
60.00	0.00	0.00	135.42	3.57	17.84	-71.36	153.26	-67.79

Table 0-6: Bending and membrane meridional and hoop forces of model 6 due to dead load

	ψ = α-Ø		Bending field (kN/m)		Membrane field (kN/m)		Total field (kN/m)	
Ø^0	Deg.	Rad.	NΘ	NØ	NΘ	NØ	NΘ	NØ
0.00	66.42	1.16	0.00	0.00	-50.57	-50.57	-50.57	-50.57
10.00	56.42	0.98	0.00	0.00	-48.64	-50.95	-48.64	-50.95
20.00	46.42	0.81	0.00	0.00	-42.90	-52.14	-42.90	-52.14
25.83	40.59	0.71	0.00	0.00	-37.80	-53.23	-37.80	-53.23
30.00	36.42	0.64	0.00	0.00	-33.39	-54.20	-33.39	-54.20
36.87	29.55	0.52	0.00	0.00	-24.72	-56.19	-24.72	-56.19
40.00	26.42	0.46	0.00	0.00	-20.21	-57.27	-20.21	-57.27
45.56	20.86	0.36	0.00	0.00	-11.33	-59.49	-11.32	-59.49
50.00	16.42	0.29	0.14	0.00	-3.45	-61.56	-3.31	-61.56
53.13	13.29	0.23	-0.02	0.01	2.53	-63.21	2.51	-63.20
60.00	6.42	0.11	-2.43	-0.14	16.86	-67.42	14.42	-67.56
66.42	0.00	0.00	87.87	1.64	31.78	-72.24	119.65	-70.60

Table 0-7: Table Bending and membrane meridional and hoop forces of model 7 due to dead load

	ψ = α-Ø		Bending field (kN/m)		Membrane field (kN/m)		Total field (kN/m)	
$Ø^0$	Deg.	Rad.	NΘ	NØ	NΘ	NØ	NΘ	NØ
0.00	72.53	1.27	0.00	0.00	-48.59	-48.59	-48.59	-48.59
10.00	62.53	1.09	0.00	0.00	-46.74	-48.96	-46.74	-48.96
20.00	52.53	0.92	0.00	0.00	-41.22	-50.10	-41.22	-50.10
25.83	46.70	0.82	0.00	0.00	-36.33	-51.15	-36.33	-51.15
30.00	42.53	0.74	0.00	0.00	-32.08	-52.08	-32.08	-52.08
36.87	35.66	0.62	0.00	0.00	-23.76	-53.99	-23.76	-53.99
40.00	32.53	0.57	0.00	0.00	-19.42	-55.03	-19.42	-55.03
45.56	26.97	0.47	0.00	0.00	-10.88	-57.16	-10.88	-57.16
50.00	22.53	0.39	0.00	0.00	-3.31	-59.16	-3.31	-59.16
53.13	19.40	0.34	0.01	0.00	2.43	-60.74	2.44	-60.74
60.00	12.53	0.22	0.01	0.00	16.20	-64.79	16.21	-64.78
66.42	6.11	0.11	-2.00	-0.05	30.54	-69.41	28.54	-69.46
70.00	2.53	0.04	11.64	0.01	39.18	-72.41	50.82	-72.40
72.53	0.00	0.00	40.59	0.36	45.57	-74.74	86.16	-74.38

Table 0-8: Bending and membrane meridional and hoop forces of model 8 due to dead load

	ψ = α-Ø		Bending field (kN/m)		Membrane field (kN/m)		Total field (kN/m)	
$Ø^0$	Deg.	Rad.	NΘ	NØ	NΘ	NØ	NΘ	NØ
0.00	78.45	1.37	0.00	0.00	-47.31	-47.31	-47.31	-47.31
10.00	68.45	1.19	0.00	0.00	-45.51	-47.67	-45.51	-47.67
20.00	58.45	1.02	0.00	0.00	-40.13	-48.78	-40.13	-48.78
25.83	52.62	0.92	0.00	0.00	-35.37	-49.80	-35.37	-49.80
30.00	48.45	0.85	0.00	0.00	-31.24	-50.70	-31.24	-50.70
36.87	41.58	0.73	0.00	0.00	-23.13	-52.56	-23.13	-52.56
40.00	38.45	0.67	0.00	0.00	-18.90	-53.57	-18.90	-53.57
45.56	32.89	0.57	0.00	0.00	-10.60	-55.65	-10.60	-55.65
50.00	28.45	0.50	0.00	0.00	-3.22	-57.59	-3.22	-57.59
53.13	25.32	0.44	0.00	0.00	2.37	-59.13	2.37	-59.13
60.00	18.45	0.32	-0.04	0.00	15.77	-63.08	15.73	-63.08
66.42	12.03	0.21	0.58	0.00	29.73	-67.58	30.31	-67.58
70.00	8.45	0.15	0.86	0.03	38.14	-70.50	39.00	-70.48
72.53	5.92	0.10	-4.09	0.01	44.37	-72.77	40.28	-72.76
78.45	0.00	0.00	-9.61	-0.36	59.89	-78.83	50.28	-79.19

Table 0-9: Bending and membrane meridional and hoop forces of model 9 due to dead load

	ψ = α-Ø		Bending field (kN/m)		Membrane field (kN/m)		Total field (kN/m)	
$Ø^0$	Deg.	Rad.	NΘ	NØ	NΘ	NØ	NΘ	NØ
0.00	84.27	1.47	0.00	0.00	-46.58	-46.58	-46.58	-46.58
10.00	74.27	1.30	0.00	0.00	-44.81	-46.94	-44.81	-46.94
20.00	64.27	1.12	0.00	0.00	-39.52	-48.03	-39.52	-48.03
25.83	58.44	1.02	0.00	0.00	-34.82	-49.03	-34.82	-49.03
30.00	54.27	0.95	0.00	0.00	-30.76	-49.93	-30.76	-49.93
36.87	47.40	0.83	0.00	0.00	-22.77	-51.76	-22.77	-51.76
40.00	44.27	0.77	0.00	0.00	-18.61	-52.75	-18.61	-52.75
45.56	38.71	0.68	0.00	0.00	-10.43	-54.80	-10.43	-54.80
50.00	34.27	0.60	0.00	0.00	-3.17	-56.71	-3.17	-56.71
53.13	31.14	0.54	0.00	0.00	2.33	-58.23	2.33	-58.23
60.00	24.27	0.42	0.01	0.00	15.53	-62.11	15.53	-62.11
66.42	17.85	0.31	-0.14	0.00	29.28	-66.54	29.13	-66.55
70.00	14.27	0.25	0.17	0.00	37.56	-69.42	37.73	-69.42
72.53	11.74	0.20	1.66	0.01	43.68	-71.65	45.34	-71.64
78.45	5.82	0.10	-8.06	0.04	58.97	-77.62	50.91	-77.59
80.00	4.27	0.07	-29.15	-0.05	63.20	-79.38	34.05	-79.43
84.27	0.00	0.00	-65.93	-0.51	75.40	-84.71	9.48	-85.22

Table 0-10: Bending and membrane meridional and hoop forces of model 10 due to dead load

	ψ = α-Ø		Bending field (kN/m)		Membrane field (kN/m)		Total field (kN/m)	
$Ø^0$	Deg.	Rad.	NΘ	NØ	NΘ	NØ	NΘ	NØ
0.00	90.00	1.57	0.00	0.00	-46.35	-46.35	-46.35	-46.35
10.00	80.00	1.40	0.00	0.00	-44.59	-46.70	-44.59	-46.70
20.00	70.00	1.22	0.00	0.00	-39.32	-47.79	-39.32	-47.79
25.83	64.17	1.12	0.00	0.00	-34.65	-48.79	-34.65	-48.79
30.00	60.00	1.05	0.00	0.00	-30.60	-49.68	-30.60	-49.68
36.87	53.13	0.93	0.00	0.00	-22.66	-51.50	-22.66	-51.50
40.00	50.00	0.87	0.00	0.00	-18.52	-52.49	-18.52	-52.49
45.56	44.44	0.78	0.00	0.00	-10.38	-54.52	-10.38	-54.52
50.00	40.00	0.70	0.00	0.00	-3.16	-56.43	-3.16	-56.43
53.13	36.87	0.64	0.00	0.00	2.32	-57.94	2.32	-57.94
60.00	30.00	0.52	0.00	0.00	15.45	-61.80	15.45	-61.80
66.42	23.58	0.41	0.01	0.00	29.13	-66.21	29.14	-66.21
70.00	20.00	0.35	-0.10	0.00	37.37	-69.07	37.26	-69.08
72.53	17.47	0.30	-0.27	0.00	43.47	-71.30	43.19	-71.30
78.45	11.55	0.20	3.14	0.01	58.67	-77.24	61.81	-77.23
80.00	10.00	0.17	5.68	0.03	62.89	-78.98	68.56	-78.95
84.27	5.73	0.10	-13.88	0.03	75.03	-84.28	61.15	-84.25
90.00	0.00	0.00	-131.48	0.00	92.70	-92.70	-38.78	-92.70

Table 0-11: Bending and membrane meridional and hoop forces of model 1 due to live load

:`	ψ = α-Ø		Bending field (kN/m)		Membrane field (kN/m)		Total field (kN/m)	
	Deg.	Rad.	NΘ	NØ	NΘ	NØ	NΘ	NØ
0.00	25.83	0.45	0.00	0.00	-8.61	-8.61	-8.61	-8.61
10.00	15.83	0.28	0.00	0.00	-8.09	-8.61	-8.09	-8.61
20.00	5.83	0.10	-1.74	-0.12	-6.59	-8.61	-8.34	-8.72
25.83	0.00	0.00	40.67	2.88	-5.34	-8.61	35.33	-5.72

Table 0-12: Bending and membrane meridional and hoop forces of model 2 due to live load

Ø^0	ψ = α-Ø		Bending field (kN/m)		Membrane field (kN/m)		Total field (kN/m)	
	Deg.	Rad.	NΘ	NØ	NΘ	NØ	NΘ	NØ
0.00	36.87	0.64	0.00	0.00	-6.25	-6.25	-6.25	-6.25
10.00	26.87	0.47	0.00	0.00	-5.87	-6.25	-5.87	-6.25
20.00	16.87	0.29	0.00	0.00	-4.79	-6.25	-4.79	-6.25
25.83	11.04	0.19	-0.01	0.01	-3.88	-6.25	-3.88	-6.24
30.00	6.87	0.12	-1.16	-0.06	-3.13	-6.25	-4.29	-6.31
36.87	0.00	0.00	27.22	0.00	-1.75	-6.25	25.47	-6.25

Table 0-13: Bending and membrane meridional and hoop forces of model 3 due to live load

Ø^0	ψ = α-Ø		Bending field (kN/m)		Membrane field (kN/m)		Total field (kN/m)	
	Deg.	Rad.	NΘ	NØ	NΘ	NØ	NΘ	NØ
0.00	45.56	0.80	0.00	0.00	-5.25	-5.25	-5.25	-5.25
10.00	35.56	0.62	0.00	0.00	-4.93	-5.25	-4.93	-5.25
20.00	25.56	0.45	0.00	0.00	-4.02	-5.25	-4.02	-5.25
25.83	19.73	0.34	0.00	0.00	-3.26	-5.25	-3.26	-5.25
30.00	15.56	0.27	0.02	0.00	-2.63	-5.25	-2.60	-5.25
36.87	8.69	0.15	-0.59	-0.01	-1.47	-5.25	-2.06	-5.27
40.00	5.56	0.10	-0.23	-0.06	-0.91	-5.25	-1.14	-5.31
45.56	0.00	0.00	20.16	0.00	0.10	-5.25	20.26	-5.25

Table 0-14: Bending and membrane meridional and hoop forces of model 4 due to live load

Ø^0	ψ = α-Ø		Bending field (kN/m)		Membrane field (kN/m)		Total field (kN/m)	
	Deg.	Rad.	NΘ	NØ	NΘ	NØ	NΘ	NØ
0.00	53.13	0.93	0.00	0.00	-4.69	-4.69	-4.69	-4.69
10.00	43.13	0.75	0.00	0.00	-4.41	-4.69	-4.41	-4.69
20.00	33.13	0.58	0.00	0.00	-3.59	-4.69	-3.59	-4.69
25.83	27.30	0.48	0.00	0.00	-2.91	-4.69	-2.91	-4.69
30.00	23.13	0.40	0.00	0.00	-2.35	-4.69	-2.35	-4.69
36.87	16.26	0.28	0.02	0.00	-1.31	-4.69	-1.29	-4.69
40.00	13.13	0.23	0.01	0.00	-0.81	-4.69	-0.80	-4.69
45.56	7.57	0.13	-0.66	-0.02	0.09	-4.69	-0.57	-4.72
50.00	3.13	0.05	5.58	0.05	0.81	-4.69	6.39	-4.65
53.13	0.00	0.00	15.15	0.00	1.31	-4.69	16.47	-4.69

Table 0-15: Bending and membrane meridional and hoop forces of model 5 due to live load

:Ø^0	ψ = α-Ø		Bending field (kN/m)		Membrane field (kN/m)		Total field (kN/m)	
	Deg.	Rad.	NΘ	NØ	NΘ	NØ	NΘ	NØ
0.00	60.00	1.05	0.00	0.00	-4.33	-4.33	-4.33	-4.33
10.00	50.00	0.87	0.00	0.00	-4.07	-4.33	-4.07	-4.33
20.00	40.00	0.70	0.00	0.00	-3.32	-4.33	-3.32	-4.33
25.83	34.17	0.60	0.00	0.00	-2.69	-4.33	-2.69	-4.33
30.00	30.00	0.52	0.00	0.00	-2.17	-4.33	-2.16	-4.33
36.87	23.13	0.40	0.00	0.00	-1.21	-4.33	-1.21	-4.33
40.00	20.00	0.35	0.00	0.00	-0.75	-4.33	-0.75	-4.33
45.56	14.44	0.25	0.02	0.00	0.08	-4.33	0.10	-4.33
50.00	10.00	0.17	-0.24	0.00	0.75	-4.33	0.51	-4.33
53.13	6.87	0.12	-0.41	-0.02	1.21	-4.33	0.80	-4.35
60.00	0.00	0.00	10.96	0.00	2.17	-4.33	13.12	-4.33

Table 0-16: Bending and membrane meridional and hoop forces of model 6 due to live load

Ø^0	ψ = α-Ø		Bending field (kN/m)		Membrane field (kN/m)		Total field (kN/m)	
	Deg.	Rad.	NΘ	NØ	NΘ	NØ	NΘ	NØ
0.00	66.42	1.16	0.00	0.00	-4.09	-4.09	-4.09	-4.09
10.00	56.42	0.98	0.00	0.00	-3.84	-4.09	-3.84	-4.09
20.00	46.42	0.81	0.00	0.00	-3.13	-4.09	-3.13	-4.09
25.83	40.59	0.71	0.00	0.00	-2.54	-4.09	-2.54	-4.09
30.00	36.42	0.64	0.00	0.00	-2.05	-4.09	-2.05	-4.09
36.87	29.55	0.52	0.00	0.00	-1.15	-4.09	-1.15	-4.09
40.00	26.42	0.46	0.00	0.00	-0.71	-4.09	-0.71	-4.09
45.56	20.86	0.36	0.00	0.00	0.08	-4.09	0.08	-4.09
50.00	16.42	0.29	0.01	0.00	0.71	-4.09	0.72	-4.09
53.13	13.29	0.23	0.00	0.00	1.15	-4.09	1.14	-4.09
60.00	6.42	0.11	-0.20	-0.01	2.05	-4.09	1.85	-4.10
66.42	0.00	0.00	7.11	0.00	2.78	-4.09	9.89	-4.09

Table 0-17: Bending and membrane meridional and hoop forces of model 7 due to live load

Ø^0	ψ = α-Ø		Bending field (kN/m)		Membrane field (kN/m)		Total field (kN/m)	
	Deg.	Rad.	NΘ	NØ	NΘ	NØ	NΘ	NØ
0.00	72.53	1.27	0.00	0.00	-3.93	-3.93	-3.93	-3.93
10.00	62.53	1.09	0.00	0.00	-3.69	-3.93	-3.69	-3.93
20.00	52.53	0.92	0.00	0.00	-3.01	-3.93	-3.01	-3.93
25.83	46.70	0.82	0.00	0.00	-2.44	-3.93	-2.44	-3.93
30.00	42.53	0.74	0.00	0.00	-1.97	-3.93	-1.97	-3.93
36.87	35.66	0.62	0.00	0.00	-1.10	-3.93	-1.10	-3.93
40.00	32.53	0.57	0.00	0.00	-0.68	-3.93	-0.68	-3.93
45.56	26.97	0.47	0.00	0.00	0.08	-3.93	0.08	-3.93
50.00	22.53	0.39	0.00	0.00	0.68	-3.93	0.68	-3.93
53.13	19.40	0.34	0.00	0.00	1.10	-3.93	1.10	-3.93
60.00	12.53	0.22	0.00	0.00	1.97	-3.93	1.97	-3.93
66.42	6.11	0.11	-0.16	0.00	2.67	-3.93	2.51	-3.94
70.00	2.53	0.04	0.94	0.00	3.01	-3.93	3.95	-3.93
72.53	0.00	0.00	3.28	0.00	3.22	-3.93	6.51	-3.93

Table 0-18: Bending and membrane meridional and hoop forces of model 8 due to live load

Ø^0	ψ = α-Ø		Bending field (kN/m)		Membrane field (kN/m)		Total field (kN/m)	
	Deg.	Rad.	NΘ	NØ	NΘ	NØ	NΘ	NØ
0.00	78.45	1.37	0.00	0.00	-3.83	-3.83	-3.83	-3.83
10.00	68.45	1.19	0.00	0.00	-3.60	-3.83	-3.60	-3.83
20.00	58.45	1.02	0.00	0.00	-2.93	-3.83	-2.93	-3.83
25.83	52.62	0.92	0.00	0.00	-2.37	-3.83	-2.37	-3.83
30.00	48.45	0.85	0.00	0.00	-1.91	-3.83	-1.91	-3.83
36.87	41.58	0.73	0.00	0.00	-1.07	-3.83	-1.07	-3.83
40.00	38.45	0.67	0.00	0.00	-0.66	-3.83	-0.66	-3.83
45.56	32.89	0.57	0.00	0.00	0.07	-3.83	0.07	-3.83
50.00	28.45	0.50	0.00	0.00	0.66	-3.83	0.66	-3.83
53.13	25.32	0.44	0.00	0.00	1.07	-3.83	1.07	-3.83
60.00	18.45	0.32	0.00	0.00	1.91	-3.83	1.91	-3.83
66.42	12.03	0.21	0.05	0.00	2.60	-3.83	2.65	-3.83
70.00	8.45	0.15	0.07	0.00	2.93	-3.83	3.00	-3.83
72.53	5.92	0.10	-0.33	0.00	3.14	-3.83	2.81	-3.83
78.45	0.00	0.00	-0.78	0.00	3.52	-3.83	2.74	-3.83

Table 0-19: Bending and membrane meridional and hoop forces of model 9 due to live load

Ø^0	ψ = α-Ø		Bending field (kN/m)		Membrane field (kN/m)		Total field (kN/m)	
	Deg.	Rad.	NΘ	NØ	NΘ	NØ	NΘ	NØ
0.00	84.27	1.47	0.00	0.00	-3.77	-3.77	-3.77	-3.77
10.00	74.27	1.30	0.00	0.00	-3.54	-3.77	-3.54	-3.77
20.00	64.27	1.12	0.00	0.00	-2.89	-3.77	-2.89	-3.77
25.83	58.44	1.02	0.00	0.00	-2.34	-3.77	-2.34	-3.77
30.00	54.27	0.95	0.00	0.00	-1.88	-3.77	-1.88	-3.77
36.87	47.40	0.83	0.00	0.00	-1.06	-3.77	-1.06	-3.77
40.00	44.27	0.77	0.00	0.00	-0.65	-3.77	-0.65	-3.77
45.56	38.71	0.68	0.00	0.00	0.07	-3.77	0.07	-3.77
50.00	34.27	0.60	0.00	0.00	0.65	-3.77	0.65	-3.77
53.13	31.14	0.54	0.00	0.00	1.06	-3.77	1.06	-3.77
60.00	24.27	0.42	0.00	0.00	1.88	-3.77	1.88	-3.77
66.42	17.85	0.31	-0.01	0.00	2.56	-3.77	2.55	-3.77
70.00	14.27	0.25	0.01	0.00	2.89	-3.77	2.90	-3.77
72.53	11.74	0.20	0.13	0.00	3.09	-3.77	3.22	-3.77
78.45	5.82	0.10	-0.65	0.00	3.47	-3.77	2.81	-3.77
80.00	4.27	0.07	-2.36	0.00	3.54	-3.77	1.18	-3.77
84.27	0.00	0.00	-5.33	0.00	3.69	-3.77	-1.64	-3.77

Table 0-20: Bending and membrane meridional and hoop forces of model 10 due to live load

Ø^0	ψ = α-Ø		Bending field (kN/m)		Membrane field (kN/m)		Total field (kN/m)	
	Deg.	Rad.	NΘ	NØ	NΘ	NØ	NΘ	NØ
0.00	90.00	1.57	0.00	0.00	-3.75	-3.75	-3.75	-3.75
10.00	80.00	1.40	0.00	0.00	-3.52	-3.75	-3.52	-3.75
20.00	70.00	1.22	0.00	0.00	-2.87	-3.75	-2.87	-3.75
25.83	64.17	1.12	0.00	0.00	-2.33	-3.75	-2.33	-3.75
30.00	60.00	1.05	0.00	0.00	-1.88	-3.75	-1.87	-3.75
36.87	53.13	0.93	0.00	0.00	-1.05	-3.75	-1.05	-3.75
40.00	50.00	0.87	0.00	0.00	-0.65	-3.75	-0.65	-3.75
45.56	44.44	0.78	0.00	0.00	0.07	-3.75	0.07	-3.75
50.00	40.00	0.70	0.00	0.00	0.65	-3.75	0.65	-3.75
53.13	36.87	0.64	0.00	0.00	1.05	-3.75	1.05	-3.75
60.00	30.00	0.52	0.00	0.00	1.88	-3.75	1.88	-3.75
66.42	23.58	0.41	0.00	0.00	2.55	-3.75	2.55	-3.75
70.00	20.00	0.35	-0.01	0.00	2.87	-3.75	2.86	-3.75
72.53	17.47	0.30	-0.02	0.00	3.07	-3.75	3.05	-3.75
78.45	11.55	0.20	0.25	0.00	3.45	-3.75	3.70	-3.75
80.00	10.00	0.17	0.46	0.00	3.52	-3.75	3.98	-3.75
84.27	5.73	0.10	-1.12	0.00	3.68	-3.75	2.55	-3.75
90.00	0.00	0.00	-10.64	0.00	3.75	-3.75	-6.89	-3.75

APPENDIX B: SAP2000 analysis results of all models for each load cases

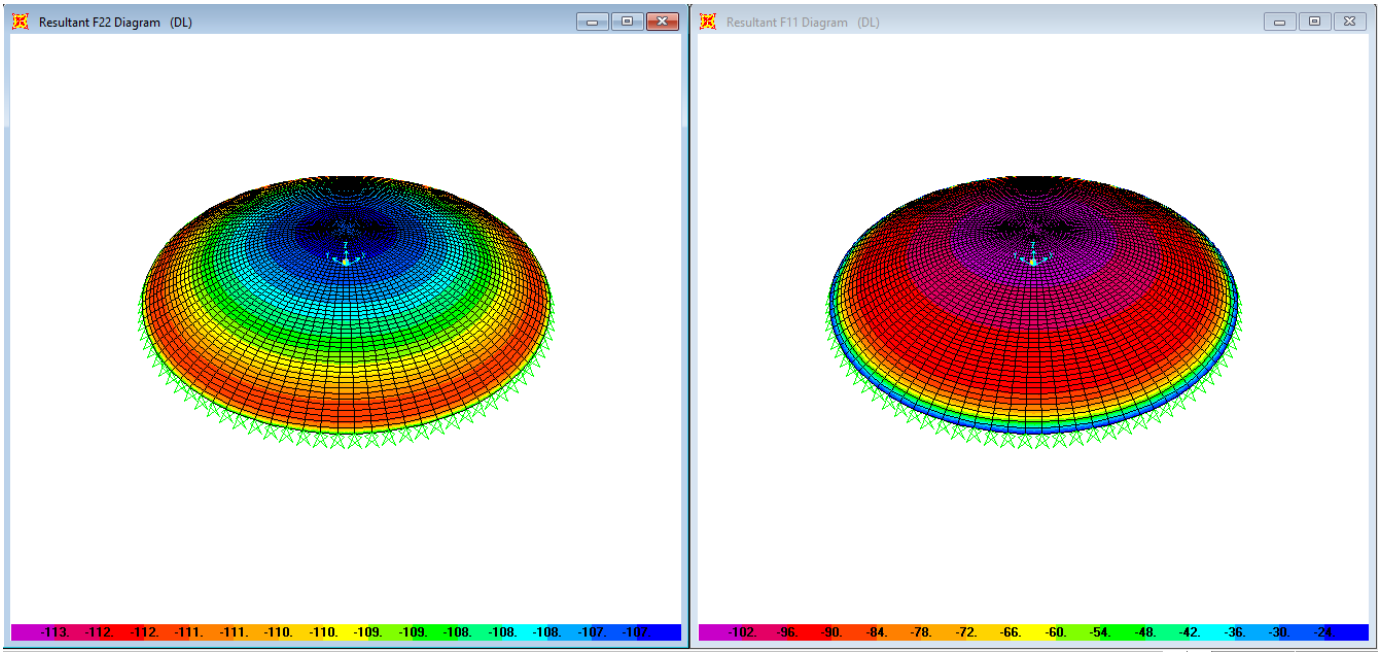

Figure 0-1: Resultant meridional and hoop forces of model 1 due to dead load

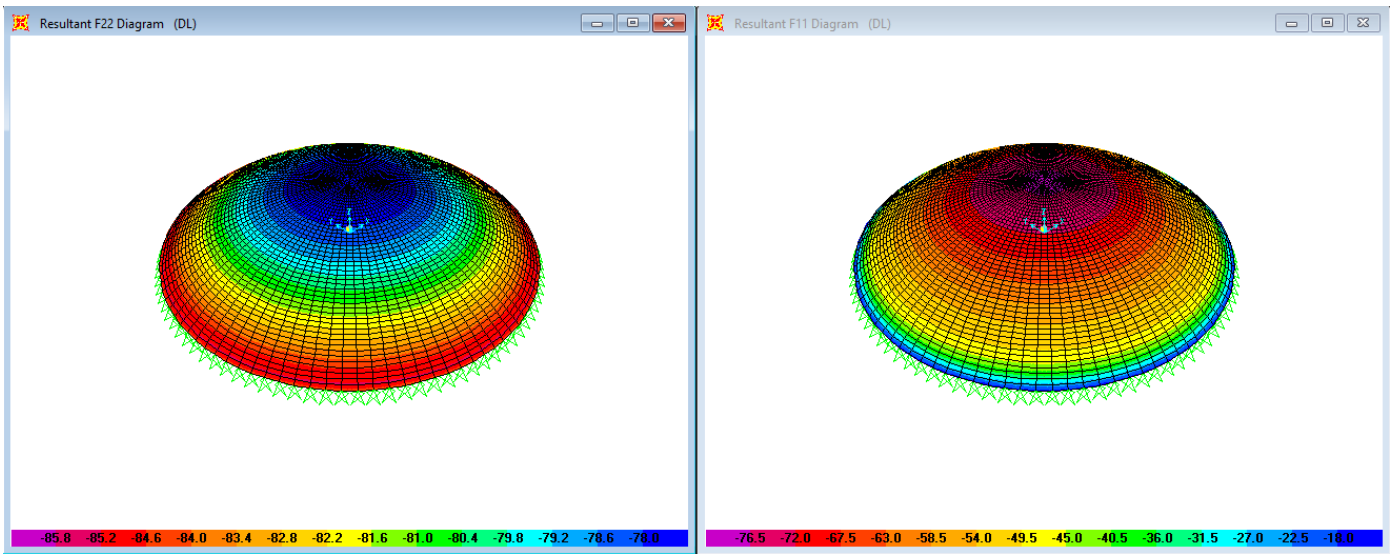

Figure 0-2: Resultant meridional and hoop forces of model 2 due to dead load

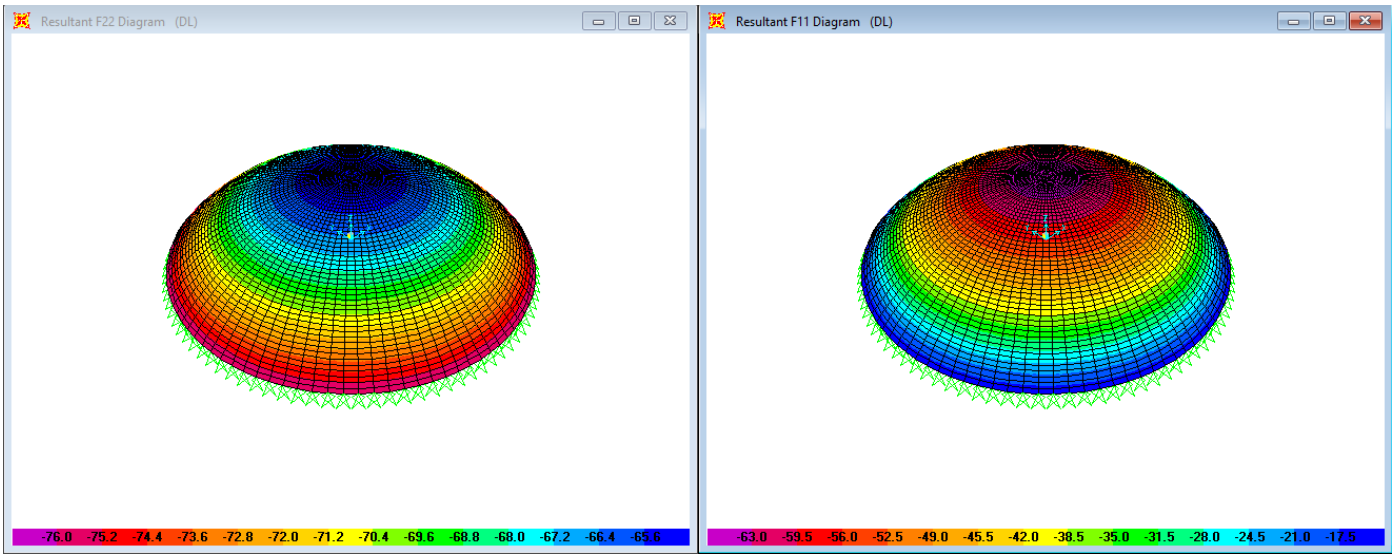

Figure 0-3: Resultant meridional and hoop forces of model 3 due to dead load

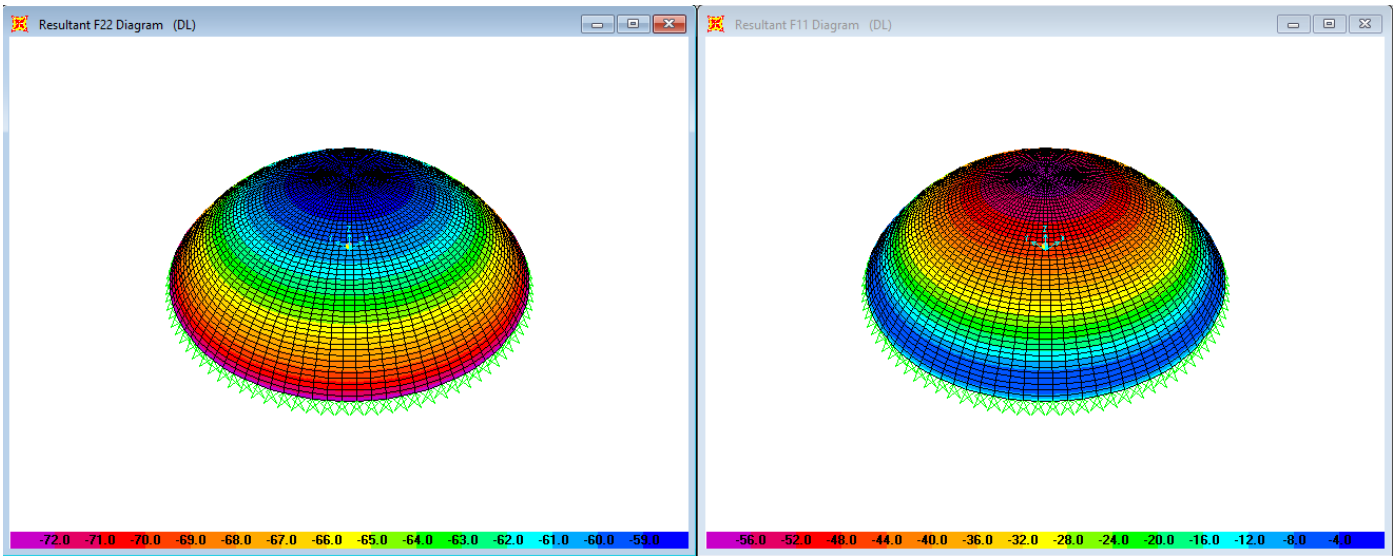

Figure 0-4: Resultant meridional and hoop forces of model 4 due to dead load

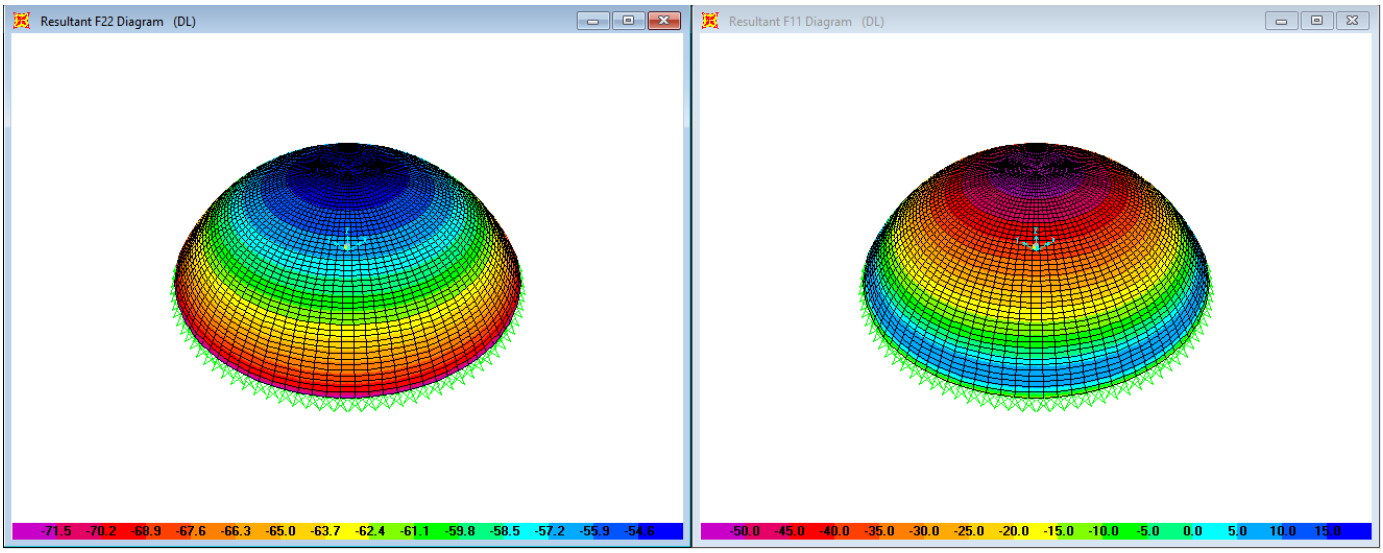

Figure 0-5: Resultant meridional and hoop forces of model 5 due to dead load

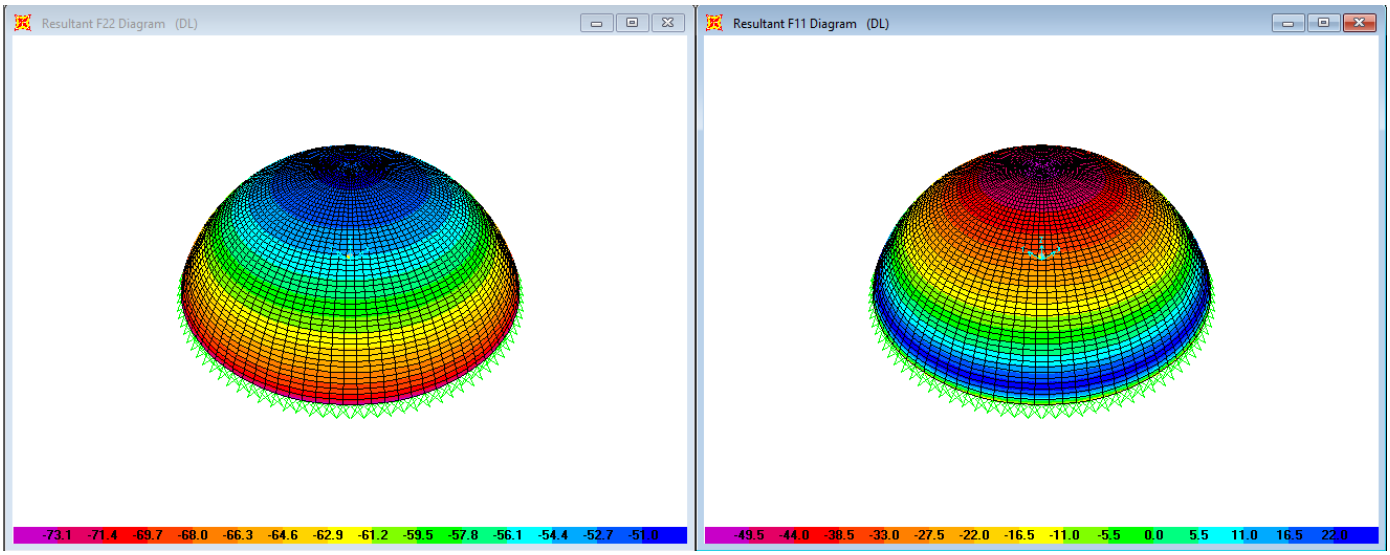

Figure 0-6: Resultant meridional and hoop forces of model 6 due to dead load

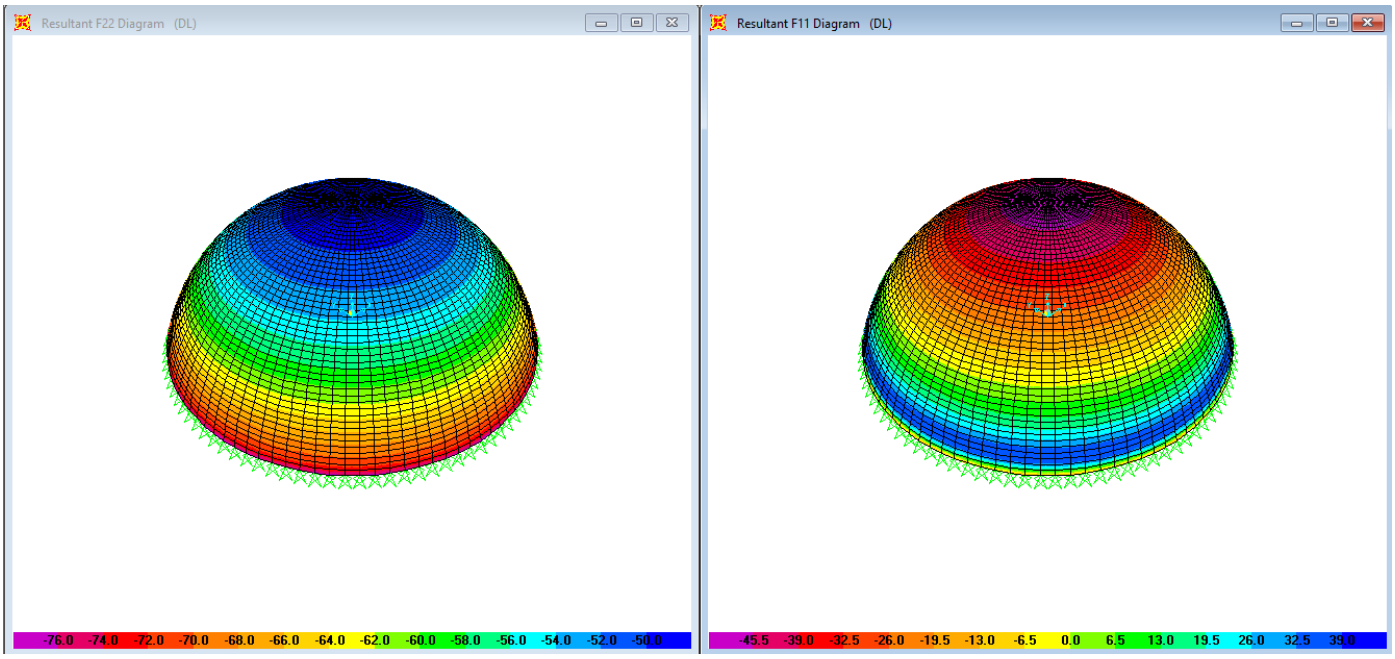

Figure 0-7: Resultant meridional and hoop forces of model 7 due to dead load

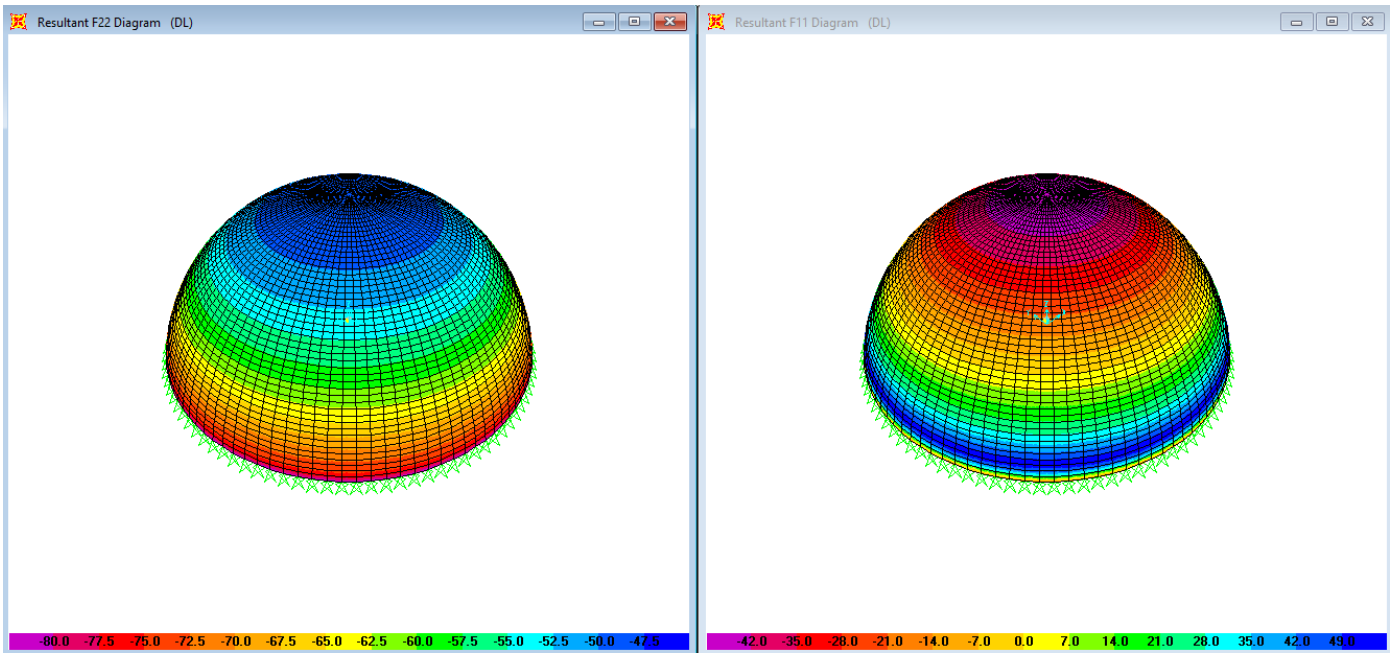

Figure 0-8: Resultant meridional and hoop forces of model 8 due to dead load

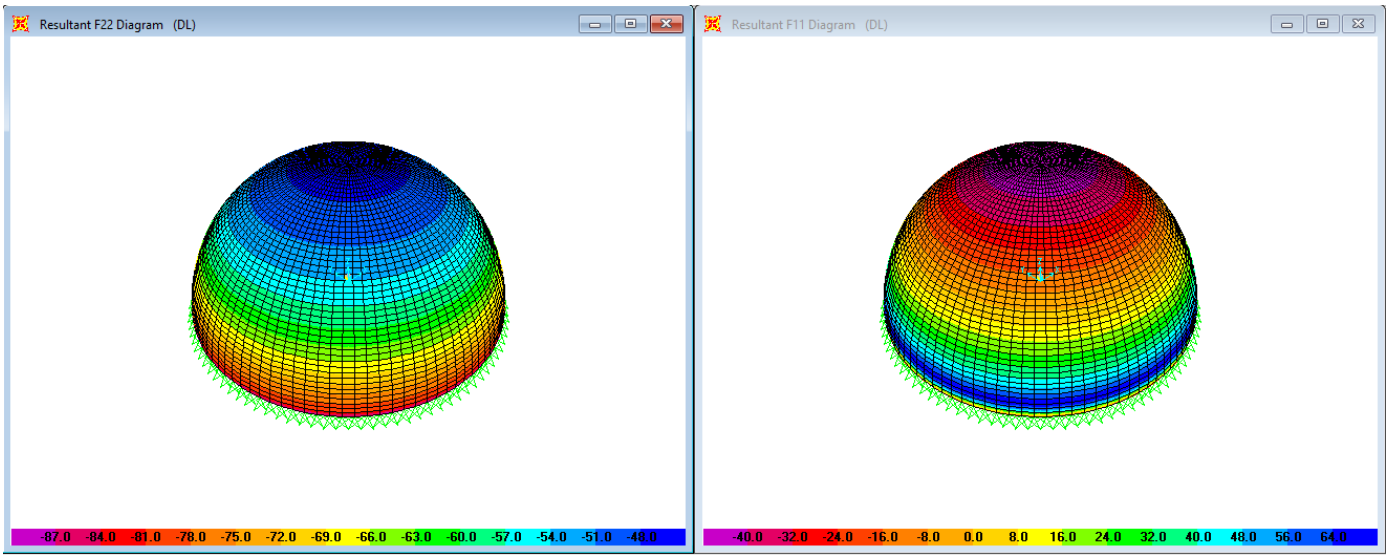

Figure 0-9: Resultant meridional and hoop forces of model 9 due to dead load

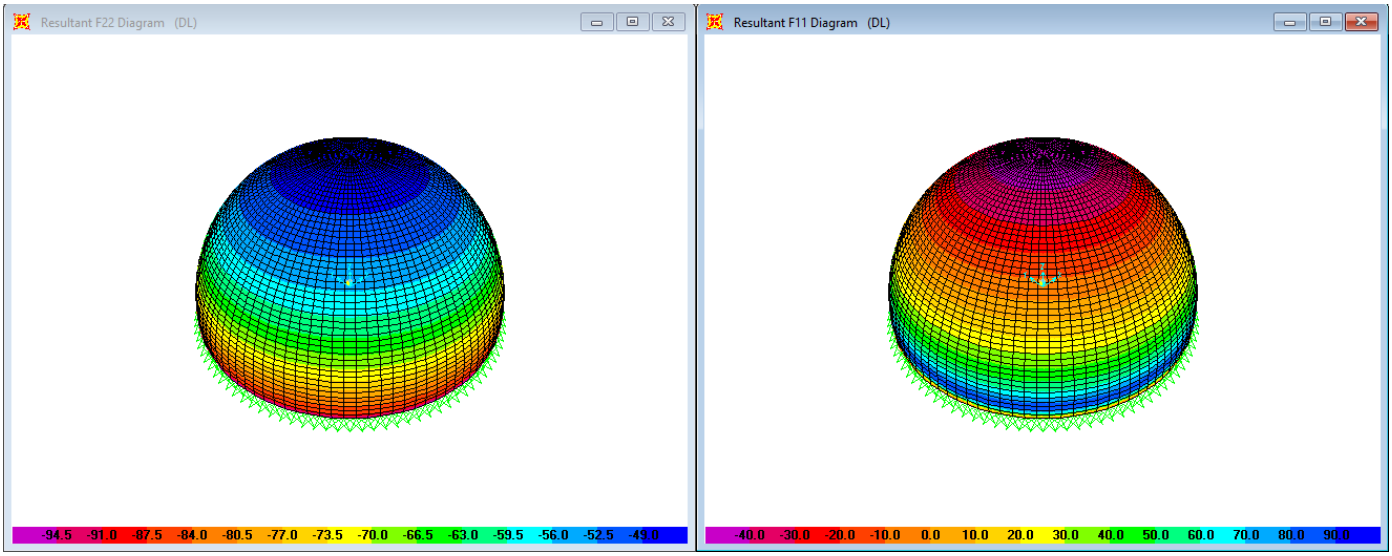

Figure 0-10: Resultant meridional and hoop forces of model 10 due to dead load

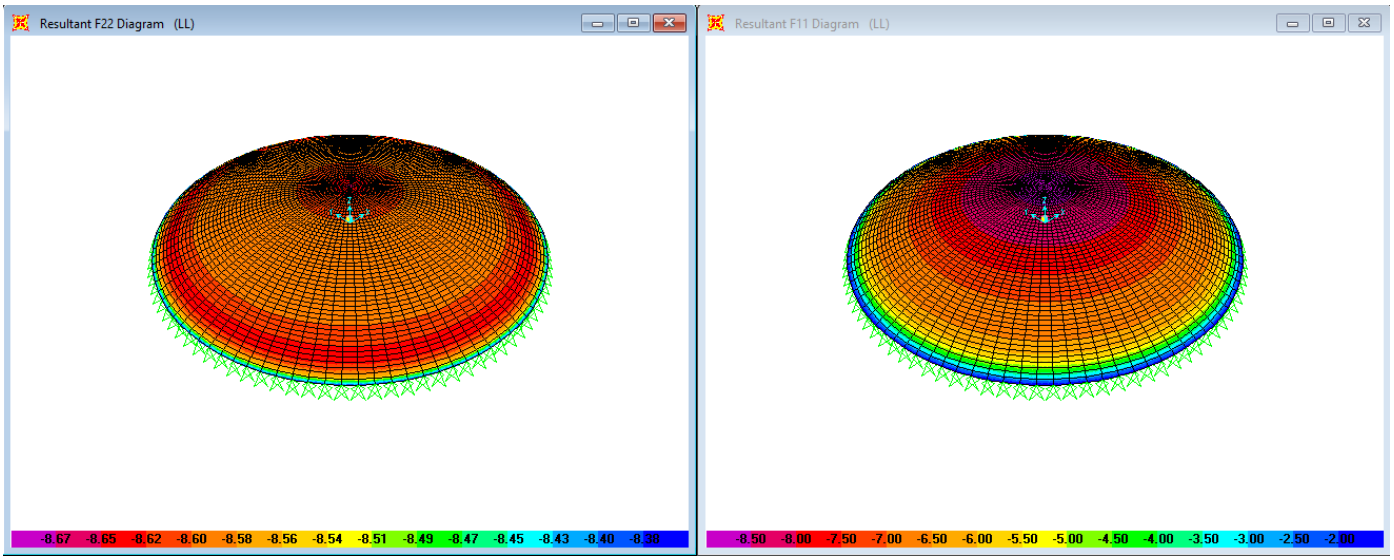

Figure 0-11: Resultant meridional and hoop forces of model 1 due to live load

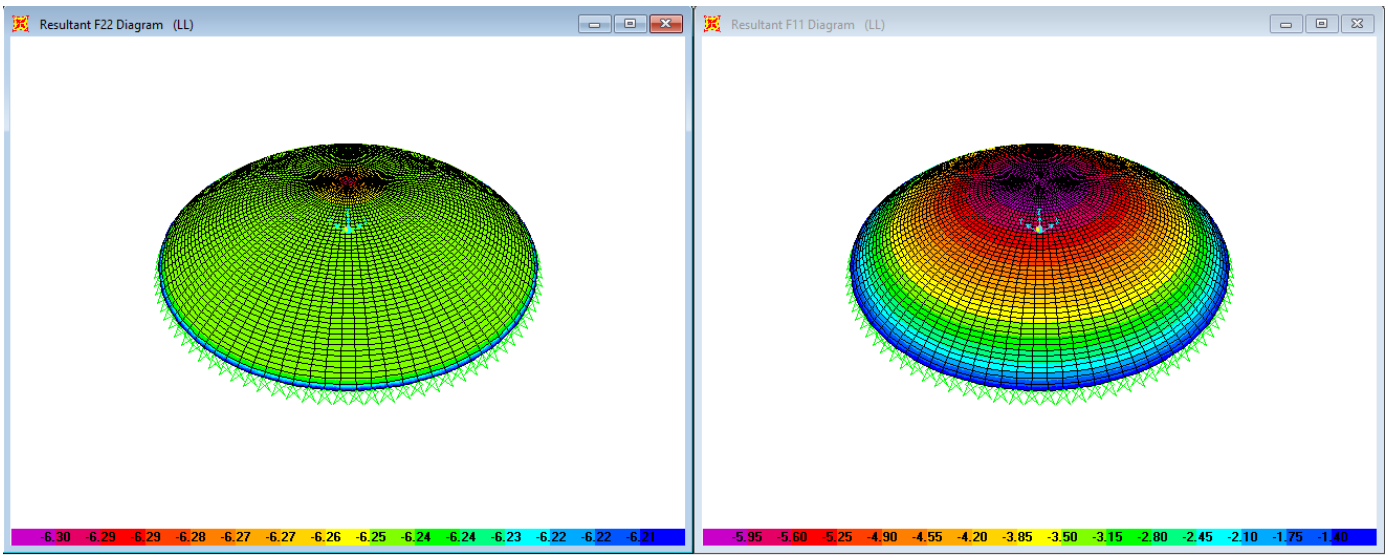

Figure 0-12: Resultant meridional and hoop forces of model 2 due to live load

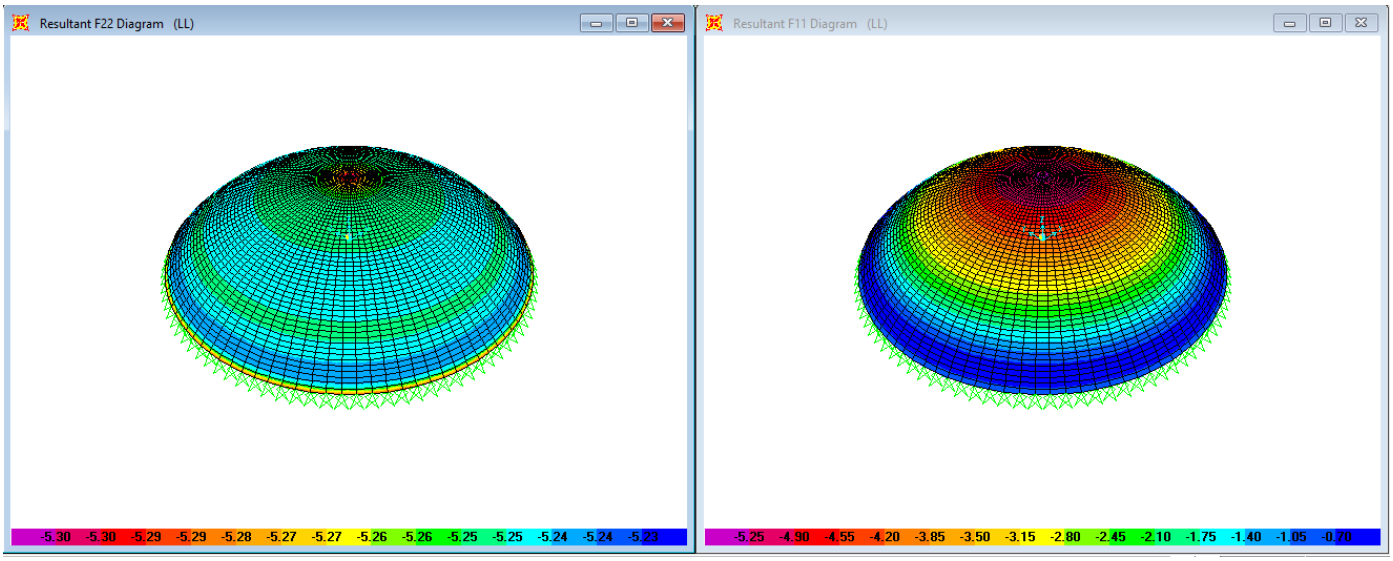

Figure 0-13: Resultant meridional and hoop forces of model 3 due to live load

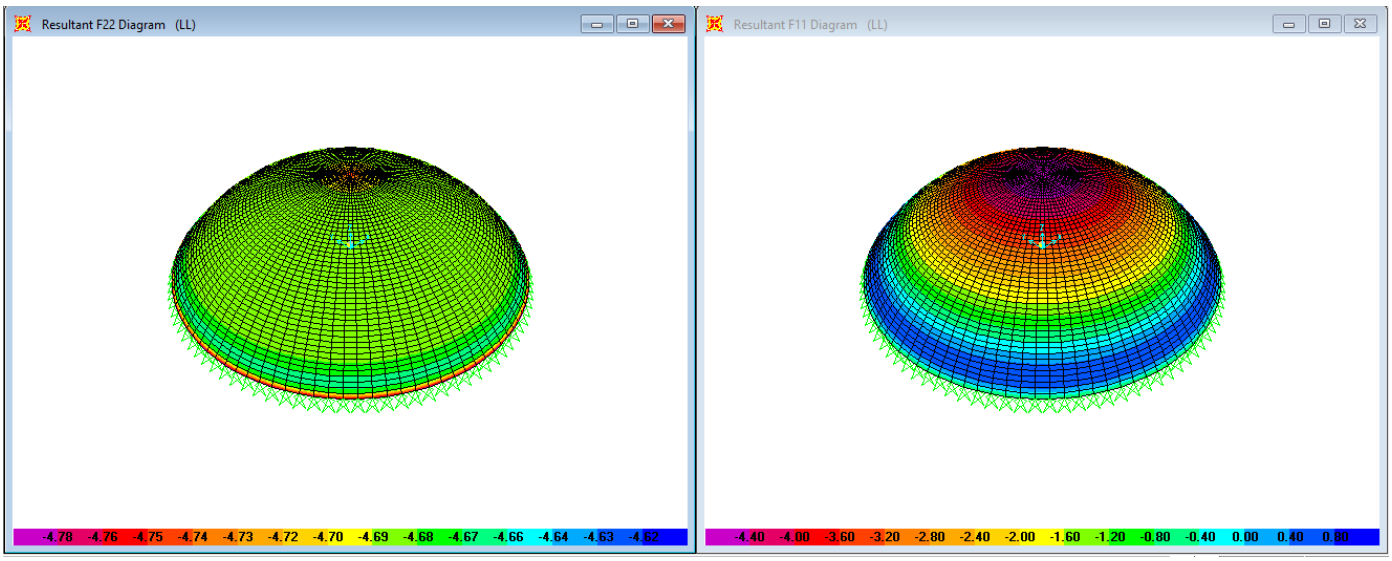

Figure 0-14: Resultant meridional and hoop forces of model 4 due to live load

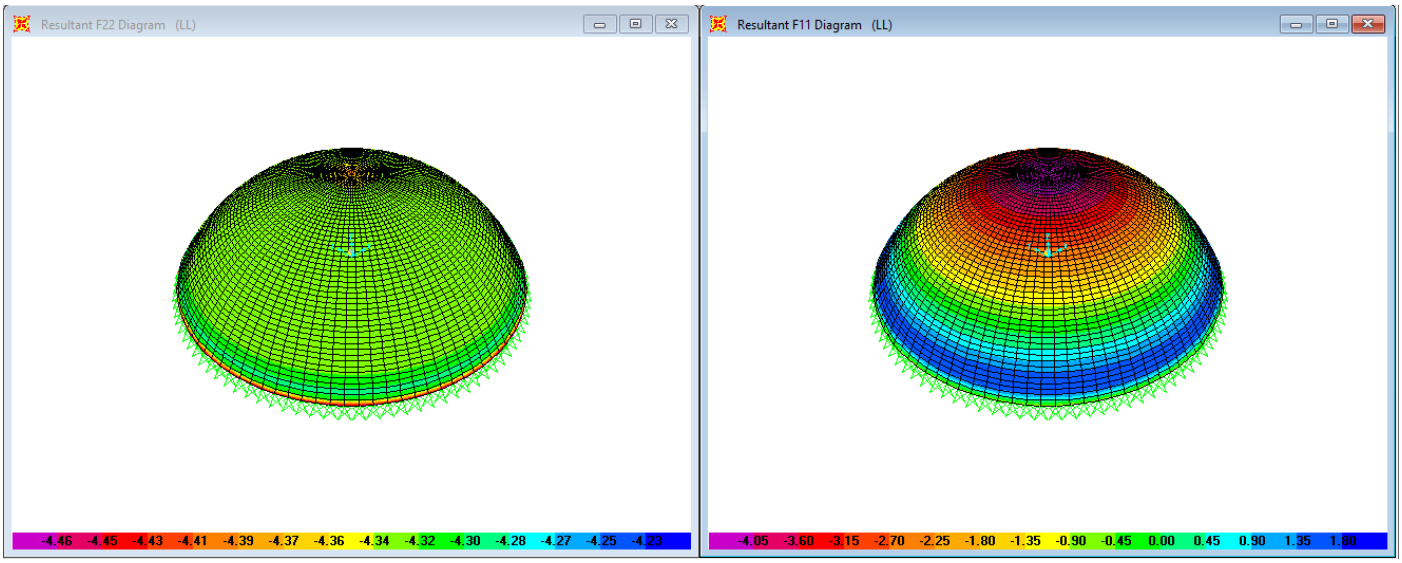

Figure 0-15: Resultant meridional and hoop forces of model 5 due to live load

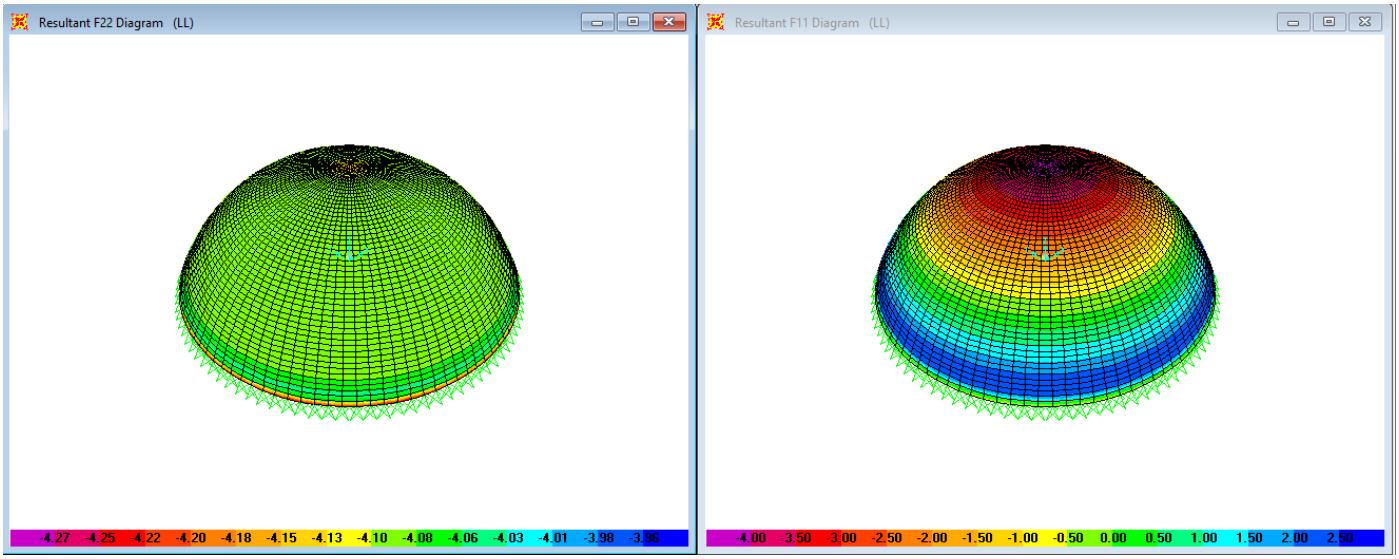

Figure 0-16: Resultant meridional and hoop forces of model 6 due to live load

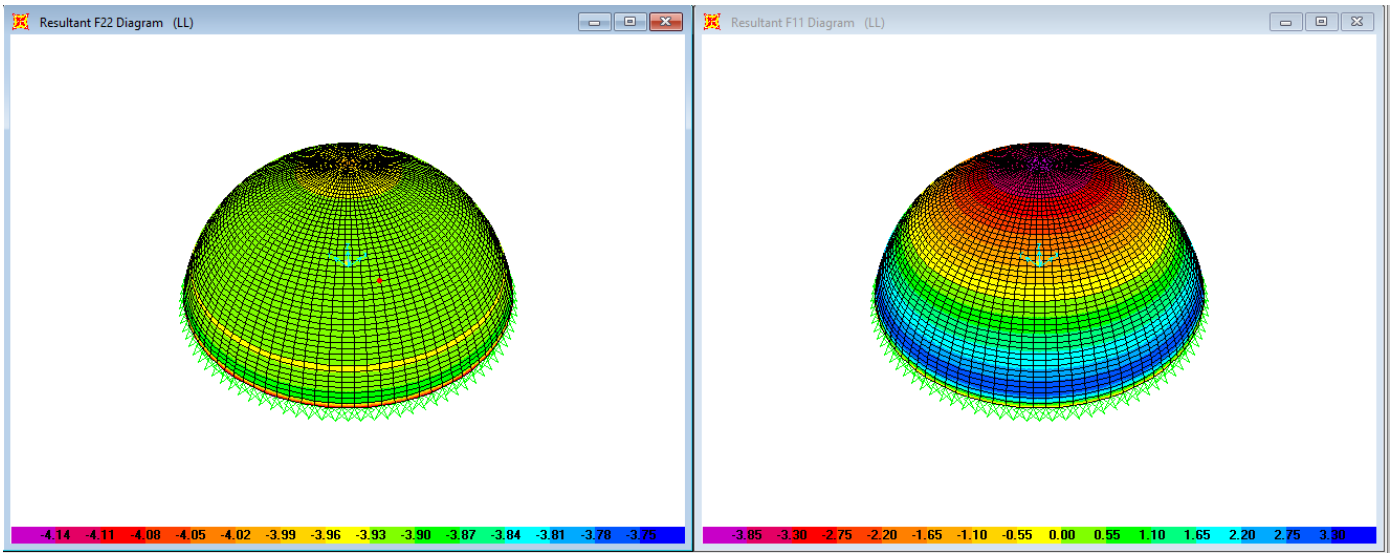

Figure 0-17: Resultant meridional and hoop forces of model 8 due to live load

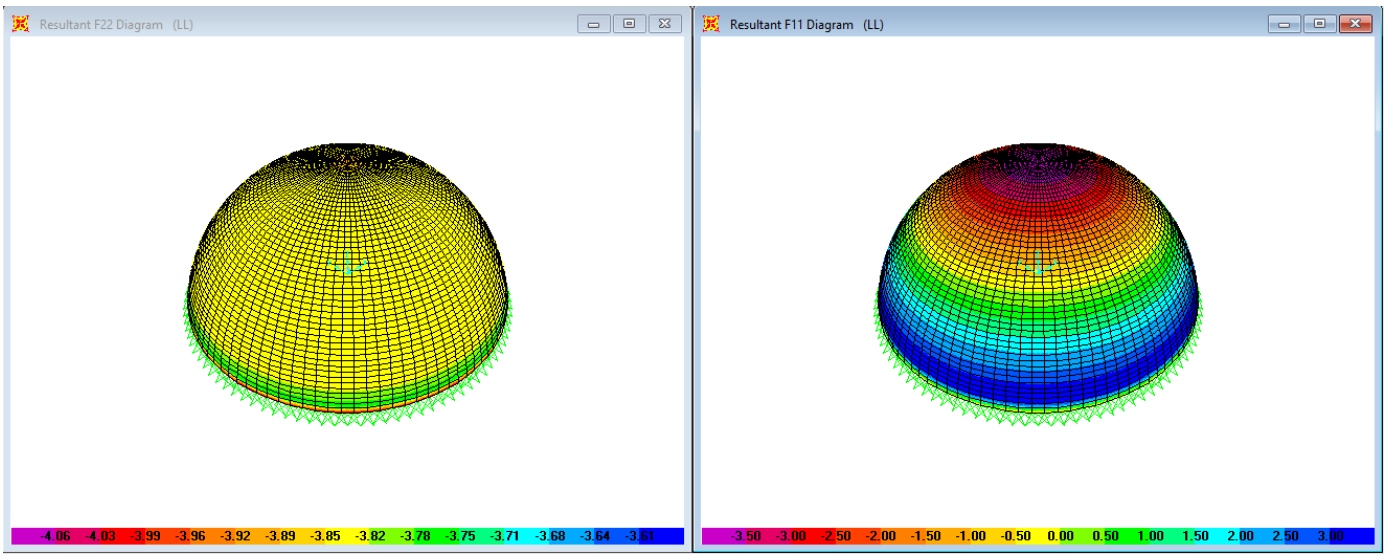

Figure 0-18: Resultant meridional and hoop forces of model 8 due to live load

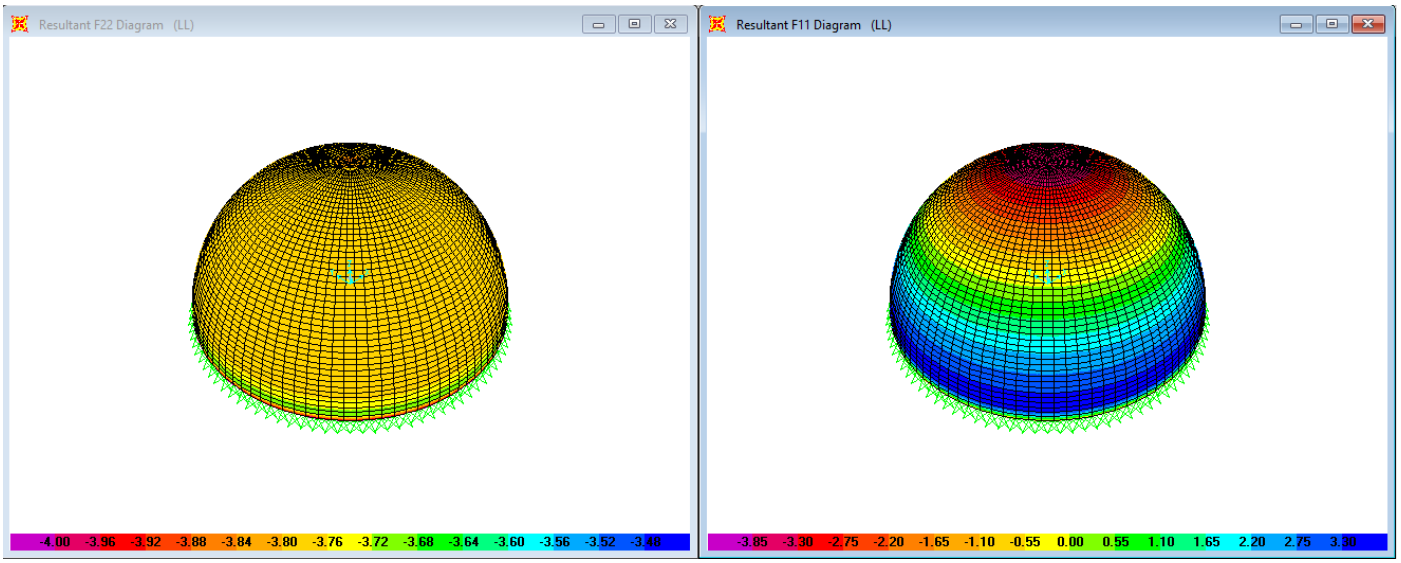

Figure 0-19: Resultant meridional and hoop forces of model 9 due to live load

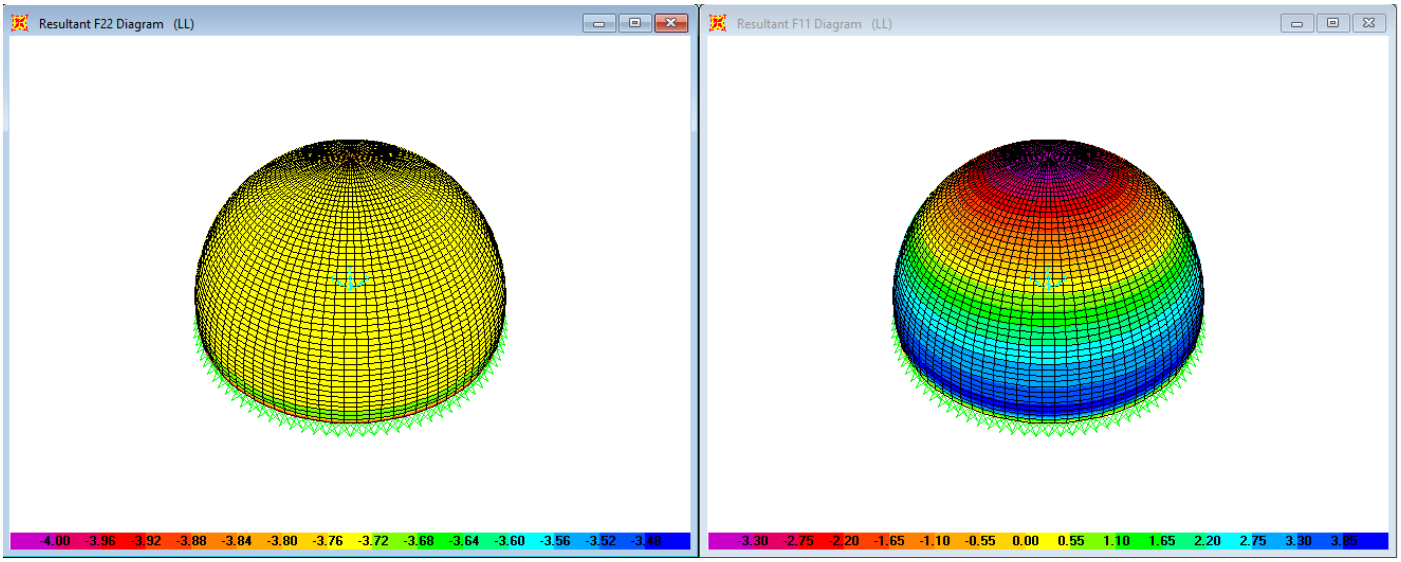

Figure 0-20: Resultant meridional and hoop forces of model 10 due to live load

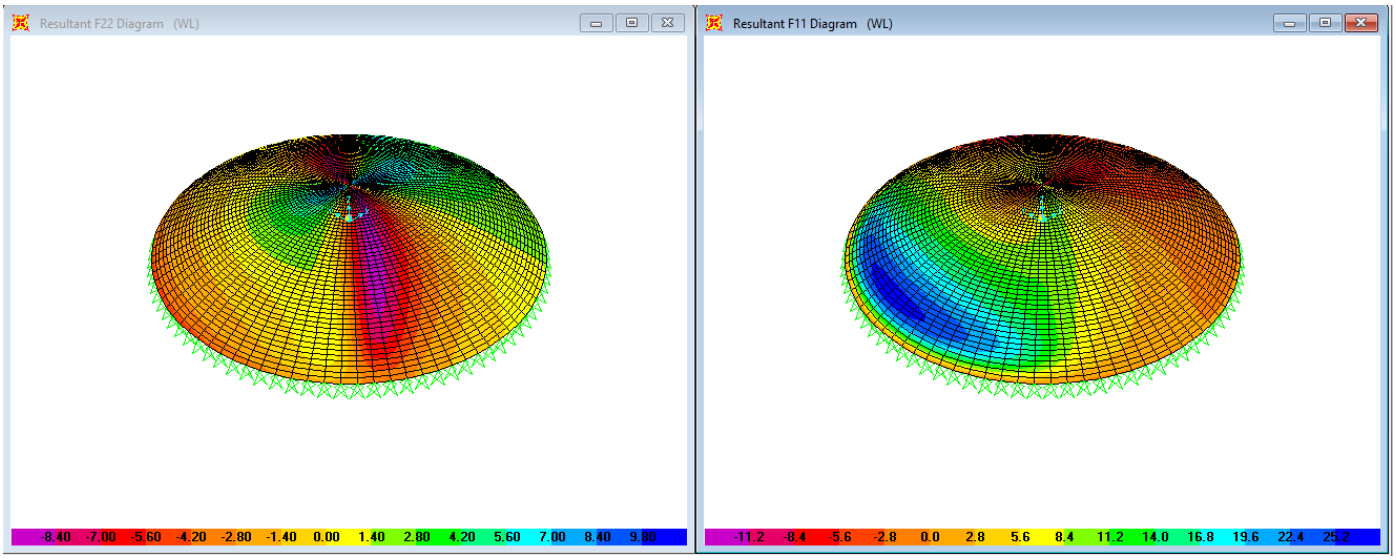

Figure 0-21: Resultant meridional and hoop forces of model 1 due to wind load

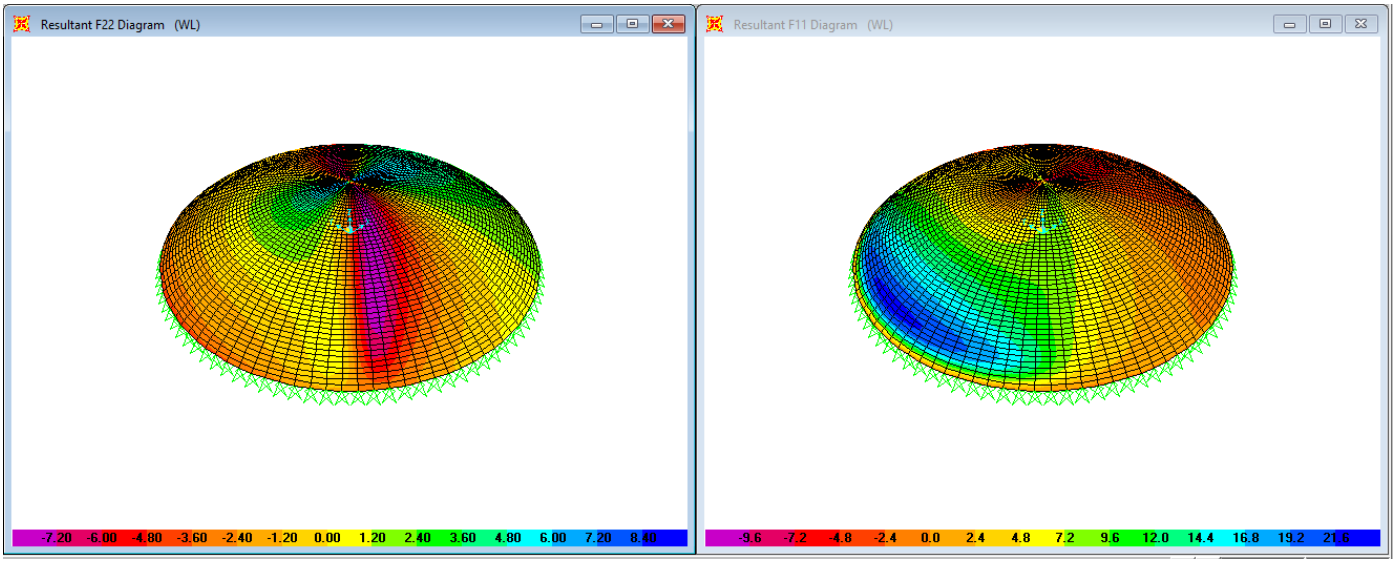

Figure 0-22: Resultant meridional and hoop forces of model 2 due to wind load

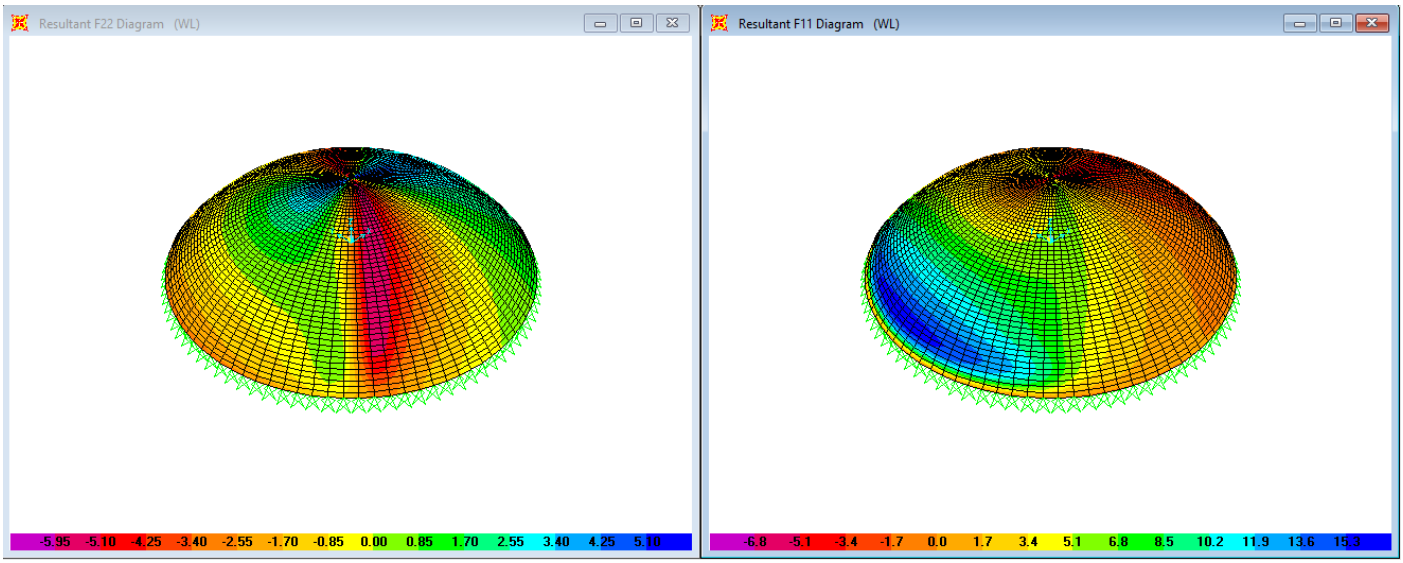

Figure 0-23: Resultant meridional and hoop forces of model 3 due to wind load

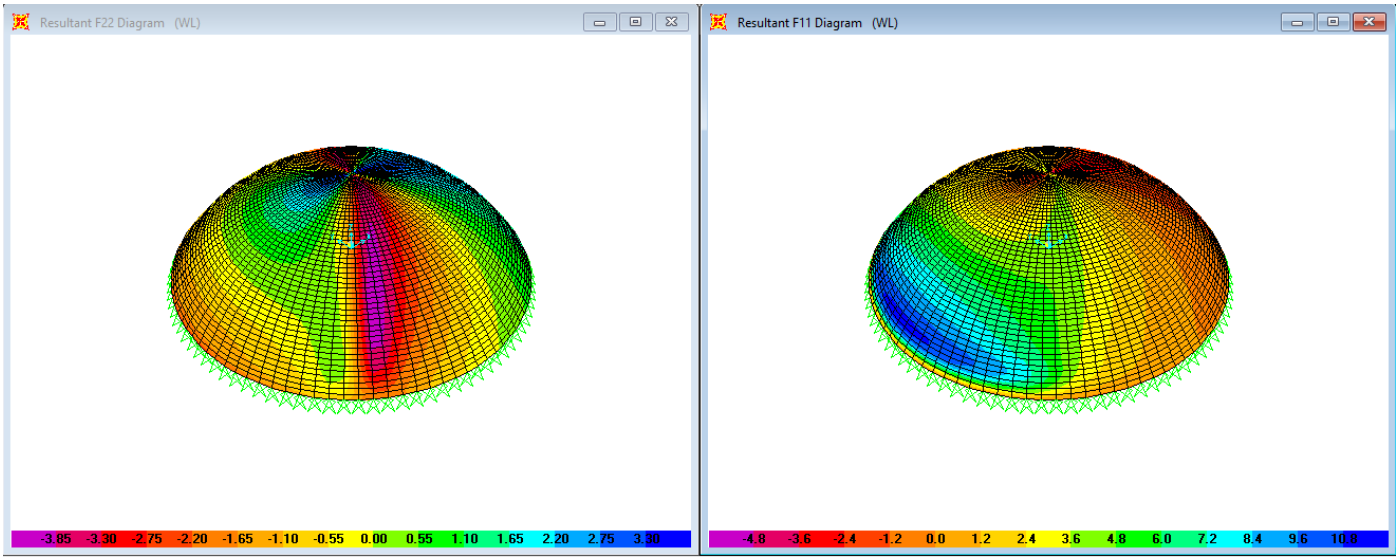

Figure 0-24: Resultant meridional and hoop forces of model 4 due to wind load

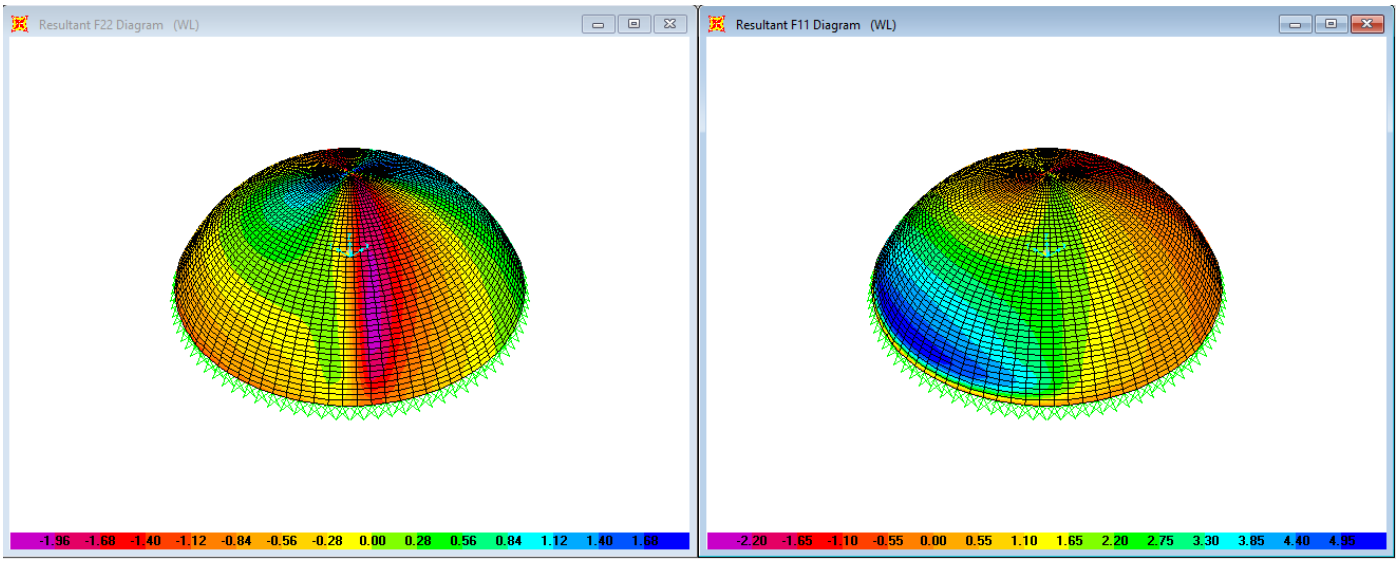

Figure 0-25: Resultant meridional and hoop forces of model 5 due to wind load

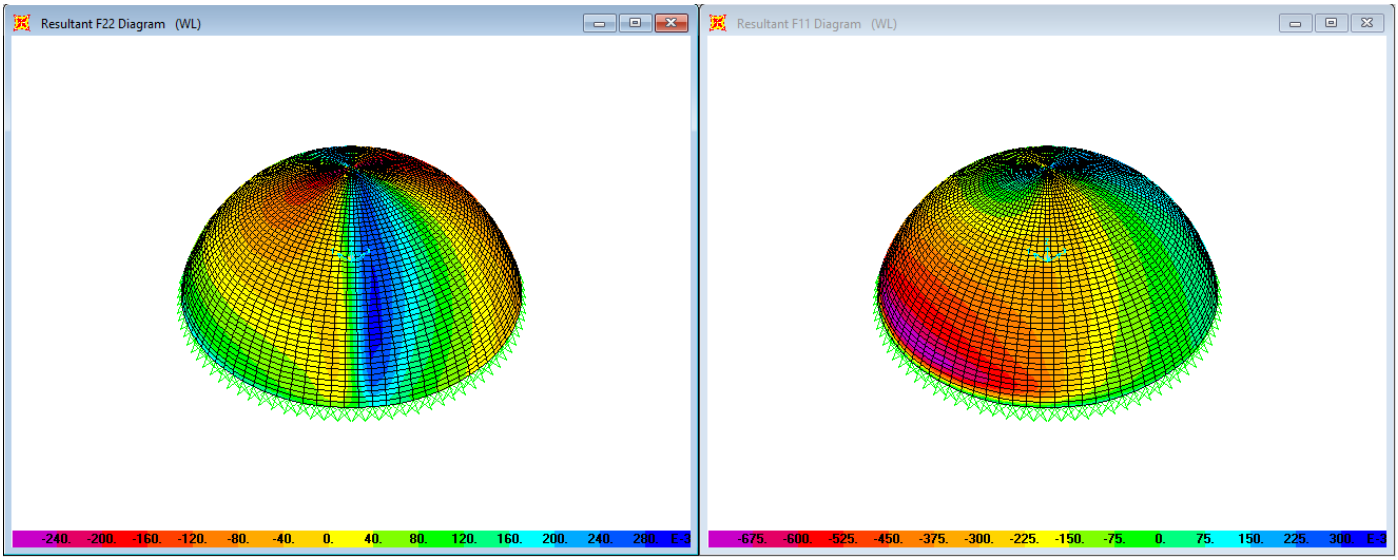

Figure 0-26: Resultant meridional and hoop forces of model 6 due to wind load

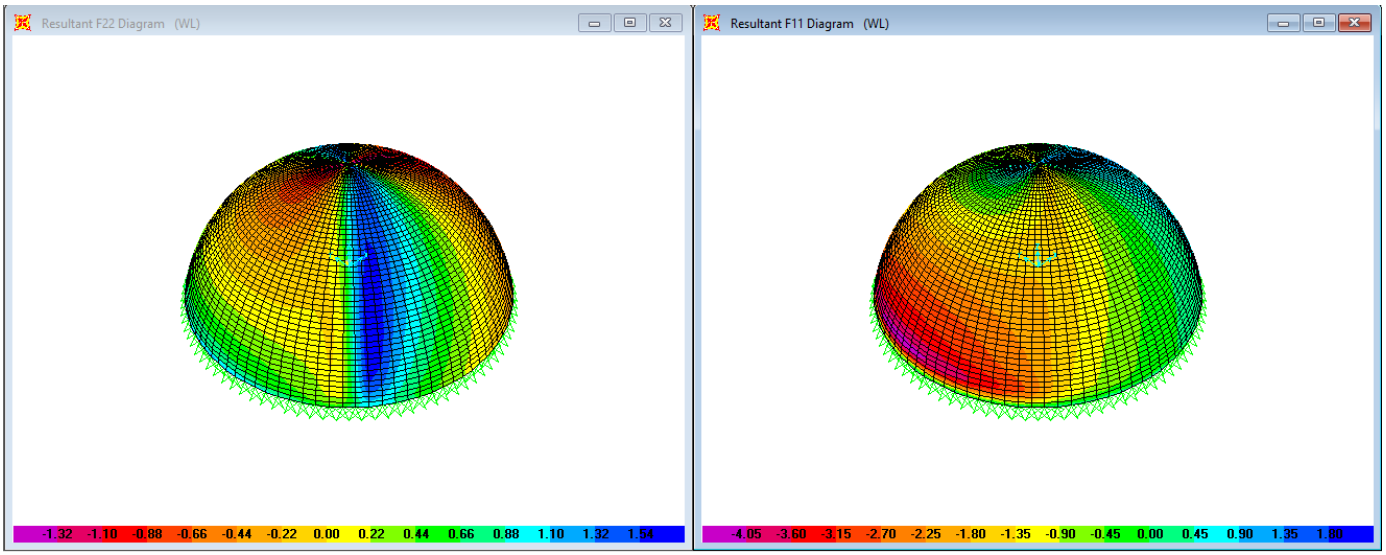

Figure 0-27: Resultant meridional and hoop forces of model 7 due to wind load

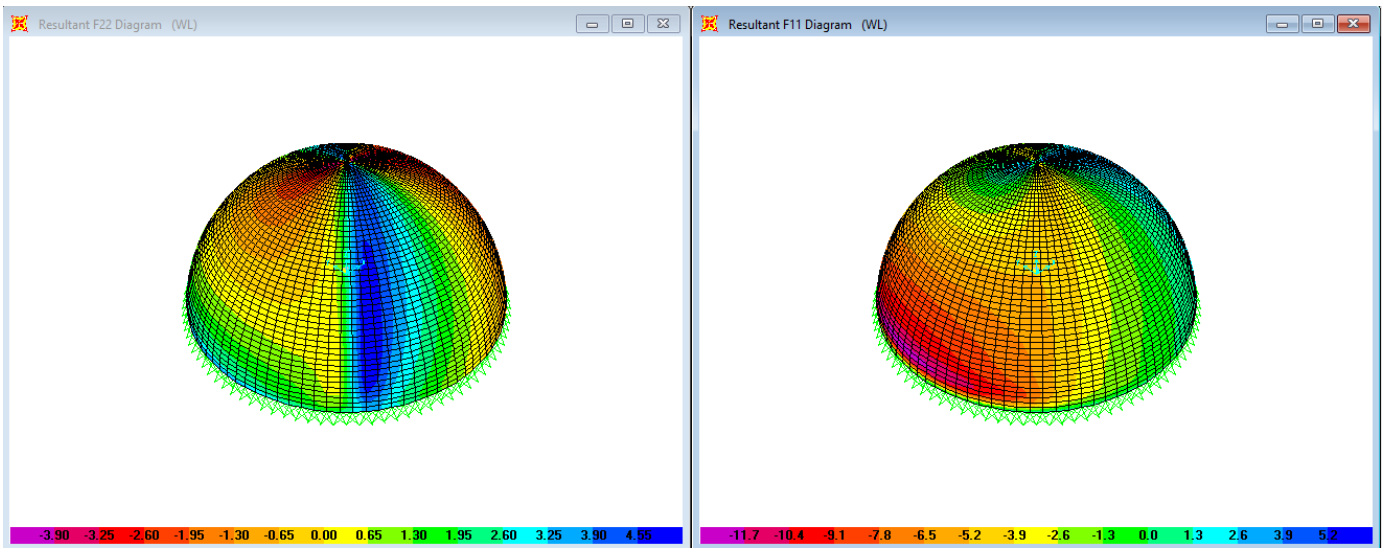

Figure 0-28: Resultant meridional and hoop forces of model 8 due to wind load

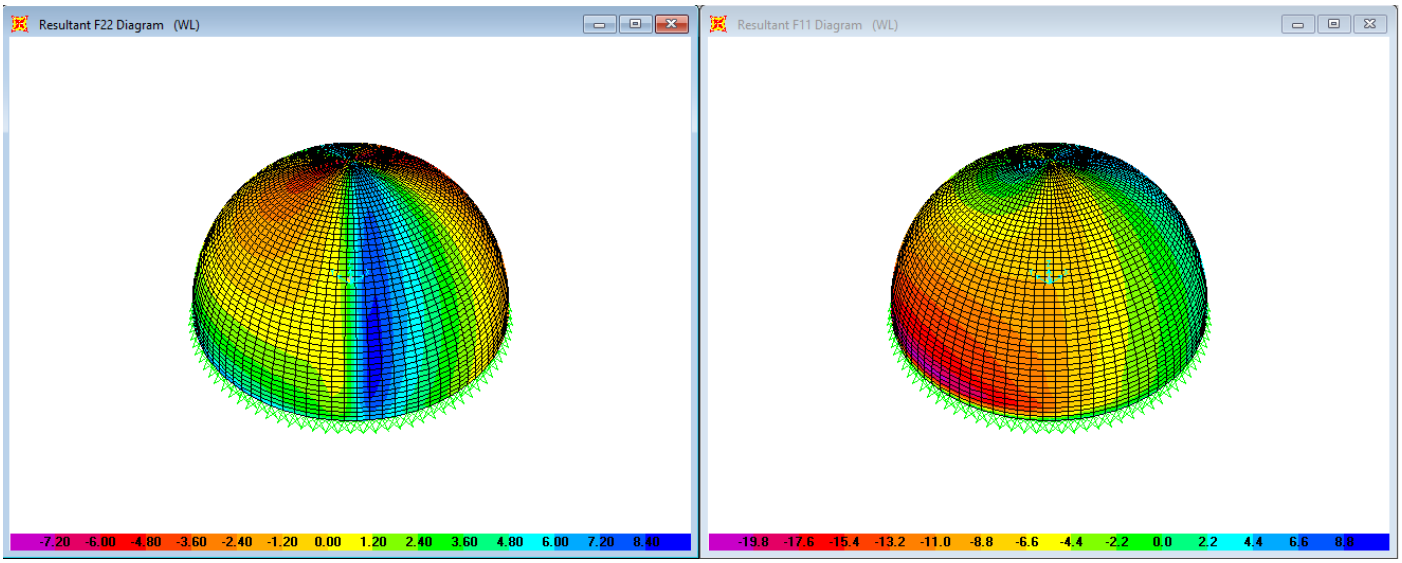

Figure 0-29: Resultant meridional and hoop forces of model 9 due to wind load

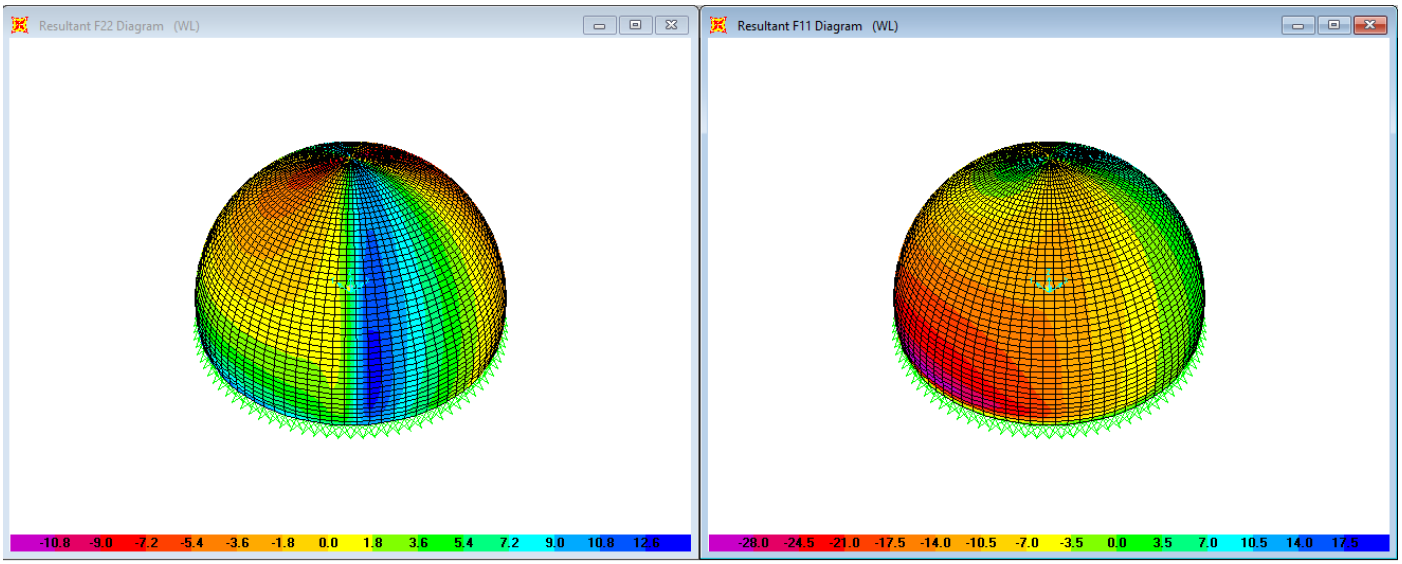

Figure 0-30: Resultant meridional and hoop forces of model 10 due to wind load